NSF/ENG-86023

PB87-148169

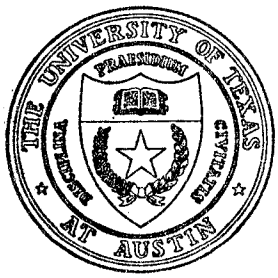

PMFSEL REPORT NO. 86-5
MAY 1986

SEISMIC STRENGTHENING OF A REINFORCED CONCRETE FRAME USING STRUCTURAL STEEL BRACING

By

Elizabeth A. Jones
James O. Jirsa

Report on a Research Project
Sponsored by
National Science Foundation
Grant No. CEE-8201205

PHIL M. FERGUSON STRUCTURAL ENGINEERING LABORATORY
Department of Civil Engineering / Bureau of Engineering Research
The University of Texas at Austin

The contents of this report reflect the views of the authors who are responsible for the facts and accuracy of the data presented herein. The contents do not necessarily reflect the view or policies of the National Science Foundation. This report does not constitute a standard, specification, or regulation.

50272-101

REPORT DOCUMENTATION PAGE	1. REPORT NO. NSF/ENG-86023	2.	3. Recipient's Accession No. PB87-148169/AS
4. Title and Subtitle: Seismic Strengthening of a Reinforced Concrete Frame Using Structural Steel Bracing			5. Report Date: May 1986 6.
7. Author(s): E.A. Jones; J.O. Jirsa			8. Performing Organization Rept. No. PMFSEL 86-5
9. Performing Organization Name and Address: University of Texas, Phil M. Ferguson Structural Engineering Laboratory, 10100 Burnet Road, Austin, TX 78758			10. Project/Task/Work Unit No. 11. Contract(C) or Grant(G) No. (C) (G) CEE8201205
12. Sponsoring Organization Name and Address: Directorate for Engineering (ENG), National Science Foundation, 1800 G Street, N.W., Washington, DC 20550			13. Type of Report & Period Covered 14.

15. Supplementary Notes

16. Abstract (Limit: 200 words)

A two-thirds scale model of two bays and two stories of the exterior moment resisting frame of a reinforced concrete building was constructed. The test specimen, which had deep spandrel beams and short narrow columns, was strengthened with an exposed structural steel diagonal bracing scheme in order to increase the lateral capacity of the structure for earthquake loads. Construction and fabrication of the strengthening scheme are discussed. The model was subjected to reversed, cyclic loads producing maximum interstory drifts of 1.3 percent. The behavior of the model is discussed, with special emphasis on the load-drift relationships of the frame. The load carried by the wide flange braces and the forces carried in steel collector members are examined. Slip between the steel elements and the concrete frame was also measured. The importance of quality control in fabrication of epoxy-grouted bolts used to attach the steel collectors to the concrete frame and of welded brace connections is discussed.

17. Document Analysis a. Descriptors

Structural engineering
Buildings
Braces
Tests
Reinforced concrete
Maintenance
Cyclic loads
Buckling

b. Identifiers/Open-Ended Terms

Earthquake engineering

c. COSATI Field/Group

18. Availability Statement	19. Security Class (This Report)	21. No. of Pages
NTIS	20. Security Class (This Page)	22. Price

SEISMIC STRENGTHENING OF A REINFORCED CONCRETE FRAME USING STRUCTURAL STEEL BRACING

by

Elizabeth A. Jones

and

James O. Jirsa

Report on a Research Project

Sponsored by

National Science Foundation

Grant No. CEE-8201205

Phil M. Ferguson Structural Engineering Laboratory
Department of Civil Engineering
BUREAU OF ENGINEERING RESEARCH
THE UNIVERSITY OF TEXAS AT AUSTIN

May 1986

A C K N O W L E D G M E N T S

The research was conducted as part of the Master of Science program of Elizabeth A. Jones under the direction of Dr. James O. Jirsa. The expert advice given by Dr. Joseph Yura was very helpful with the design and analysis of the steel bracing. This research was conducted jointly with the firm of H.J. Degenkolb Associates, Inc., San Francisco, California. Appreciation is expressed for the help provided by Loring Wyllie, Jr., Chris Poland, James O. Malley and others of that firm. The authors would like to express appreciation to the National Science Foundation who supported this research under Grant No. CEE-8201205.

The authors would also like to extend gratitude to the entire staff at Ferguson Structural Engineering Laboratory. Special thanks go to Dick Marshall and Pat Ball for their willing cooperation and hard work on the lab floor, and to Jean Gehrke, Terri Nally, and Carol Booth for their expert and speedy drafting and typing.

The authors are indebted to Carol Roach, Tommy Bush, and Marc Badoux who provided friendship, support, and hard work throughout the project and made it an enjoyable experience.

TABLE OF CONTENTS

TABLE OF CONTENTS (Continued)

LIST OF TABLES

LIST OF FIGURES

LIST OF FIGURES (continued)

LIST OF FIGURES (continued)

LIST OF FIGURES (continued)

LIST OF FIGURES (continued)

LIST OF FIGURES (continued)

CHAPTER 1

INTRODUCTION

1.1 Need for Strengthening

Many existing structures in high risk earthquake areas are inadequate in their ability to withstand seismic loads. Although these buildings were designed and constructed following the structural codes in effect at the time, their lateral-load resisting systems are deficient in terms of the stricter and more complex codes of today.

Significant changes in the Structural Engineers Association of California Recommended Lateral Force Requirements and Commentary [1], have taken place in the past fifteen years. The SEAOC code, which serves as a standard for many regional and city codes, was altered as a result of earthquake engineering research funded after the 1971 San Fernando Earthquake. Major changes in the specifications involved proportioning of members and reinforcement details in reinforced concrete structures.

Often, an owner will choose to strengthen, as well as repair, a building damaged by an earthquake rather than construct a new building. Other reasons for seismic strengthening include forced compliance with local building codes caused by changes in occupancy, and voluntary measures taken by owners for safety or financial interests.

1.2 Strengthening Techniques

Some of the more common methods of seismic strengthening are shown in Fig. 1.1. These include infilling walls, adding wingwalls to existing columns, attaching structural steel braces, and encasing columns. In general, the first three methods are regarded as techniques to increase strength. Encasing columns may be used to increase ductility rather than strength.

The purpose of column encasement is to improve the shear strength of the columns, thereby increasing the ductility of the structure by avoiding a brittle shear failure. The "wrapping" techniques include steel straps welded to steel angles at each corner, a steel case filled with grout, or a concrete coat with a steel mesh. When a column is encased, an increase in flexural

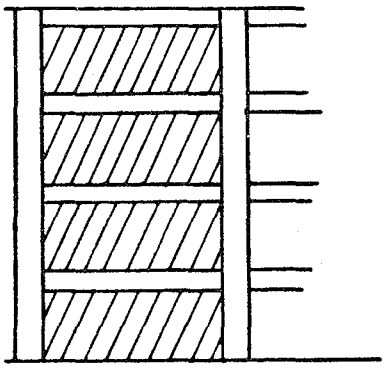

a) Infilled Walls

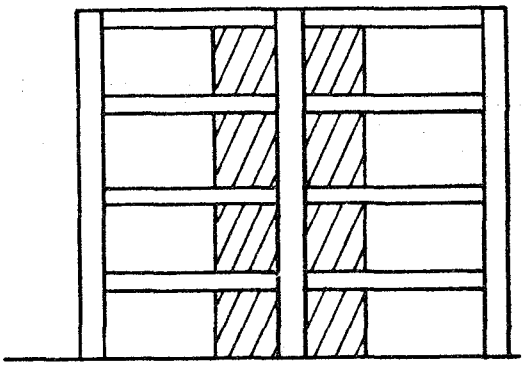

b) Wingwalls

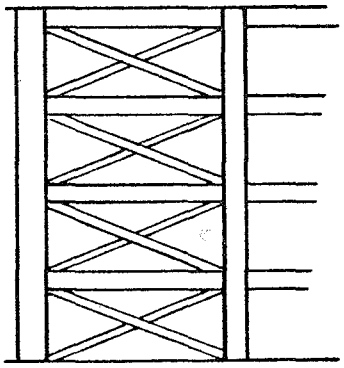

c) Steel Braces

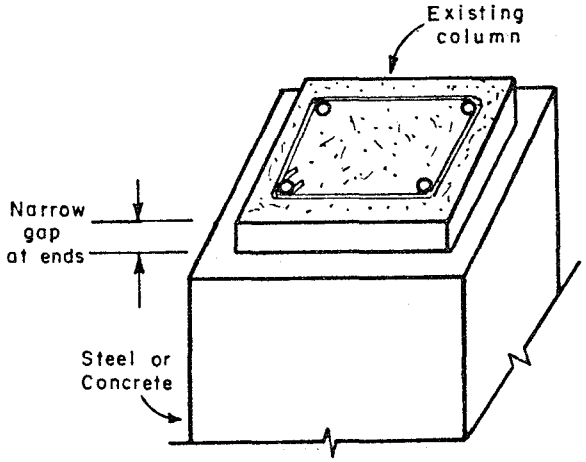

d) Column Encasement
- steel straps
- steel case filled with grout
- reinforced concrete coat

Fig. 1.1 Seismic Strengthening Techniques

capacity which would result in a shear failure mechanism must be avoided. Often a gap is left at the ends of a column to prevent an increase in flexural capacity.

Wingwalls, or side walls, can be precast or cast-in-place elements attached to the existing columns. By increasing both the flexural and shear strength of columns, addition of wingwalls will usually transfer the failure mechanism from the columns to the beams. Anchorage of the vertical steel reinforcement in the wingwalls must be provided in one of two ways. Either the steel is embedded in the beams above and below, or the vertical bars are continued through sections of the wingwalls which are cast against the beam faces. The most important detail in the design of wingwalls is the connection between the new and old concrete. Shear transfer between the old and new may be accomplished through an arrangement of shear keys, or by grouted dowels or wedge anchors into the existing elements.

Several steel bracing arrangements are shown in Fig. 1.2. Possible patterns include X-braces, K-shape, diamond shape, and eccentric braces. Steel bracing can be designed to carry all or part of the lateral design loads. An important consideration is the transfer of load from the concrete frame to the steel system. Vertical and horizontal steel members, which are attached to the concrete columns and beams, may be used to make this transfer.

The selection of a strengthening method depends on the desired result: an increase in strength, an increase in ductility, or a combination of the two. Aesthetics, economics, and construction are all important factors to consider when choosing a strengthening scheme. In order to minimize interference with the normal operation of a building, it is vital to consider the method of construction.

1.3 Example

The most likely candidate for seismic strengthening is a building which has satisfactory gravity load capacity, is clearly deficient in its lateral load system, and is economically feasible to strengthen. In the United States, structures meeting the above conditions are a number of reinforced concrete buildings constructed in California during the 1950's and 1960's.

During this time period, the trend was to concentrate the lateral resistance in the exterior frames and leave the interior frames as flat slabs on columns. This type of design

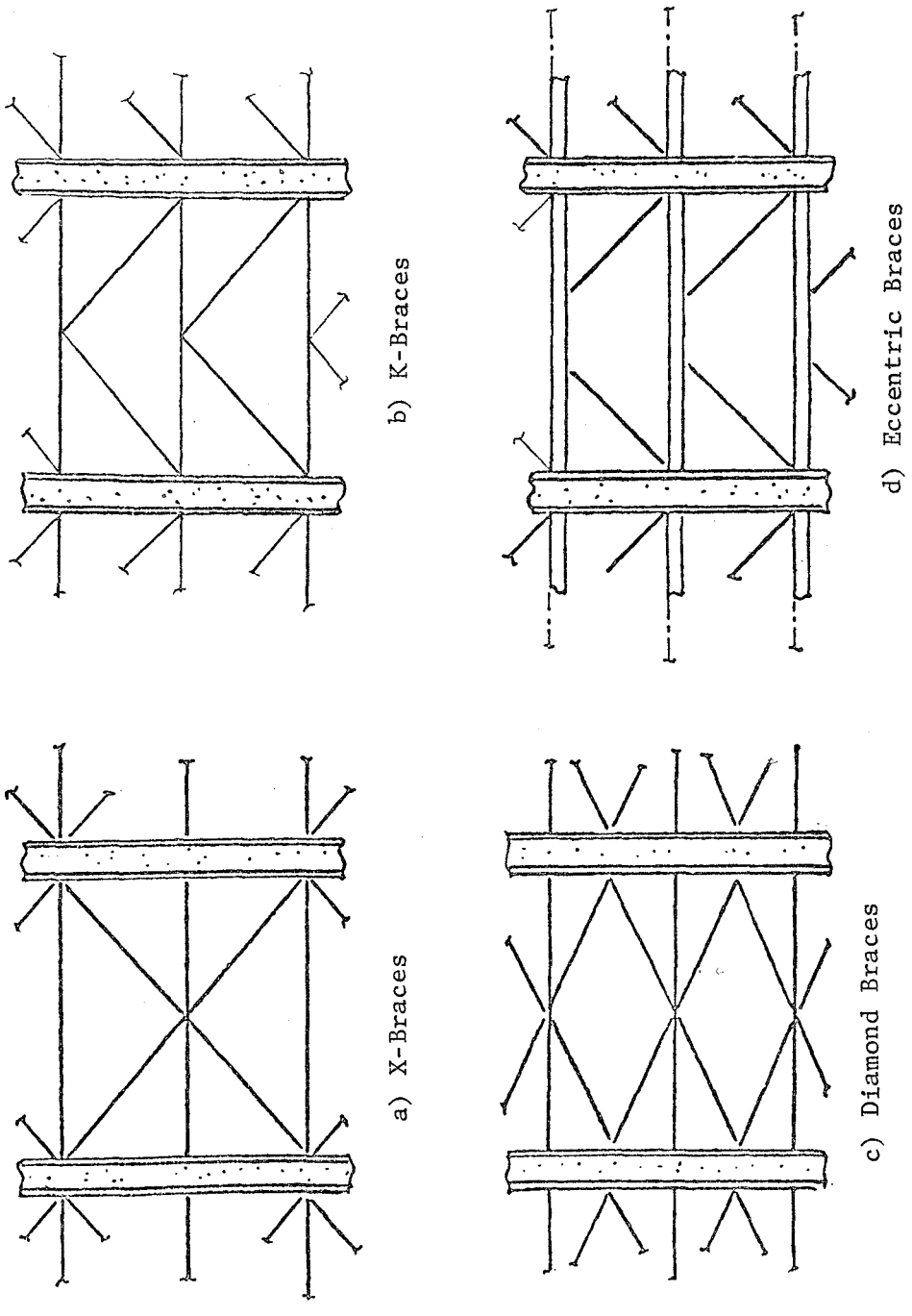

Fig. 1.2 Steel bracing patterns

allowed larger vertical clearances on the interior and, thus, a reduction in the overall height of the building. Because the lateral earthquake design loads were much lower thirty years ago, it was possible to carry the loads entirely in the outer frames.

Due to the increase in earthquake design loads, these outer frames are not strong enough by today's standards. In addition, the columns are underdesigned because the building codes at the time did not emphasize the possibility of shear failure in columns, nor did they offer the detailing requirements which are now in use. Therefore, it is economically feasible to strengthen the exterior frames only on these structures and, thus, reduce the interference with the function of the building.

A specific example of the type of building suitable for seismic strengthening is the weak column/strong beam system shown in Fig. 1.3. The exterior moment-resisting frame consists of deep spandrel beams framing into slender columns. The weak link of the example building is the short column, often referred to as a "captive" column. These columns are sometimes created when non-structural walls are added which reduce the clear height of the columns. Figure 1.4 shows the relationship between the moments and shears in a column subjected to lateral load. As the length (L) of a column is decreased, the shear force (V) increases for a given end moment (M) resulting from the displacement (Δ).

The columns of the example building will fail under lateral load long before the beams develop their flexural strength. The column shear failure will be brittle, resulting in a sudden loss of capacity and a possible collapse of the structure. Figure 1.5 shows the brittle column failure of a high school building in Japan, which took place during the 1968 Tokachi-Oki Earthquake. The failure occurred in the captive region of the column between the infilled walls.

To strengthen the weak column/strong beam building, it is necessary to increase the shear capacity of the columns or to carry the shear by an alternate load resisting system in order to change the failure mechanism of the structure. To achieve an increase in shear capacity, the columns could be strengthened by encasement. Alternatively, wingwalls could be added which would raise both the flexural and shear capacity. Another option would be to install steel bracing on the exterior frames. If the braces are designed to carry the entire lateral load, column shear failure can be avoided.

Fig. 1.3 Example Building [3]

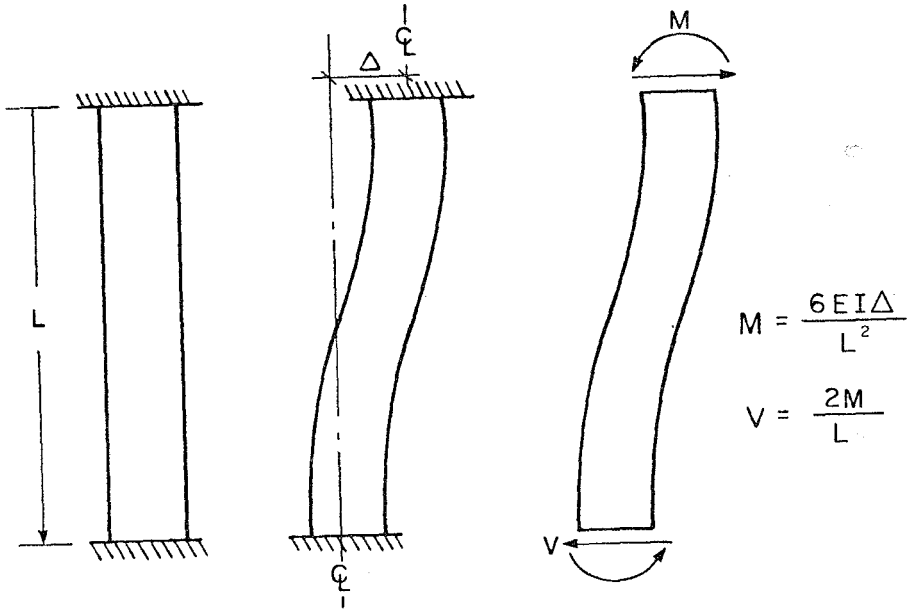

Fig. 1.4 Relationship between End Moments and Shears in a Column Subjected to Sidesway

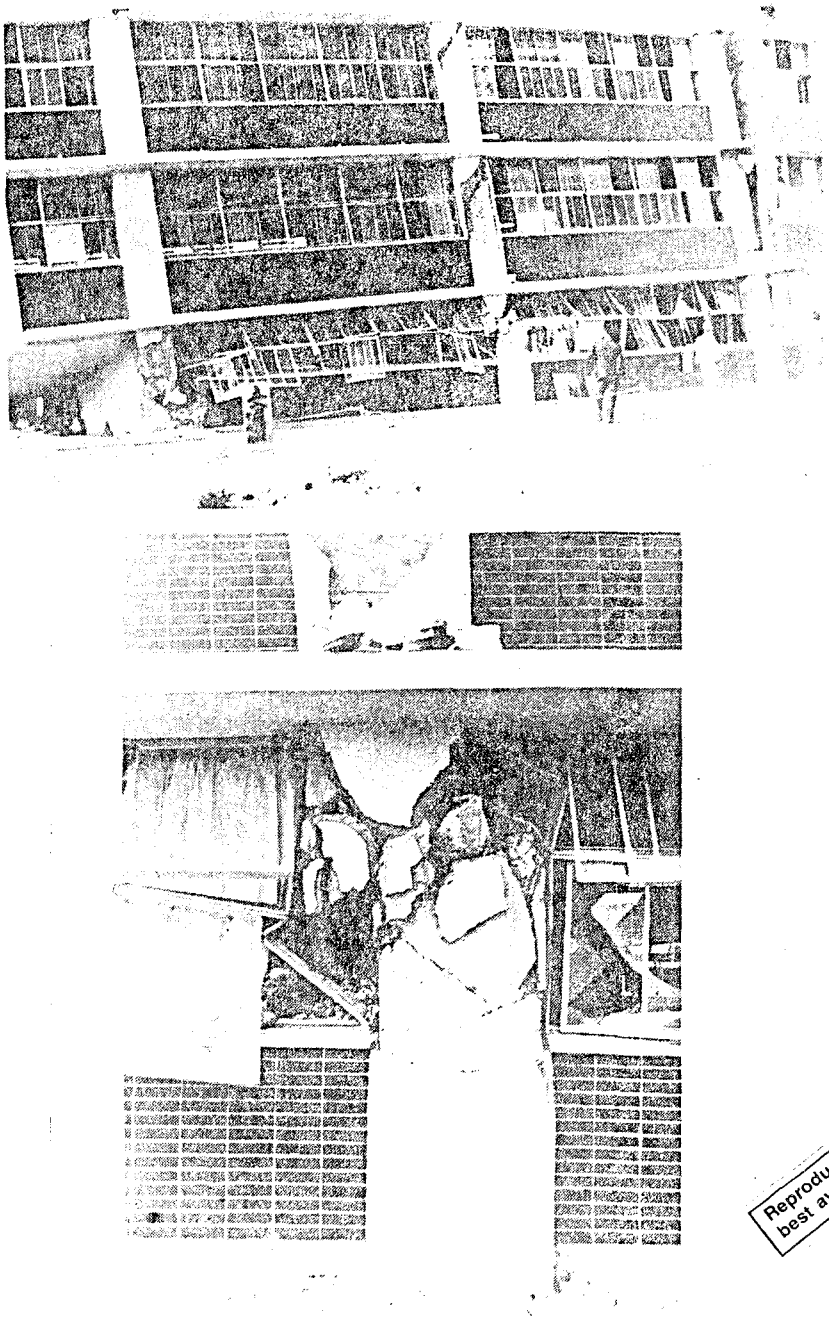

Fig. 1.5 Column Failure in Japanese Building - 1968 Tokachi-Oki Earthquake [4]

The main advantage of the steel system is that all work can be done on the exterior of the structure without complete evacuation of occupants or disruption of activities in the structure. Other advantages include preservation of natural lighting through the windows, easy conveyance, and negligible additional weight so that foundations and design lateral loads would not need extensive alteration. Possible disadvantages are the relative cost of the fabricated steel compared to reinforced concrete and the special techniques required to attach structural steel elements to concrete.

1.4 Previous Experience and Research

1.4.1 Need for Research. The Uniform Building Code and other structural codes are written for new construction using modern materials. There are no provisions for repairing or strengthening existing structures. A major unknown is the interaction of old and new materials, especially materials having different properties such as steel and concrete. Thus, there is a need for research to determine design guidelines for the strengthening of existing buildings.

Most of the large-scale experimental work on seismic strengthening in the United States has been performed on members and sub-assemblies, rather than frames. This is sufficient for testing techniques which influence primarily the strength of a section. However, to examine steel bracing or infilling systems, a larger portion of the structure must be modelled. One of the most important aspects to be investigated is detailing of the connections between new and old elements. Construction methods and detailing can greatly affect the overall response of a strengthened structure. Small-scale experimental models give little valuable information to practicing engineers to help in designing connections or overseeing construction.

Therefore, there is a need for full-scale, or nearly full-scale, models of frame assemblies.

1.4.2 Japanese Experience. Japanese engineers have acquired considerable experience in strengthening buildings for seismic loads. Major earthquakes in 1968 and 1978 led to extensive strengthening of existing buildings, development of government design guidelines, and experimental research to solve design and construction problems.

The first experience for the Japanese to strengthen a large number of existing buildings came after the 1968 Tokachi-

Oki Earthquake. Most of the damage was caused by shear failure of columns in low to middle rise buildings [5]. Many structures were strengthened even though there were no guidelines at the time.

In 1977, an advisory committee to the Japanese Ministry of Construction prepared design guidelines which were published by the Japan Building Disaster Prevention Association. The "Guideline for Seismic Retrofitting (Strengthening, Toughening, and/or Stiffening) Design of Existing Reinforced Concrete Buildings" [6,7] was meant to be used in conjunction with a guideline for evaluation of existing buildings for their seismic safety. The 1977 design guideline provided calculation procedures for infilled walls, wingwalls, and reinforced columnns.

After the Miyagiken-Oki Earthquake of 1978, many buildings were strengthened following the 1977 design guidelines. Most of the damaged buildings had been designed before 1971, when the Architectural Institute of Japan (AIJ) had revised the standard for design of reinforced concrete buildings [8]. Sugano and Endo prepared a review of 157 buildings which had been evaluated and strengthened following the 1977 guidelines [9]. Most of the structures were four stories or less, and over 70 percent were public buildings such as schools or offices. The most common method of strengthening was cast-in-situ concrete walls (45 percent of the cases). Addition of side walls comprised 15 percent of the strengthening cases, while only 1 percent were strengthened by adding steel braces. A majority of these buildings were strengthened before any major earthquake damage had occurred.

One of the few examples of steel bracing used as a seismic strengthening technique was a building at the Tohoku Institute of Technology in Sendai [6,10,11]. The reinforced concrete frame building, constructed in 1968, was damaged in the 1978 Miyagiken-Oki quake. The eight-story building, with three stories below ground, is shown in Fig. 1.6. The major damage occurred in the columns on the north side as shown in Fig. 1.6 (c). The failure in the columns was due to the infilled spandrel walls on the north facade. The spandrel walls gave the north side a stiffness four times greater than that of the other longitudinal frames, so that the north frame attracted a large proportion of the lateral load. In addition, the spandrel walls created "captive" columns which resulted in large shear forces in the columns.

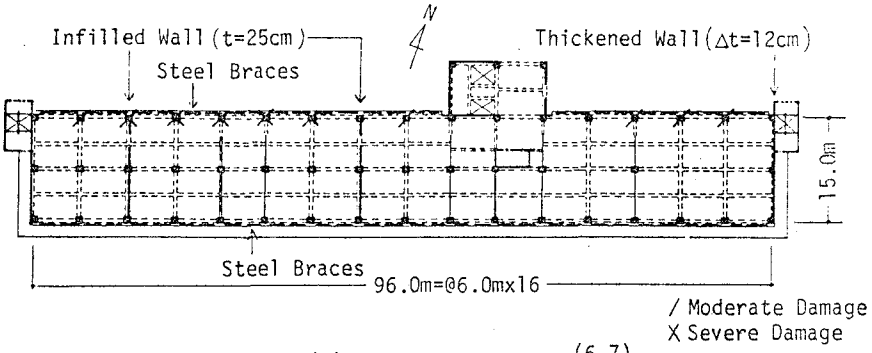

(a) Typical Floor Plan[6,7]

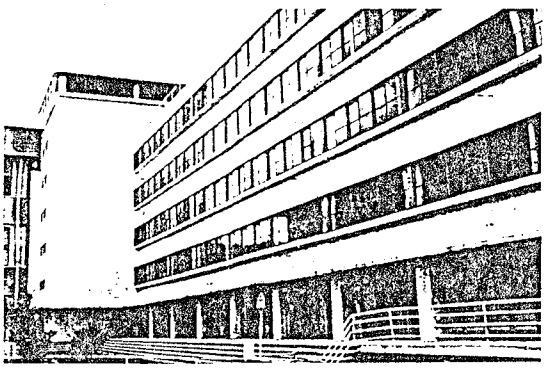

(b) North Facade

(c) Damage to a Column
(June, 1978)

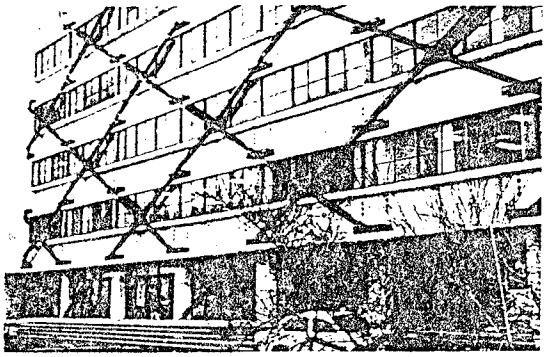

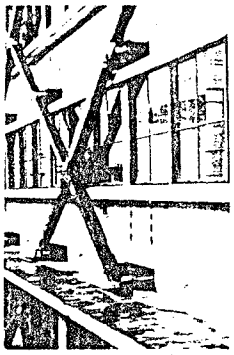

(d) After Strengthening

Fig. 1.6 Sendai School Building [11]

Retrofitting consisted of repairing old elements and adding new ones. The severely damaged portions of columns were removed, additional reinforcement was placed, and the columns were recast. In the transverse direction, some existing walls were thickened, and new shear walls were placed. Eccentric cross braces were installed on both the north and south frames to increase the lateral load capacity in the longitudinal direction. Spandrel walls were cored to reduce their strength and, thus, reduce their ability to generate large shear and flexural stresses in the columns.

The braces were H-sections of weathering steel painted with a rust-stabilizing agent. The same section was used at all levels; however, the braces were weakened at the upper levels to accelerate yielding. Three brace types (B1, B2, B3) were used as shown in Fig. 1.7 (a). Necks near the ends of a brace were produced by cutting holes in the web and outer flange. In addition, the outer flange was cut at the connection point at all levels to produce fully eccentric behavior of the braces. The cuts reduced the stiffness of the steel system, resulting in more evenly matched stiffnesses for the concrete frame and steel bracing.

A post-tensioning technique was used to connect braces to the exterior faces of the beams. Braces were attached by friction bolts to steel bases, which were post-tensioned to the concrete frame by rods passing through holes in the beam, as seen in Fig. 1.7 (b). Mortar filled the gap between the steel base and concrete surface.

Microtremor measurements performed on the completed structure showed that the strengthened building had retrieved its pre-earthquake stiffness. The period of the building in the longitudinal direction was 0.34 sec before the 1978 earthquake, 0.53 sec after it was damaged, and 0.35 sec after rehabilitation. In the transverse direction, the period went from 0.39 sec to 0.43 sec to 0.36 sec after strengthening [10].

Since the steel bracing was a new technique, experiments on the braces, connections, and spandrels were conducted. One-third scale models of the braces were tested under cyclic loading. The ultimate capacity was determined by buckling of the inner flange and web at the necked section. Slip tests on models of the connection at half scale showed that the base-to-beam connection was strong enough to develop the ultimate strength of the braces.

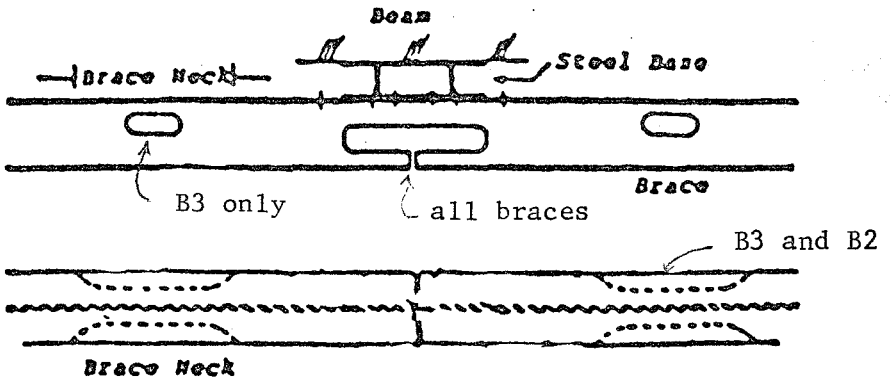

B1: 3 basement stories
B2: 1st to 3rd stories
B3: 4th to 5th stories

a) Brace Necks

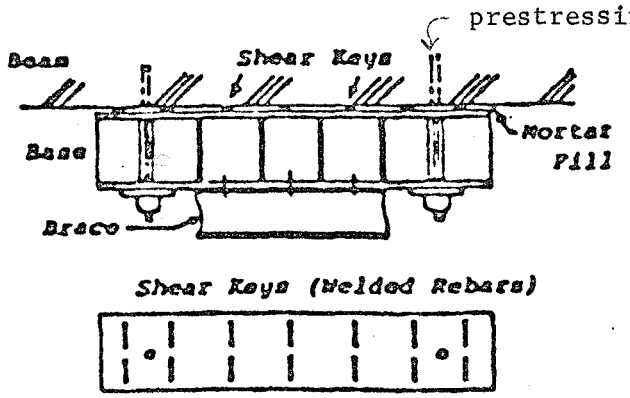

b) Connection Detail

Fig. 1.7 Bracing Details [10]

One-third scale tests on the cored spandrel beams indicated that a weakened spandrel had one-third the strength of a regular spandrel for moments producing compression in the region of the holes. Crushing of the concrete around the holes occurred at a lateral load less than that required to produce column shear failure. Therefore, the weakened spandrel beams would fail before the columns and permit development of a ductile failure mechanism.

1.4.3 Japanese Research. As of 1982 over 100 strengthened frames and 40 columns had been tested in Japan. Most of the tests were on one-third scale, single-bay, single-story specimens. More recently three-story frames have been tested. Most of the experiments were on cast-in-place infilled walls using various connection details. Other methods investigated were precast panels, concrete blocks, wingwalls, steel bracing, and steel panels. In Fig. 1.8, Sugano plotted the lateral strength versus displacement relationships for various strengthening techniques and an unstrengthened frame. The data for this graph came chiefly from two series of tests: one conducted by Higashi, the other by Sugano.

Higashi and others conducted tests on fourteen single-bay, single-story frames at one-third scale, in which the columns had poor web reinforcement [8]. Eleven types of strengthening schemes were used in addition to three control frames: two bare frames and one monolithic wall. The three schemes involving steel and the monolithic wall are shown in Fig. 1.9. Other methods included a cast-in-place wall, precast wingwalls, five types of precast walls, and steel plate wrapping of columns.

Cyclic load tests were performed for each test frame. The steel schemes increased the ultimate strength and ductility. In general, though, the initial stiffness of those frames with steel were lower than those with precast panels. The model with precast sidewalls, however, did not show notable increase in strength.

Sugano tested ten one-story, single-bay, one-third scale frames [12]. The nine strengthening schemes, along with the bare frame, consisted of two frames with monolithic walls of different thicknesses, a concrete block wall, two infilled walls with different connections, thickening of a thin wall, a steel panel bolted to the frame, steel compression braces, and tension braces. These frames may be seen in Fig. 1.10 along with their cracking patterns and hysteresis curves. The graph for the unstrengthened frame is at a different scale than the rest of the curves. The H-section compression braces were welded to plates

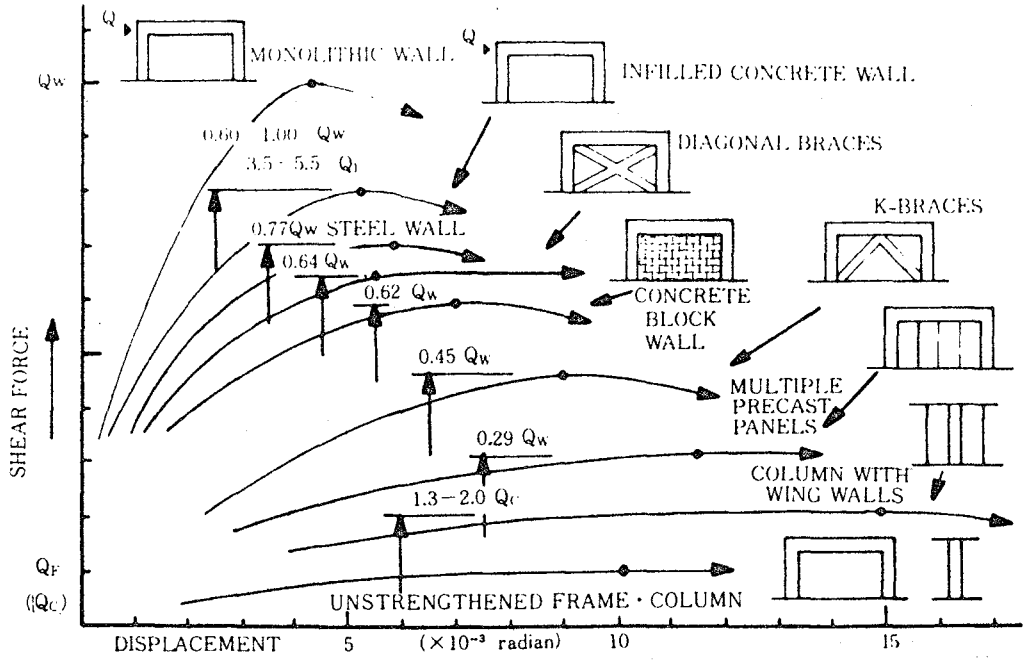

Q_c - Original column
Q_f - Original frame
Q_w - Monolithic wall

Fig. 1.8 Typical Load-Displacement Relationships for Different Strengthening Techniques [6]

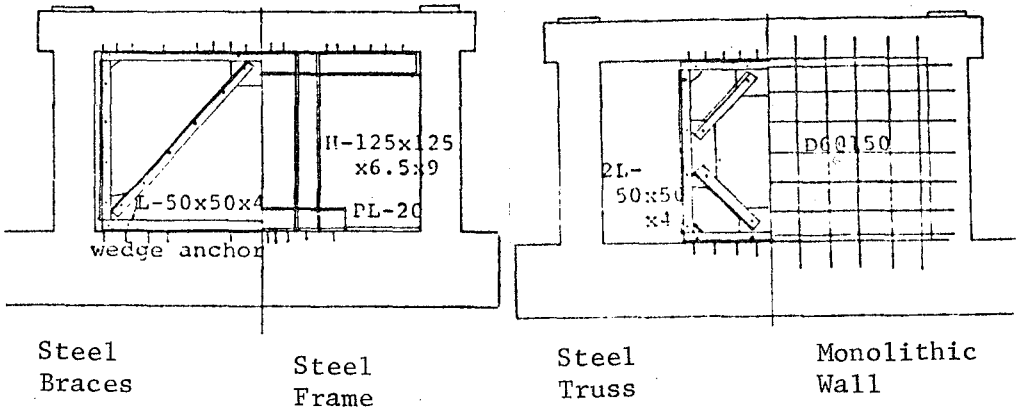

Fig. 1.9 Four of Higashi's Test Frames [8]

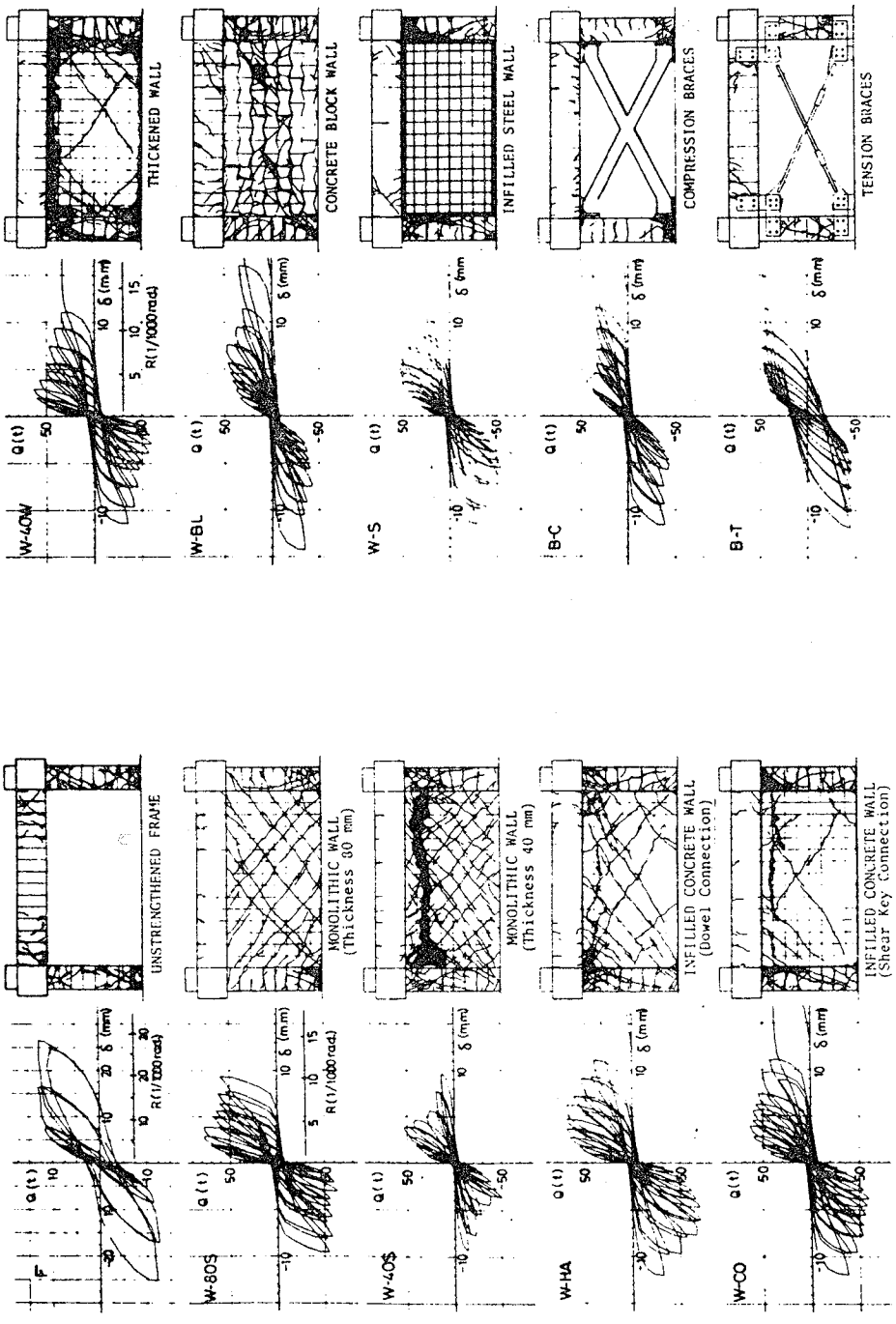

Fig. 1.10 Hysteresis Curves and Crack Patterns for Sugano's Test Frames [12]

which were attached to the frame with adjustable bolts. The tension braces, which were plain bars, were welded at their ends to plates which covered the side faces of the beams and columns.

Static, reversed cyclic loading showed that all methods increased the lateral capacity, but each frame behaved differently. The plain frame failed in a brittle manner due to shear tension in the columns. The greatest values of both strength and stiffness were observed for the infilled frames. On the other hand, the braced frames showed great energy absorption. The tension braces proved to be the most ductile of all the methods, although the increase in lateral capacity was not as significant as the increases shown by the infilled frames. For the compression-braced frame, shear sliding occurred early in the test so that the capacity was not as high; however, there was no significant deterioration of strength. The steel panel had high strength but lost capacity due to pullout of wedge anchors and shear failure of the columns. The importance of connection detailing to the hysteretic response of a structure is obvious in this series of tests.

1.5 Purpose and Scope

The objective of this study was to investigate techniques for strengthening a weak column/strong beam reinforced concrete structure to resist earthquake loads. A two-thirds scale model of a portion of an exterior moment-resisting frame was constructed. The two-bay, two-story model was tested in its unstrengthened state, and two methods of strengthening were carried out and tested: addition of reinforced concrete wingwalls to increase the column size and installation of a structural steel diagonal bracing system. All three systems, shown in Fig. 1.11, were subjected to static, cyclic lateral loads. In this thesis the design, construction, and behavior of the steel bracing technique will be discussed.

The two main features of this research which distinguished it from previous projects were the size of the model and the cooperative effort between a university research team and a structural engineering design group. The two-thirds scale model practically eliminated scale effects which are so important in modeling construction techniques. In addition, the two bays and two stories allowed a study of the redistribution of loads between the elements. Design of the prototype and strengthening schemes was carried out by H. J. Degenkolb Associates of San Francisco, while the specimen was constructed,

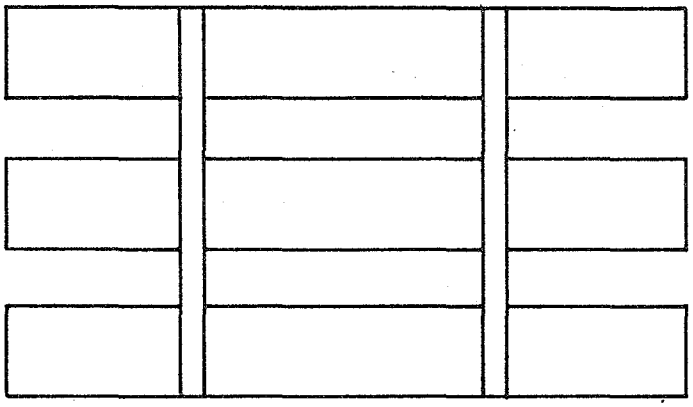

a) Unstrengthened (Bare) Frame

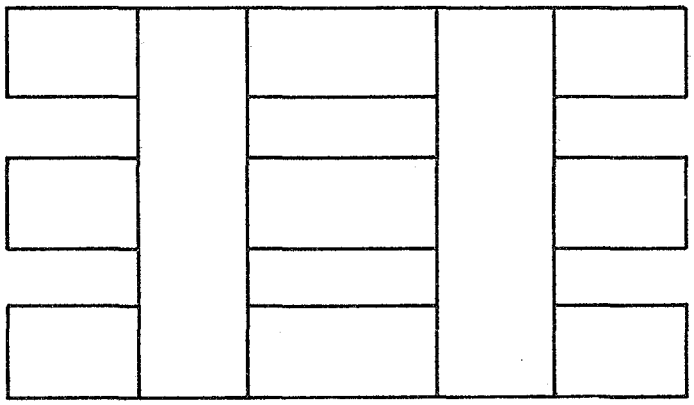

b) Strengthening by Wingwalls

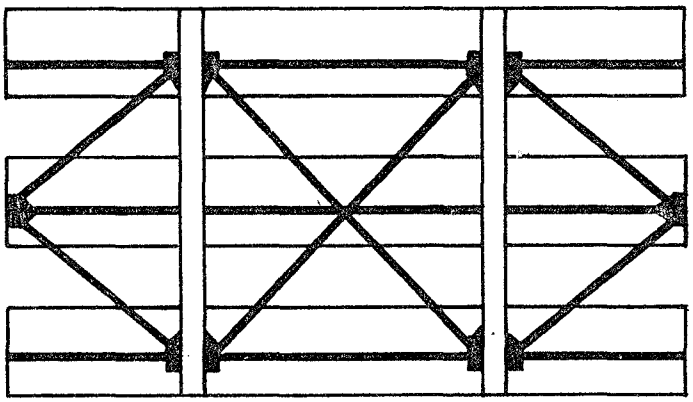

c) Strengthening by Steel Bracing

Fig. 1.11 Three Frame Systems

instrumented, and tested by a research team at The University of Texas at Austin.

CHAPTER 2

DESCRIPTION OF MODEL

2.1. Prototype Building

2.1.1 Description. The prototype for this study is typical of residential and office buildings constructed in California during the 1950's. The seven-story reinforced concrete structure, shown in Fig. 2.1 and Fig. 2.2, has deep spandrel beams and slender columns between the spandrels on the exterior frames in the longitudinal direction. Windows fill the openings between spandrels. A one-way floor slab, 6 in. deep, spans between the exterior spandrels and interior shallow beams, which are not shown in Fig. 2.1 for clarity. All reinforcing steel is Grade 40 except the column vertical steel, which is Grade 60; the specified concrete strength is 3000 psi.

The lateral load resisting system consists of four shear walls in the short direction and the moment resisting frames in the longitudinal direction. The floor slab acts as a diaphragm to distribute the lateral load. Since the interior frames are extremely flexible relative to the exterior frames in the longitudinal direction, the outer frames attract most of the lateral load.

2.1.2 Analysis. Determination of seismic loads and design of the members followed the 1955 Uniform Building Code [13]. Figure 2.2 indicates the disproportionate sizing of the members. The 72 in. by 8 in. spandrel beams with a steel area of 3.84 $in.^2$ are stronger in both flexure and shear than the 18 in. by 18 in. columns with six #10 bars.

The critical section capacity under lateral load is the column shear strength. With a design base shear force of 1064 kips, a column working shear strength of 39 kips, and assuming that only the exterior rows of columns carry the lateral load, the 18 in. columns are inadequate at the first and second levels. In the original design, it could have been assumed that the interior columns helped carry the lateral forces, in which case the columns are adequate. However, it may be unconservative to assign interior columns significant shear considering that the interior beams are only 6 in. deep compared to the 6 ft deep beams on the exterior. The spandrels produce captive columns only 4 ft in height which are almost six times stiffer than the interior columns.

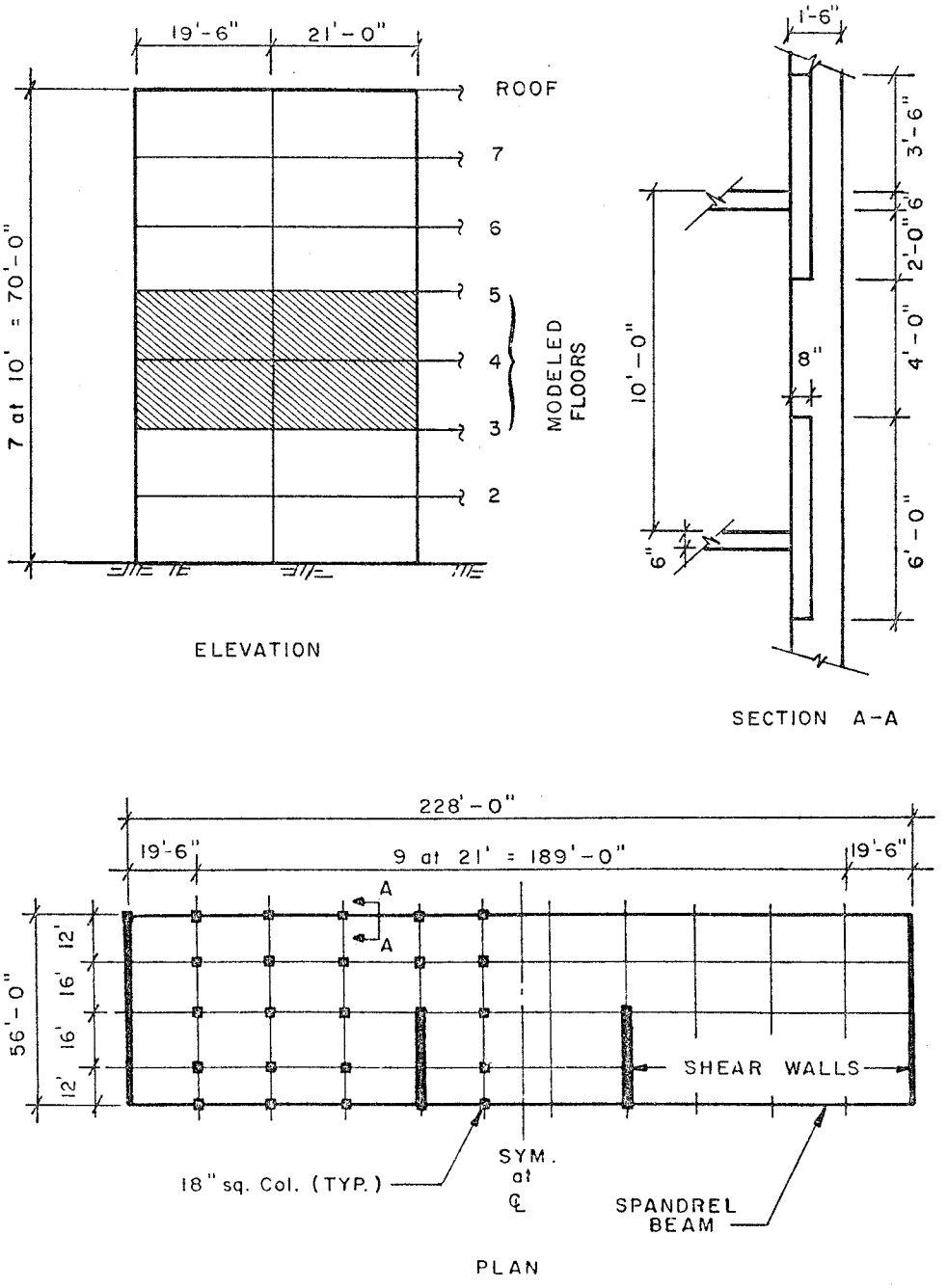

Fig. 2.1 Prototype Building

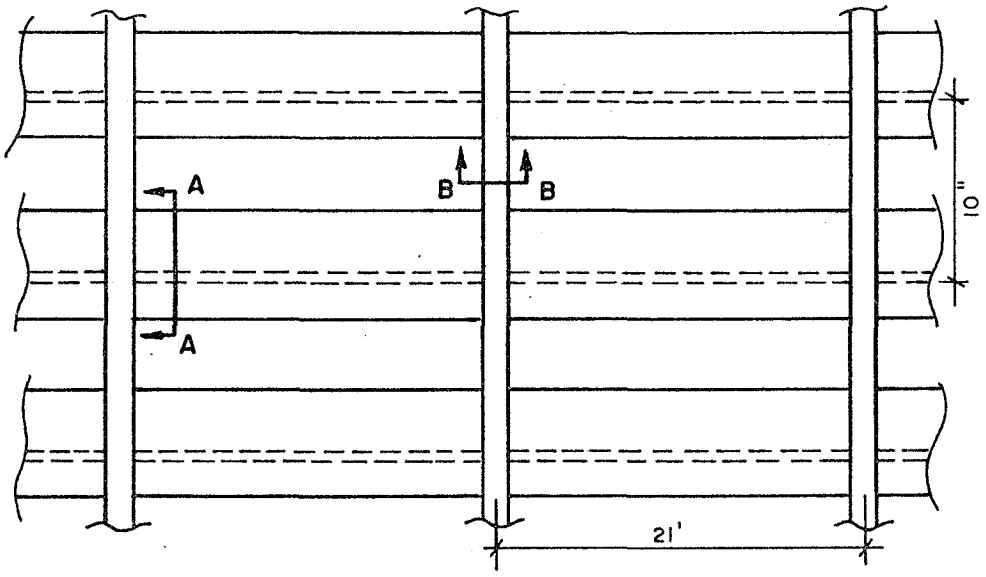

ELEVATION

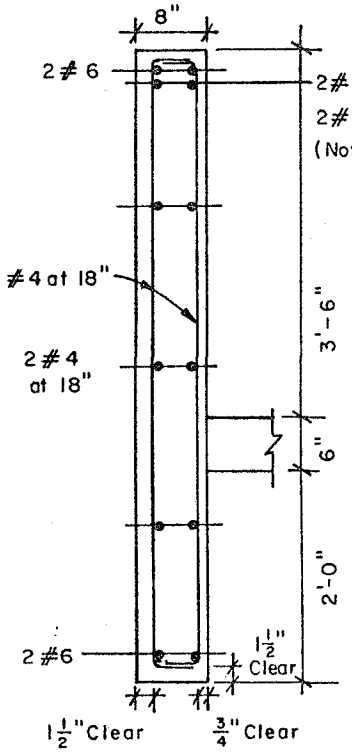

SECTION A-A

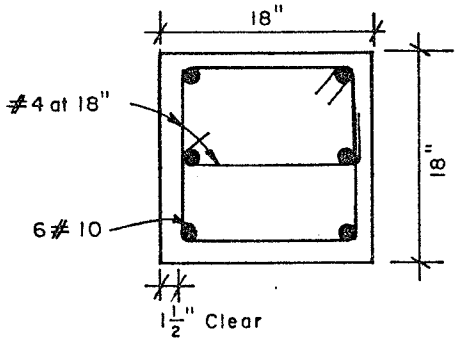

SECTION B-B

Fig. 2.2 Prototype Details

A seismic analysis indicates that the columns of the lateral load carrying system of the prototype do not meet the requirements of present building codes. The lateral design forces resulting from use of the 1982 Uniform Building Code [14] for a structure in seismic zone 4 are shown in Fig. 2.3 and are compared with the forces resulting from use of the 1955 UBC. The 1982 forces give a design base shear for earthquake load of 2378 kips, 2.2 times the 1955 value.

With the ultimate strength design method of the 1983 ACI Building Code [13], the column shear capacity is computed as follows.

$$V_n = V_c + V_s \qquad \text{where } V_c = 2\sqrt{f'_c}\, b_w d$$

$$V_s = A_v F_y\, d/s$$

$$V_c = 2\sqrt{3000} \times 18(15.5) = 30.6 \text{ kips}$$

$$V_s = 0.6(40)15.5/18 = 20.7 \text{ kips}$$

$$V_n = 51.3 \text{ kips}$$

With the third story shear of 2107 kips divided over 22 exterior columns and with the appropriate strength reduction and load factors, the required strength of 1.1(1.3)96 kips, or 137 kips, is much larger than the nominal shear capacity of, V_n, of 51. kips.

In addition to the strength requirements, ductility requirements have been added to Appendix A of the ACI 318 Code. The 18 in. column tie spacing used in the prototype is the maximum allowable spacing in the 1955 UBC and in ACI 318-83. However, if the provisions of Appendix A of ACI 318-83 are to be followed for structures in seismic zone 4, additional transverse reinforcement is required in all members which are part of the lateral load resisting system.

For the prototype column, a tie spacing of 4 in. would be required near the member ends (Section A.4.4). Since the columns are not stronger than the beams in flexure, the provisions of Section A.4.4 must be met over the full height of the columns (Section A.4.2.3). Because the joints are not confined, the 4 in. tie spacing would also be required within the joint (Section A.6.2.1).

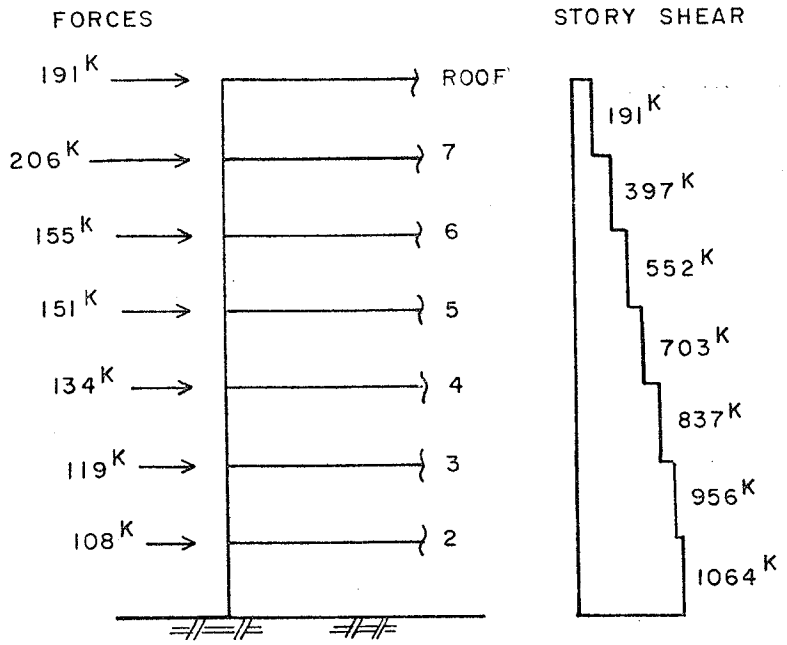

a) 1955 Loads - Entire Building

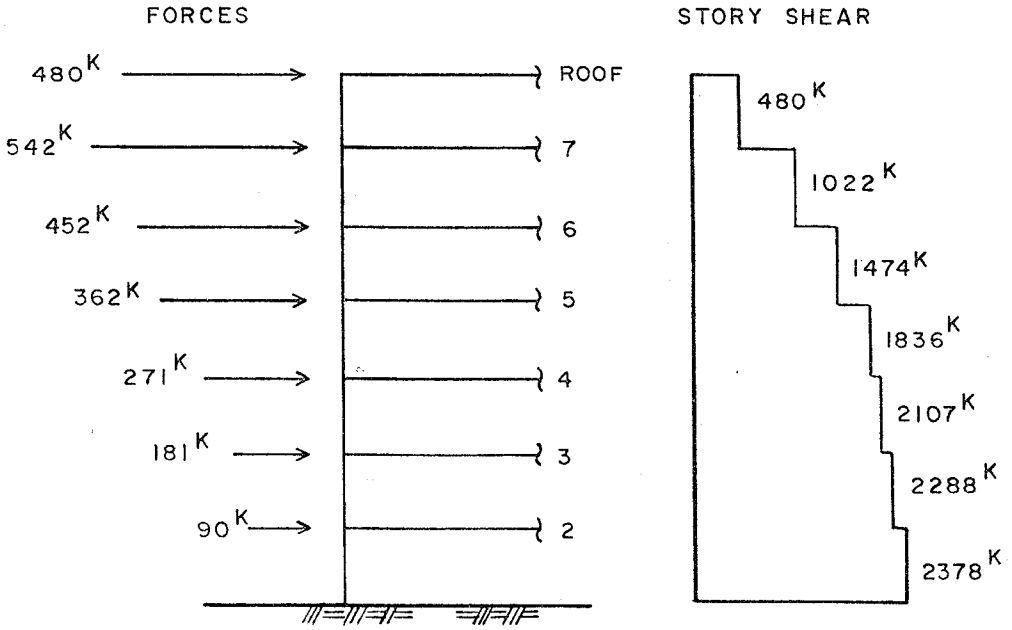

b) 1982 Loads - Entire Building

Fig. 2.3 Comparison of UBC Lateral Earthquake Loads

2.2 Two-Thirds Scale Model

The two-bay, two-story model is shown in Fig. 2.4, with reinforcement details in Fig. 2.5. All prototype dimensions were scaled down by two-thirds, resulting in 12 in. by 12 in. columns and 48 in. by 5-1/3 in. spandrel beams. The reinforcing steel in the columns consisted of six vertical #7 bars and #3 ties at 12 in. The spandrels contained pairs of #4 bars top and bottom, three intermediate rows of #3 bars, and an additional row of #5 or #4 bars to handle negative moment in the region of the columns. Beam stirrups were #3 bars at a 12 in. spacing.

The schematic in Fig. 2.6 shows the boundary conditions of the experimental model. The entire lateral load was applied at the top floor level, and horizontal reactions were provided through the bottom slab. Vertical movement at the spandrel ends (midspan of side frames) was prevented by struts fastened to the floor. The columns rested on neoprene pads on the floor, and tension links prevented uplift. The column axial load from upper floors in the prototype was neglected.

Figure 2.4 shows that a 4 ft width of slab was cast with the spandrel to provide the necessary stiffness to the beam. This also served as a work platform and as a means of applying load to the specimen and providing reactions at the base.

2.3 Concrete Strengthening Scheme

The first seismic strengthening scheme consisted of reinforced concrete piers cast against the existing columns to increase the flexural and shear capacities of the columns. The existing concrete was prepared by sandblasting to roughen the surface, and #4 dowels were epoxy-grouted into the sides of the columns and faces of the spandrels. The 5 ft wide piers are shown in Fig. 2.7.

The purpose of the concrete strengthening scheme was to force the failure mechanism into the beams by increasing the column strength. It was expected that the testing of this specimen would produce flexural hinging in the spandrels but little damage to the original columns. Since the steel strengthening scheme relies on the beams for supporting gravity loads only, it was possible to use the original bare frame for both strengthening methods. Thus, after testing the concrete strengthened frame, the new concrete was removed as will be discussed in detail in Chapter 3. The original, but damaged, specimen was then strengthened with steel bracing. Complete details of the test on the concrete pier strengthened frame are given in Ref. 24.

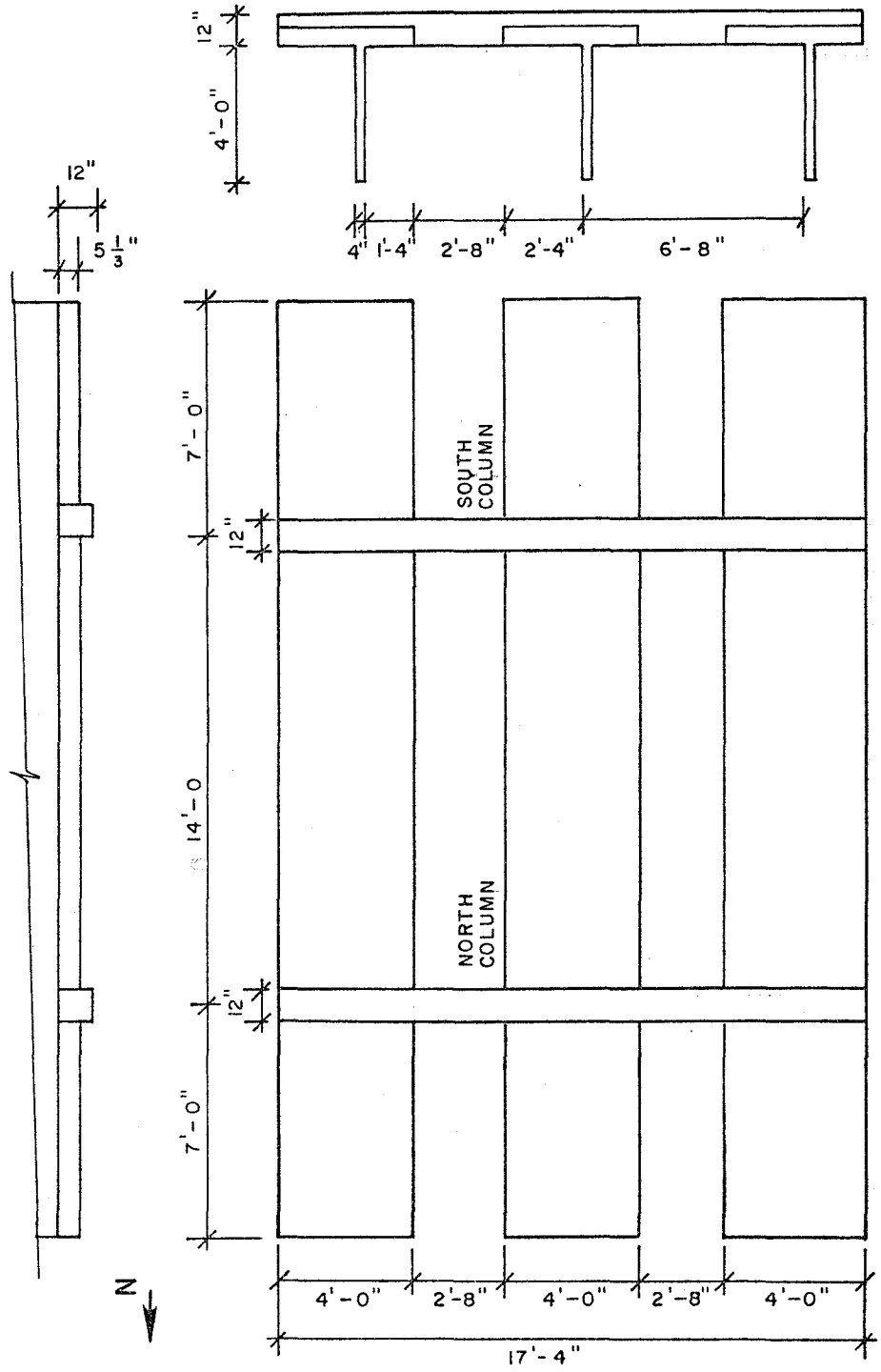

Fig. 2.4 Test specimen dimensions

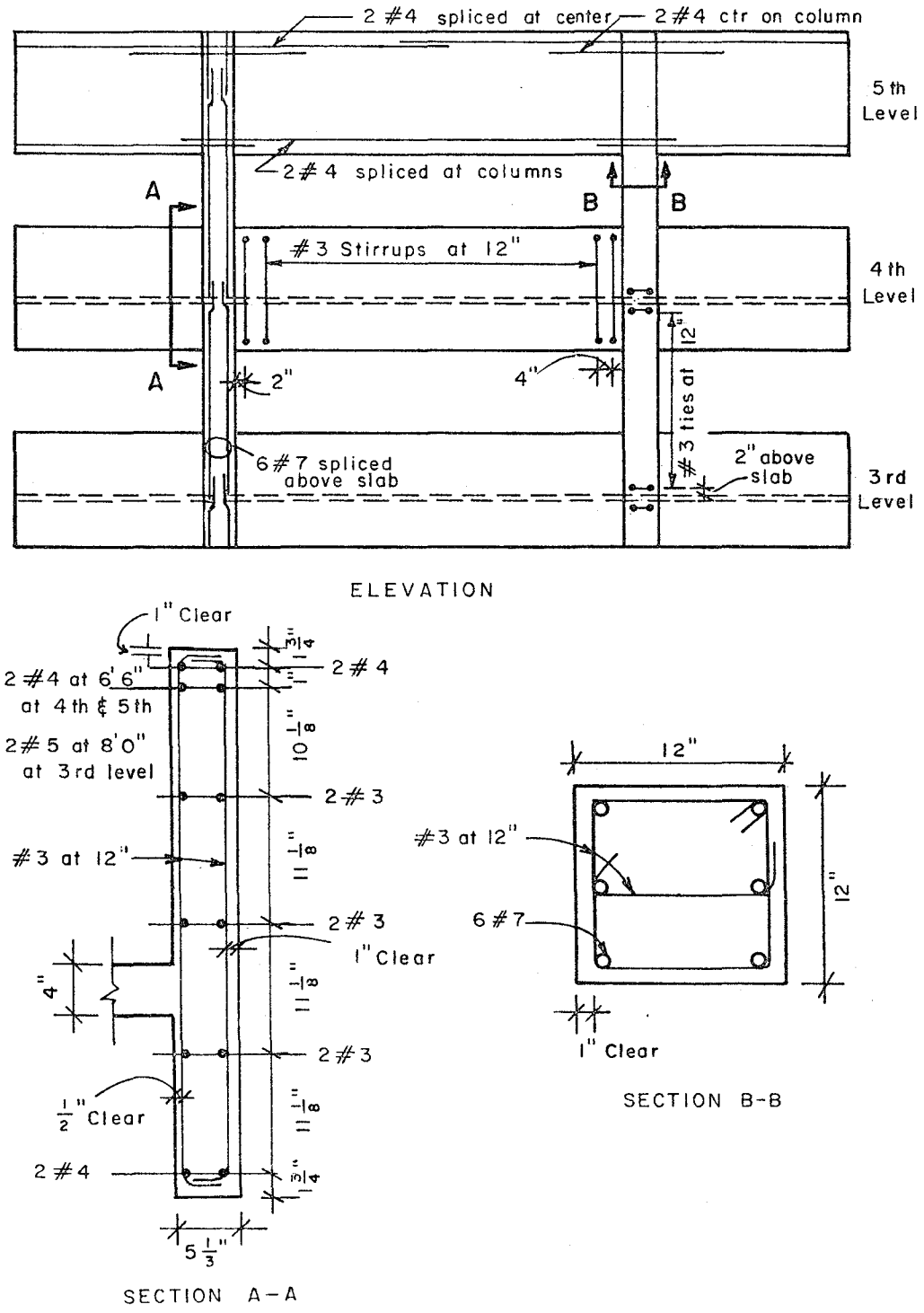

Fig. 2.5 Model reinforcement

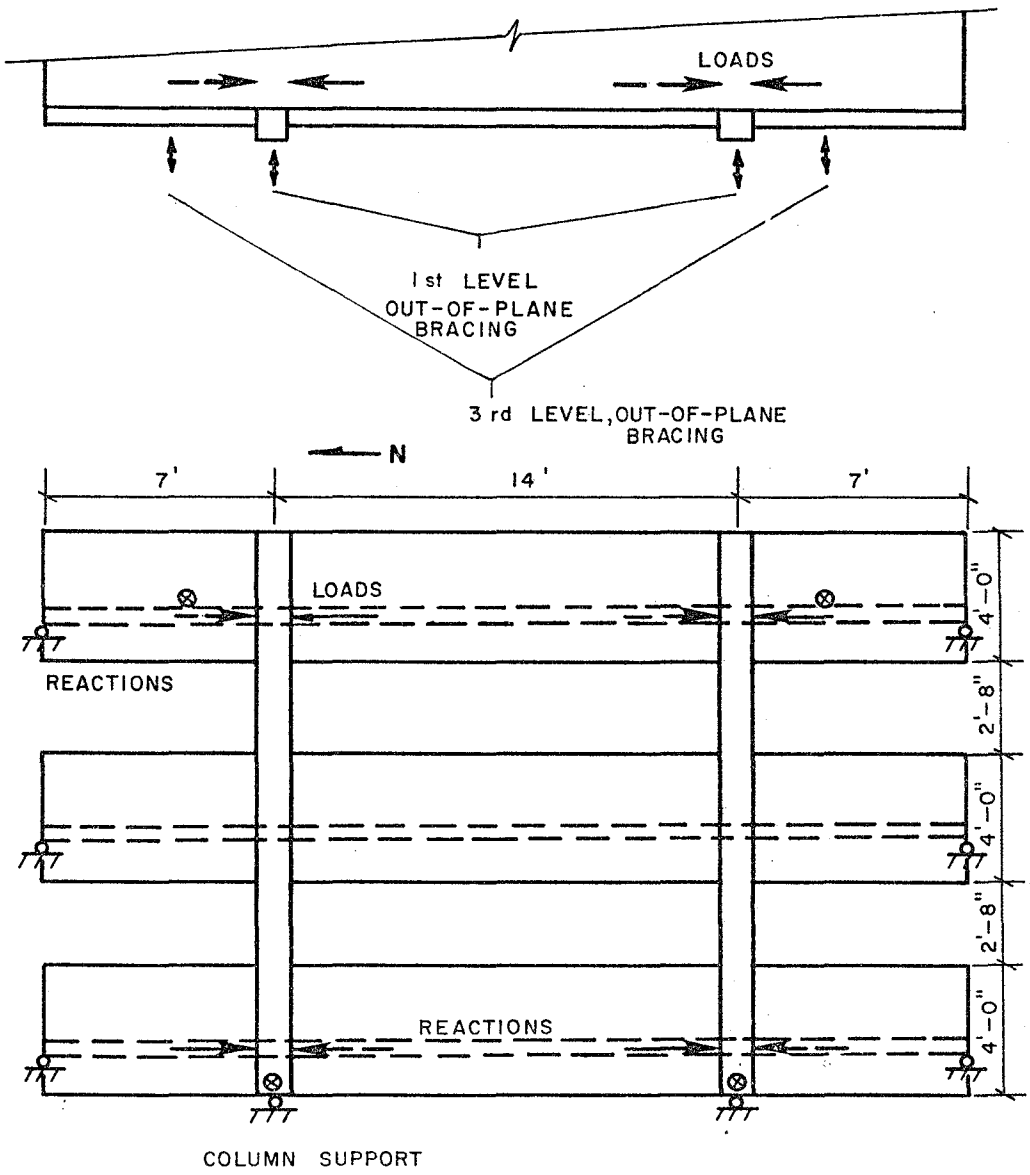

Fig. 2.6 Boundary Conditions of Test Specimen

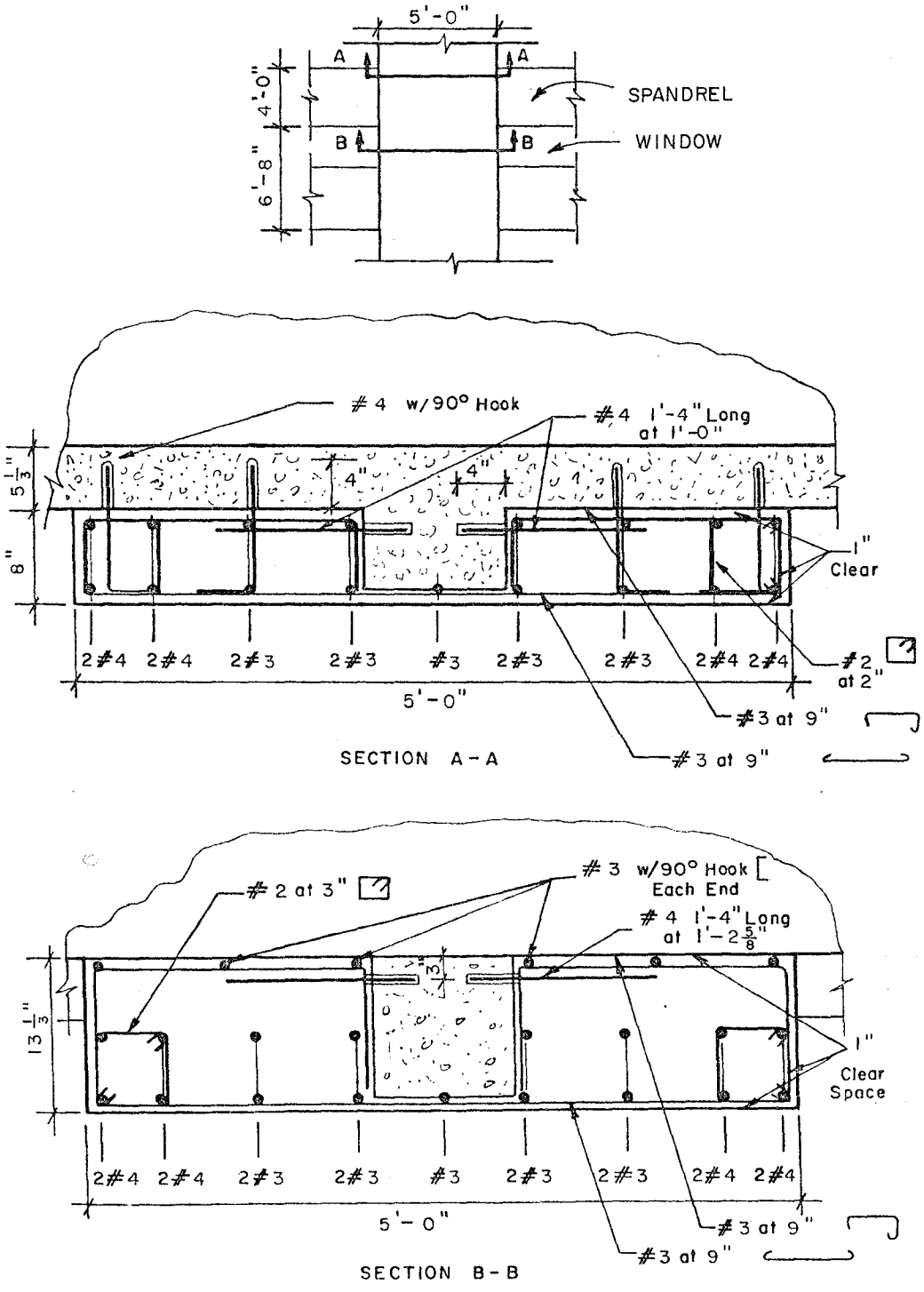

Fig. 2.7 Concrete Strengthening Scheme

2.4 Steel Strengthening Scheme

2.4.1 Overall Scheme. The strengthening scheme which will be discussed in detail here consisted of exposed structural steel diagonal braces designed to carry the entire lateral load. The bracing scheme, shown in Fig. 2.8, was to be used over eight bays of each of the two exterior frames of the prototype building. The number of braced bays was determined by the criterion that there should be no uplift of the columns due to overturning moments.

The existing concrete building must carry the gravity loads and be able to transfer the lateral loads into the exterior steel. The bracing system picks up the lateral load through steel collectors which are attached, with epoxy-grouted threaded bars, to the outside spandrel faces at the floor levels. Steel columns, attached in the same manner to both sides of the concrete column, were designed to carry the forces produced by overturning moments.

2.4.2 Design of Members. The braces were first designed for the full-scale prototype building to carry the entire seismic shear forces at each story. Earthquake loads for a building in seismic zone 4 were computed following the 1982 Uniform Building Code. Wide flange and structural tube members were considered for the braces. Although tubes are regarded as more architecturally attractive, wide flange members were chosen for easier field erection. The lateral load analysis resulted in 8 in. deep steel braces, collectors, and columns for the prototype.

An important consideration in the design of the steel strengthening scheme was that the loading system in the laboratory would be capable of failing the model braces. The maximum test load necessary to produce failure was computed by assuming that all tension braces yield as the compression braces buckle. The resulting horizontal load was added to the shear capacity of the two concrete columns. To ensure that failure would occur before a maximum lateral force of 400 kips (capacity of loading system) was reached, a value of 330 kips was set as the allowable horizontal load computed for the above failure mechanism.

The original 8 in. deep prototype members scaled down to 6 in. deep model members were too strong. Working in the two-thirds scale sizes, braces were designed which were satisfactory for the scaled-down UBC loads and also led to a horizontal failure load of about 330 kips. Reducing the area of the brace

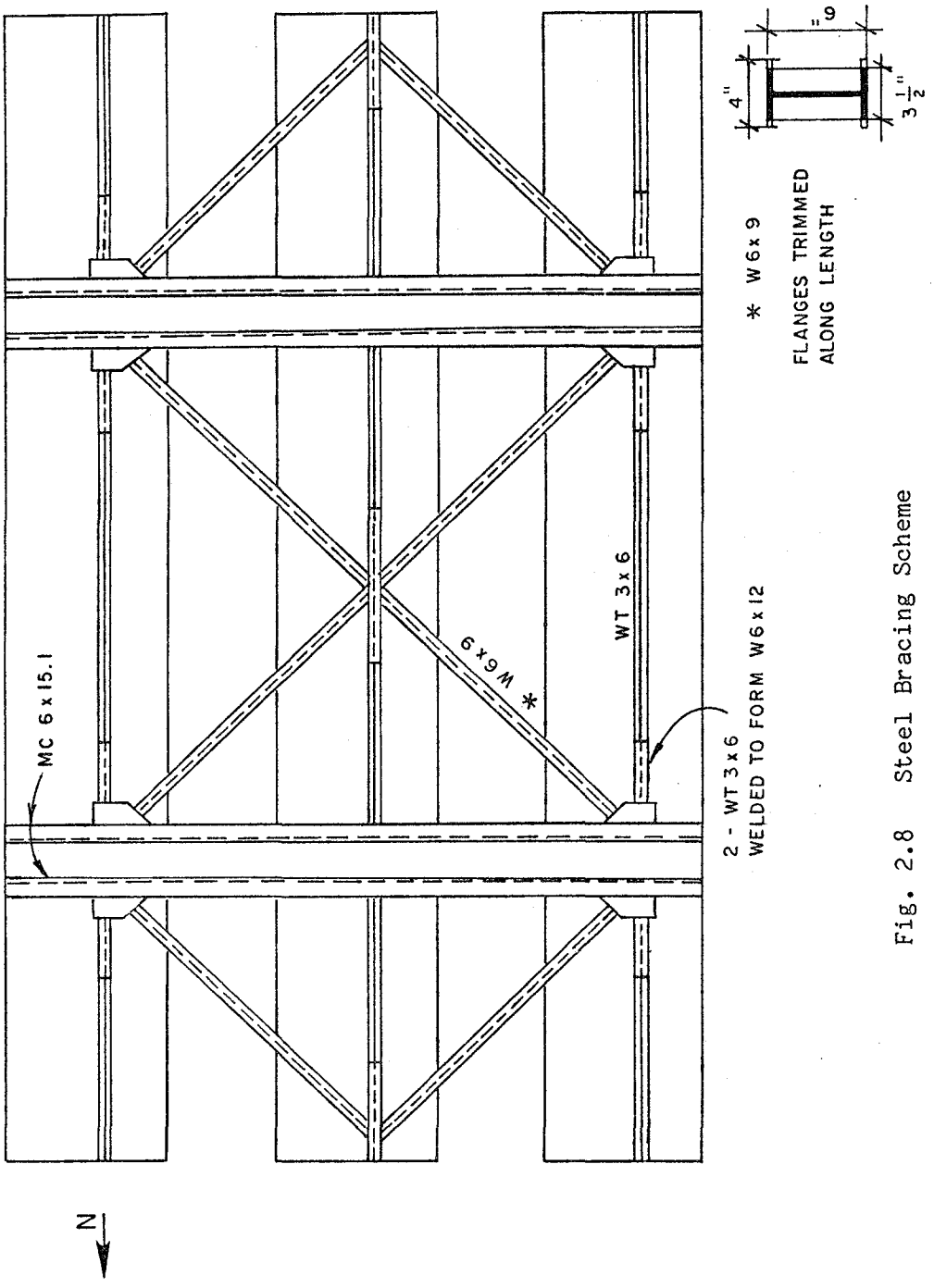

Fig. 2.8 Steel Bracing Scheme

section decreased the tension and compression capacities for the member, but the braces were still too strong. The radius of gyration about the Y-Y axis, r_y, had to be reduced in order to lower the buckling load of the brace. This resulted in fairly large slenderness, or L/r, ratios for the weak axis.

All 5 in. and 6 in. deep standard wide flange sections were too large. Rather than fabricate suitable wide flange sections from rolled plates, a standard W6X9 section was modified by removing the tips of the flanges along the length of the brace resulting in a 3-1/2 in. flange width. This reduced section has an L/r ratio of 140.

For the original prototype bracing system, design requirements were set which included limiting the effective slenderness ratio, KL/r, to 100 and preferably less than 80. The values were chosen in reference to steel strut tests performed at the University of California at Berkeley [16], where eighteen struts with three effective slenderness ratios (40, 80, 120) were tested under reversed cyclic loads. The specimens with lower KL/r values produced "fatter" hysteresis loops, indicating better energy absorption. The struts with an effective slenderness ratio of 120 had steep load-deflection curves which showed substantial deterioration of peak compression loads with each cycle.

For the pure fixed-fixed end condition (K=0.5), the modified W6X9 braces for the model have an effective slenderness ratio of 70; using the design K-factor of 0.65 yields a ratio of 91. Although the L/r ratio of 140 is high, the end restraints yield a reasonable effective slenderness ratio and satisfactory hysteretic performance. In the calculations for the expected peak capacity, it was recognized that Grade 36 steel can have a yield strength as high as 45 ksi. At a yield stress of 45 ksi, the tension capacity of one brace is 109 kips, and, with a K-factor of 0.5, the buckling load of one brace is 88 kips. Adding the horizontal components of the loads in two tension braces and two compression braces to the shear capacity of two concrete columns (63 kips) yields a lateral failure load of 338 kips. It must be noted that this estimate neglects the shear strength of the steel columns and their interaction with the concrete columns.

The steel columns and collectors in the model were each designed following two criteria. First, they had to be able to carry the forces which would be produced by the model braces at their ultimate capacity. Second, they were checked under allowable stress design using scaled-down loads from the UBC.

For example, in the prototype design the collectors would be designed to transfer the UBC lateral load at each floor level to the bracing system. For the test specimen, the collectors at one level of the model had to be able to transfer the full failure load of 338 kips. The resulting members were a structural tee, WT3X6, for the collectors and a channel, MC6X15.1, for the steel columns. Additional tee sections were field welded to the collector tees to form W6X12 wide flange sections in the brace connection regions. It was desirable to keep all members 6 in. deep to allow for simple, concentric connections.

2.4.3 Connections. Typical connections are shown in Figs. 2.9 and 2.10. The gusset plates were shop-welded to the collectors and columns, and the braces were attached on site using erection bolts and plates. Brace flanges were then field-welded to either the 1/2 in. gusset plates (Fig. 2.9) or to the flanges of the tees (Fig. 2.10). Webs were made continuous through the connection by butt-welding the web ends to 1/4 in. gusset plates inside the channels and tees.

Sizing and spacing of dowels were based on Wiener's [17] results from shear tests between steel channels and concrete blocks. Standard threaded rods, 5/8 in. in diameter and with an ultimate capacity of 11.5 kips per dowel, were used to attach the steel columns and collectors to the concrete frame. The dowels into the column were 8 in. apart and embedded 5-1/2 in., as shown in Fig. 2.11. Dowels in the collectors were on an 18 in. spacing and 4-1/2 in. embedment.

In an actual building, the floor slab transfers a portion of lateral load into the steel system at each level through the collectors. In the test specimen, all the load was applied at the third level of the model, so additional dowels were required to transfer load. The same was true at the first level of the model where the entire load was transferred to the reactions. Therefore, the dowel spacing at the first and third levels of the specimen was 9 in.

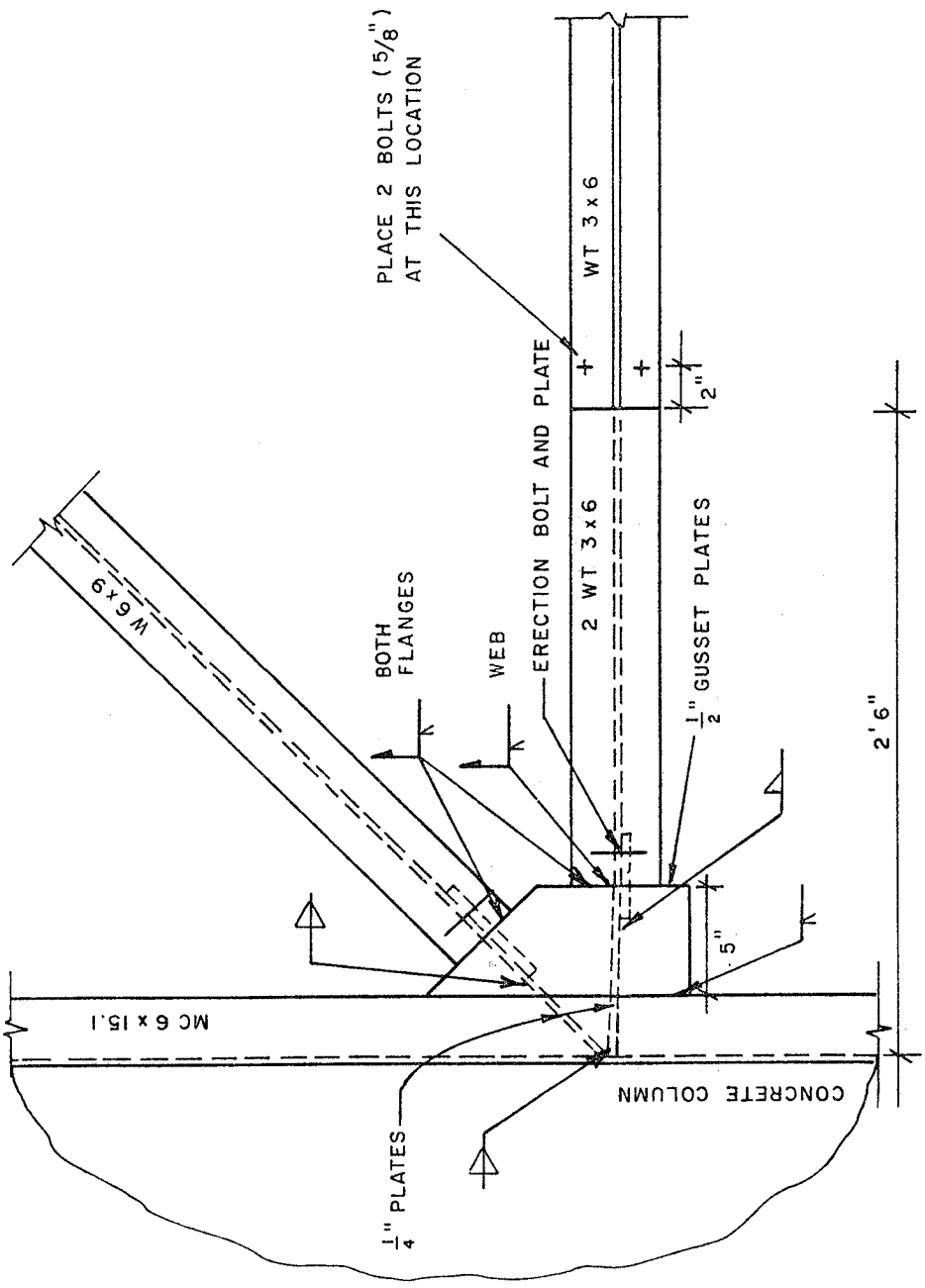

Fig. 2.9 Brace-to-Channel Connection

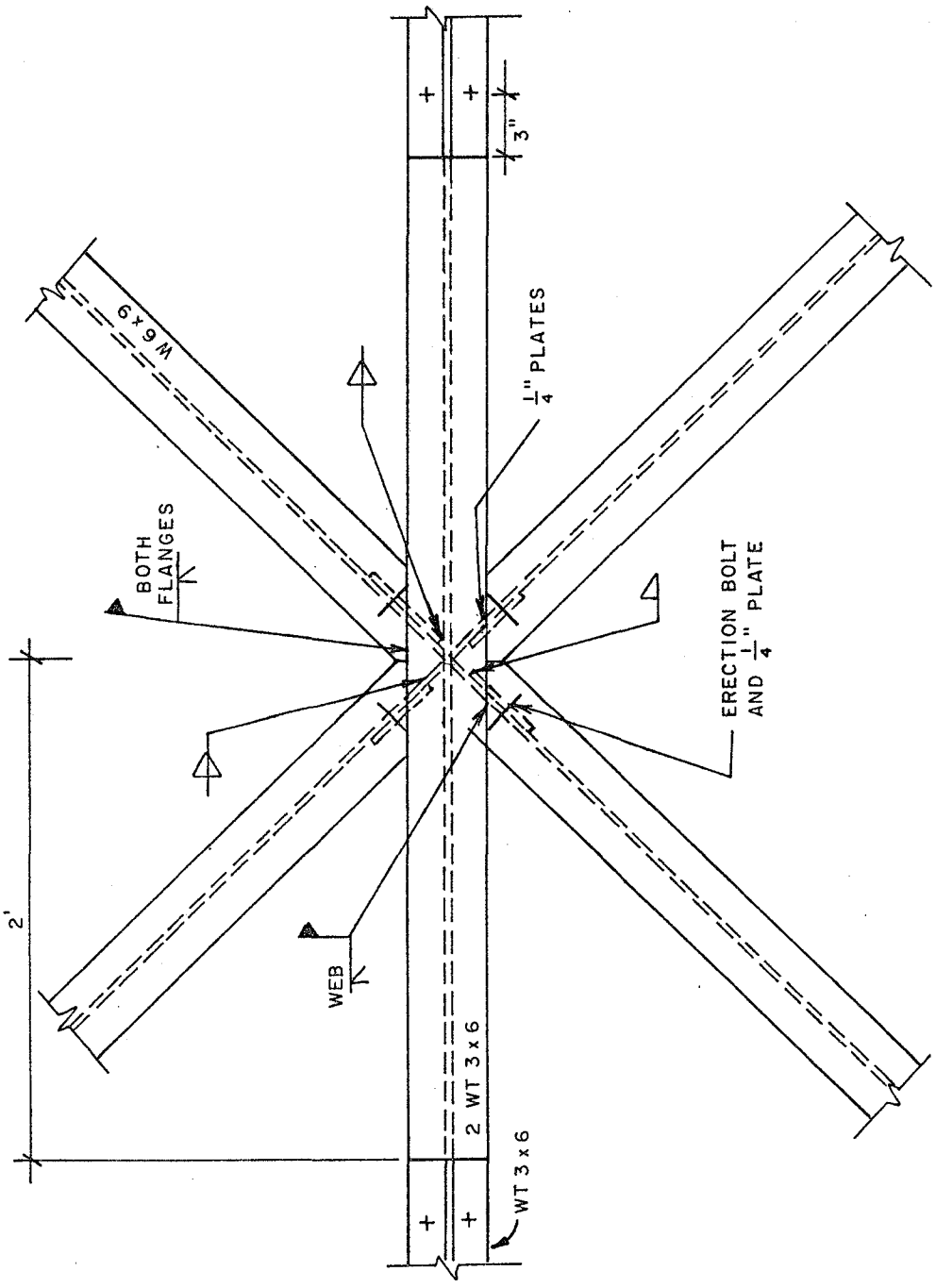

Fig. 2.10 Brace-to-Collector Connection

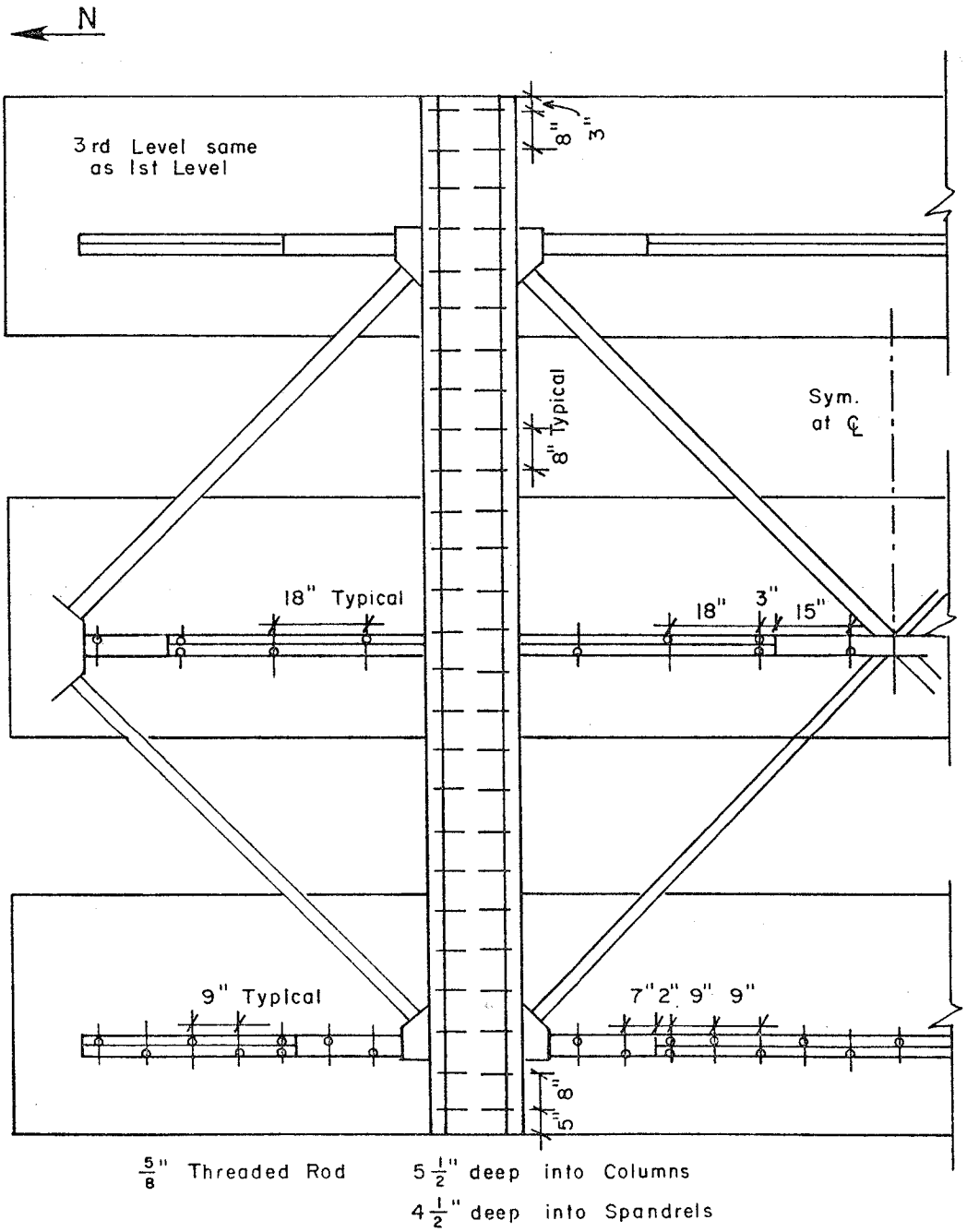

Fig. 2.11 Dowel Layout

CHAPTER 3

EXPERIMENTAL PROGRAM

3.1 Construction of Original Frame

3.1.1 Procedure. The construction of the bare frame was carried out in six stages as seen in Fig. 3.1. The bottom of each spandrel up to the top of the floor slab was cast in one stage, while the upper portion of each spandrel and the columns above (up to the next spandrel) were cast in the next stage. Formwork for the exterior of the spandrels was continuous over the full 4 ft height; therefore, forms for the lower portions of the spandrels and the slab were left in place when the upper portions of the spandrels were cast. After the second and fourth casts, forms were stripped, cleaned and erected for the next levels.

Figures 3.2 through 3.7 are photographs of the construction procedure. The slab and inside spandrel forms for the first level are shown in Fig. 3.2. These forms are in six units to allow for easier removal and for differences in slab depth described later in this chapter. Each unit consisted of the slab formwork supported by shoring and forms for the lower inside face of the spandrel, which rested on a base 4-1/4 in. above the lab floor. Neoprene pads formed the base of the columns.

The spandrel reinforcement cages were set in place on the base in two halves and spliced in the middle. The forms for the exterior of the spandrels (in four units) were set on the base, and the thickness of the spandrel was achieved using formties. The column bars (extending 18 in. above the slab) and ties were threaded into position, and the exterior column form was placed on the base. The formwork for the exterior face of the columns was bolted to the spandrel forms and extended to the bottom of the next spandrel beam. The slab steel reinforcement was placed, and the first level was cast up to the top of the slab.

For the next stage, the column exterior forms were removed to allow for the column cages to be fabricated. The vertical bars were spliced just above the slab at each level. The forms for the inside face of the spandrel were set on the concrete slab and held at the correct distance from the exterior forms with formties. Figure 3.3 shows the spandrel forms and

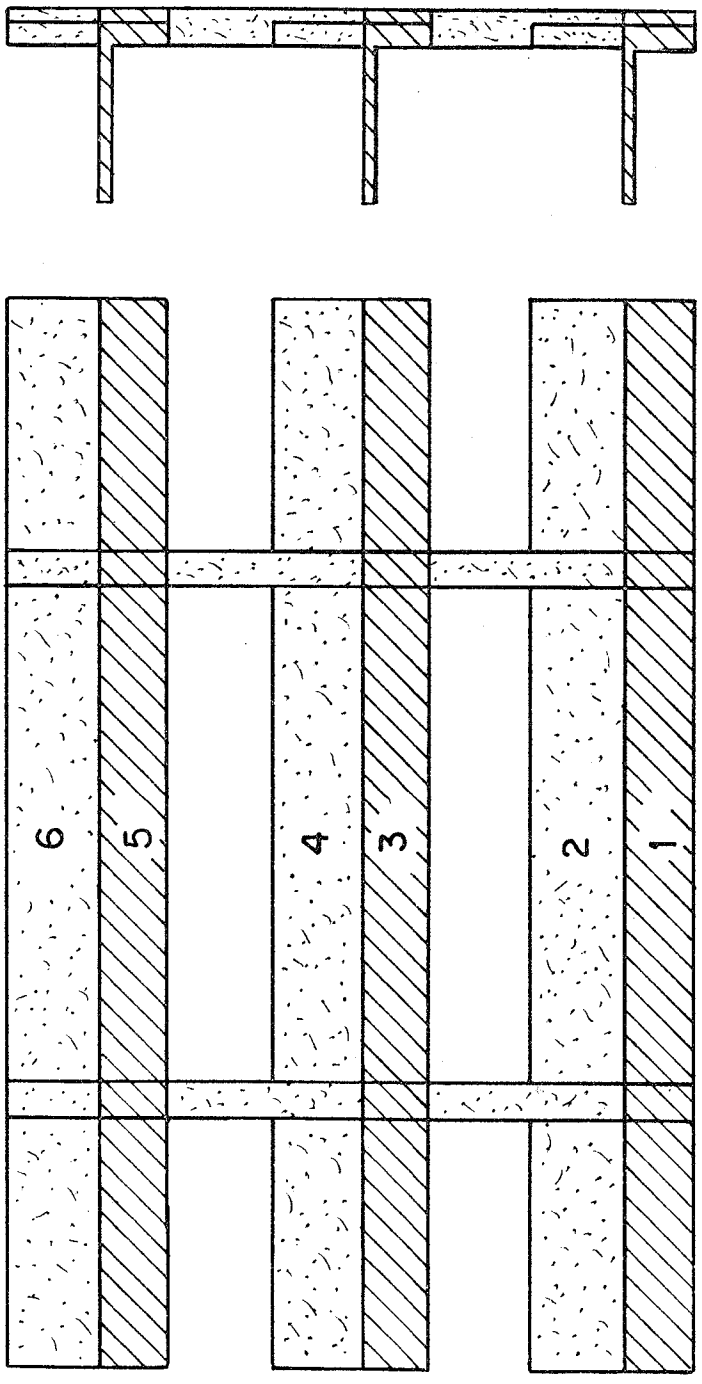

Fig. 3.1 Casting Stages

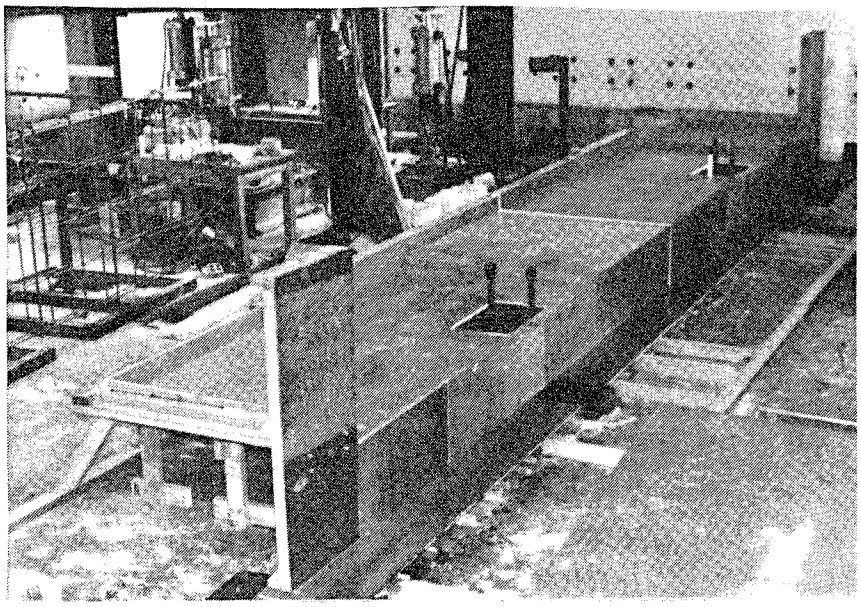

Fig. 3.2 Slab forms at first level

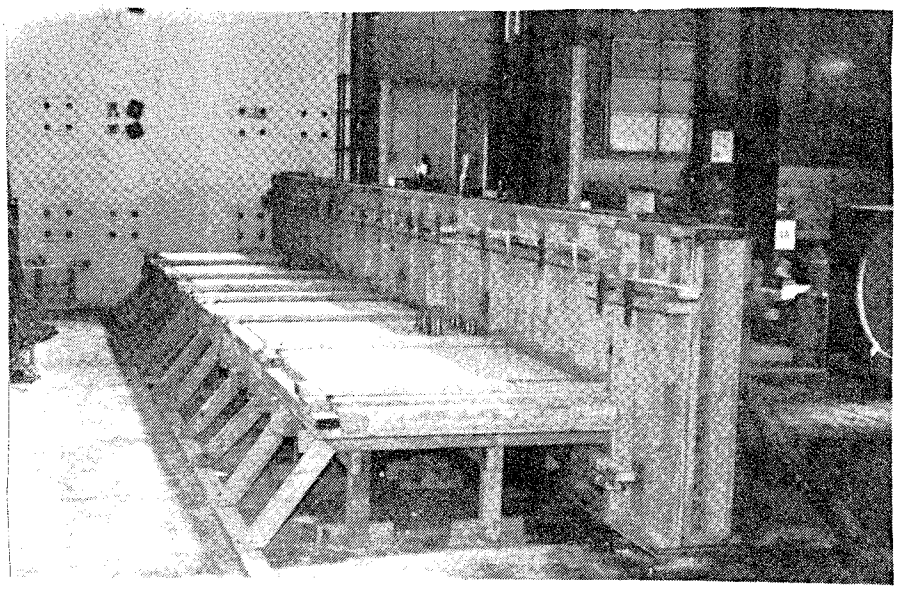

Fig. 3.3 Spandrel forms in place for second cast

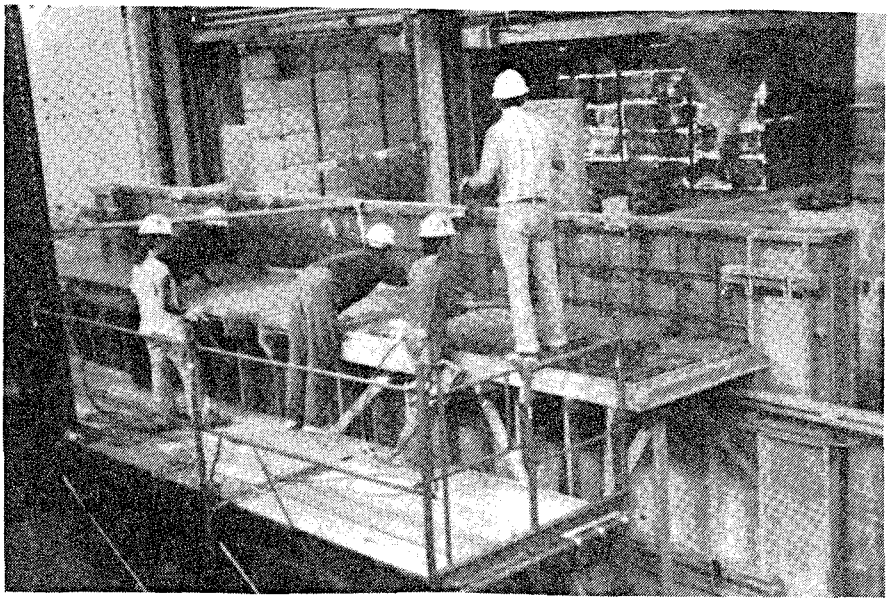

Fig. 3.4 Casting and screeding second level slab

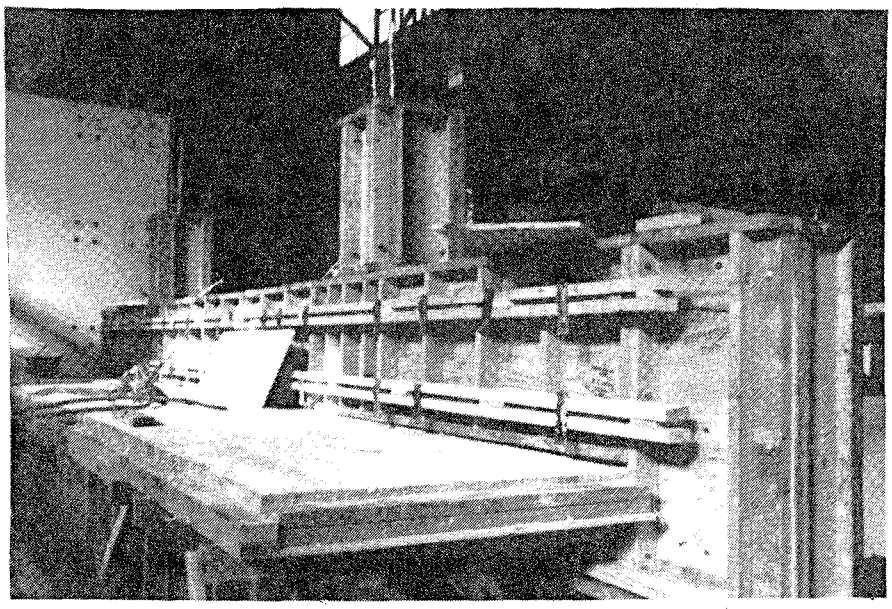

Fig. 3.5 Forms in place for fourth stage
(second level spandrel and columns)

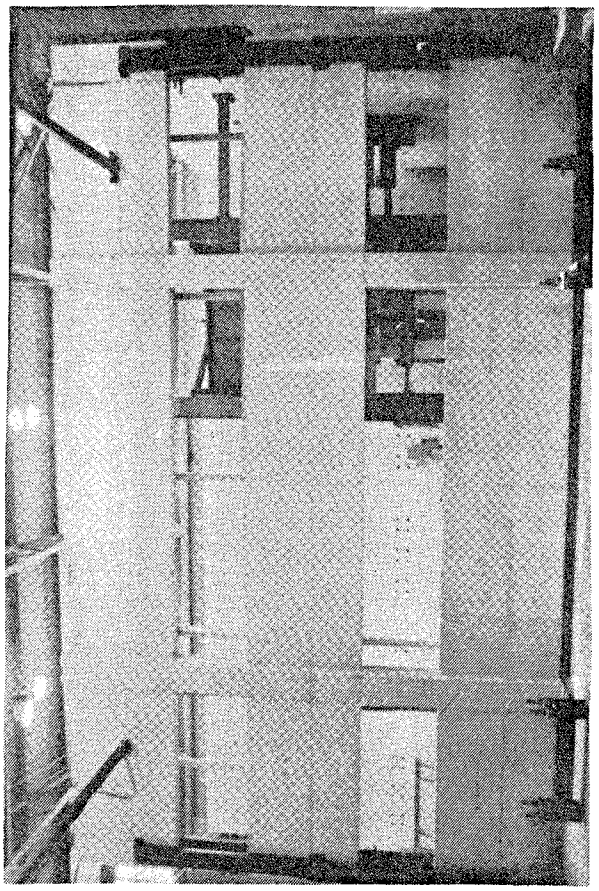

Fig. 3.7 Bare frame

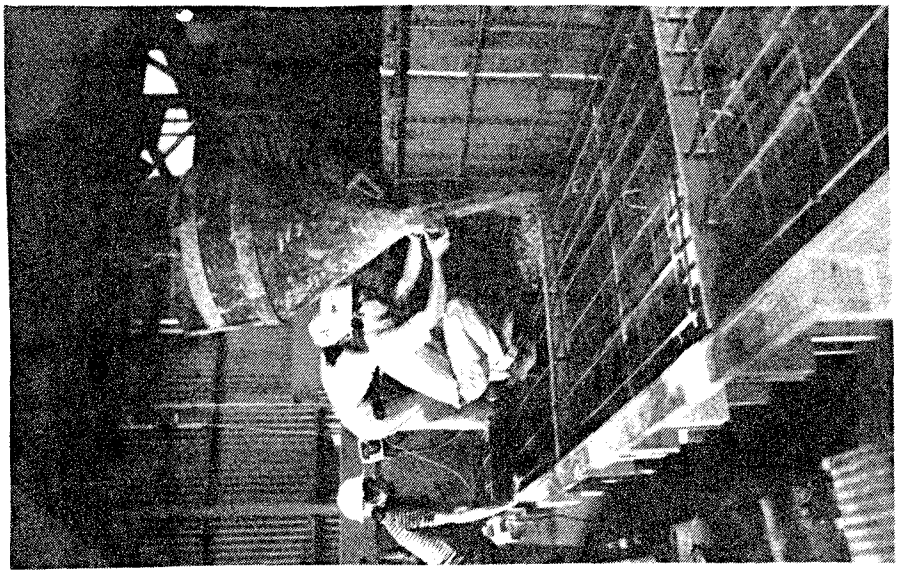

Fig. 3.6 Casting third level slab

column cages in position. The remaining column forms were assembled, and the second stage was cast.

All formwork was removed after the second stage was cast and used again for the second and third stories. Slabs were reshored with 2X4 studs at approximately 2 ft.

The construction of the upper stories proceeded in the same manner with only a few modifications. The base of the second and third level spandrels rested on large forms which were attached to the spandrels below utilizing the extruding formties. Figure 3.4 shows the spandrel forms for the third stage supported from below. The spandrel reinforcing cages had to be lowered into position over the column steel extending from the level below. Figure 3.5 shows the spandrel and column forms in place for the fourth stage, while Fig. 3.6 shows the placement of concrete for the lower spandrel at the third level.

The completed concrete frame may be seen in Fig. 3.7. After construction was finished, two 4X4 shores were placed at each level, and all other shores were removed. In addition, a wooden safety railing was installed at the second and third level floor slabs.

3.1.2 Material Strengths. Table 3.1 shows the concrete mix proportions used to reach the specified compressive strength of 3000 psi. The concrete strength was determined following ASTM C39-72 "Compressive Strength of Cylindrical Concrete Specimens" [18]. Table 3.2 shows the average concrete compressive strength (three 6x12 cylinders) for each casting stage at 28 days and at the time of testing the steel braced frame.

Mill reports were supplied for the reinforcing steel showing the average yield strengths. The Grade 60 #7 bars in the columns came from a heat with an average yield strength of 65 ksi. The #3, #4, and #5 bars, specified as Grade 40, actually had average yield strengths ranging from 57 ksi to 66 ksi.

3.2 Loading System

3.2.1 Modifications to Concrete Frame. The points of load application and vertical and horizontal restraint were seen in Fig. 2.6. Several modifications to the test specimen's dimensions were made to facilitate application of these loads and restraints. The alterations to the prototype frame may be seen in Fig. 3.8.

TABLE 3.1 Concrete Mix Proportions

Component	Quantity per Cubic Yard
Cement (Type I)	423 lbs
Gravel (maximum aggregate size = 3/4")	1735 lbs
Sand	1360 lbs
Water	30 gals
Water-Reducing Admixture	13 ozs
Air-Entraining Admixture	3 ozs

TABLE 3.2 Concrete Strength
(Avg of 3 cylinders)

Casting Stage	f'_c - 28 days (psi)	f'_c - time of test (psi)
1	4100	3930**
2	4560	4730
3	4350	4630
4	3730	4360
5	2580	3010
6	5450*	5790

*at 47 days
**Avg. of 2 cylinders

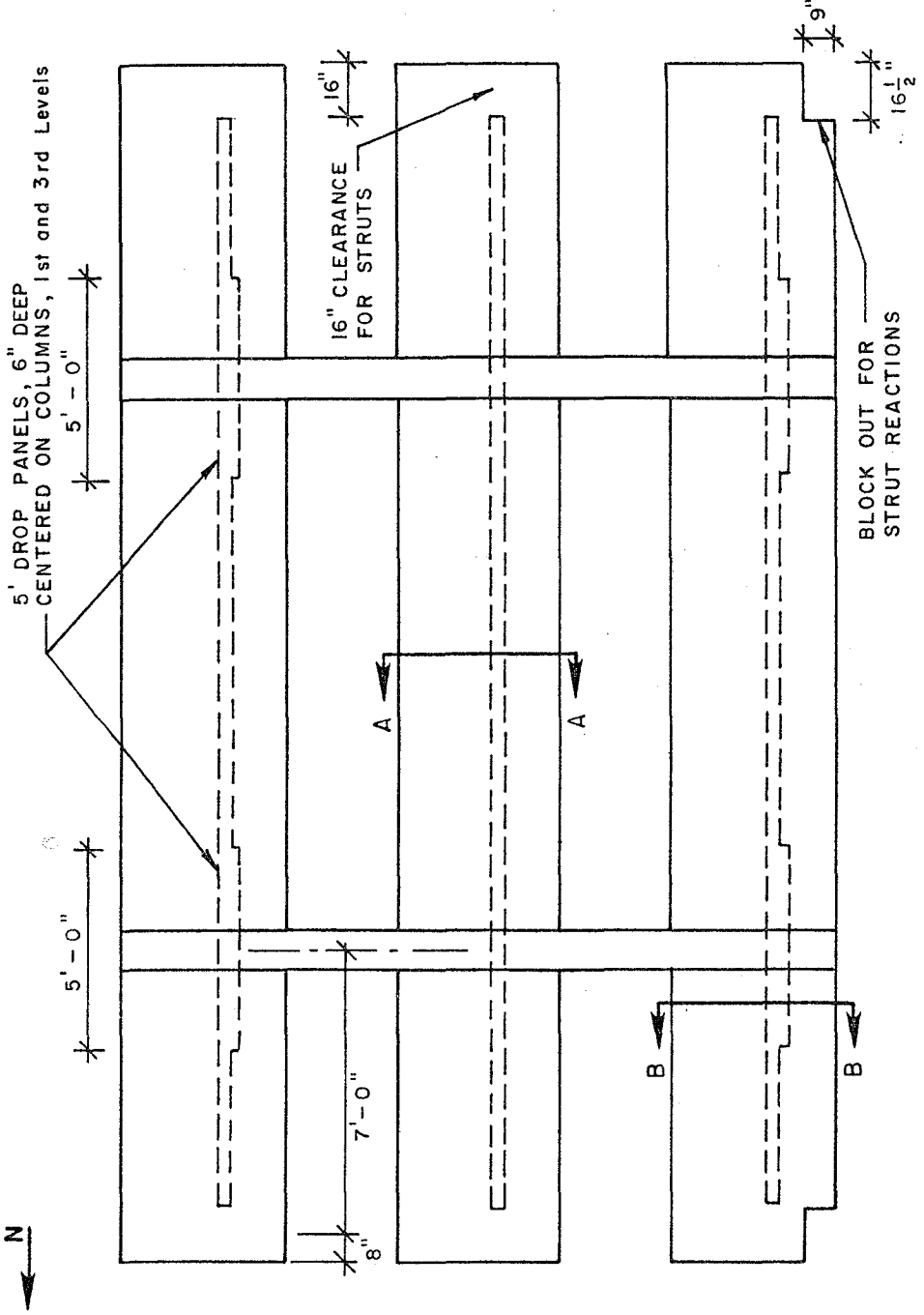

Fig. 3.8 Modifications to frame for loading

Several changes were made to accommodate the vertical struts at the ends of the spandrels. The length of the frame was increased at each end by 8 in. to allow vertical restraints to be located at what would be the center of the side spans. The floor slab was terminated 16 in. short of the spandrel end at all levels to allow space for the vertical strut members. The bottom corners of the first level spandrel were blocked out to leave clearance for the base fixtures of the struts.

To provide sufficient shear and bearing at the points of application and horizontal restraint in the floor slab, the slab thickness was increased in the regions around the columns at the first and third levels. The 5 ft wide drop panels were 6 in. deep as Fig. 3.8 shows. In addition, more slab reinforcement was placed in the drop panels, as indicated in Fig. 3.9. Typical slab reinforcement in the short direction consisted of #3's at 8 in. with 90 degree hooks into the spandrel, and, in the long direction, #3 bars on 4 in. centers near the spandrel and 8 in. centers elsewhere. For the drop panels, the spacing of the #3 bars with hooks was decreased to 4 in. The two layers of longitudinal #3 bars passed through the drop panel except for the three bars closest to the spandrel. These top bars were spliced to three #6 bars within the drop panel. Three #6 bars formed the bottom layer of reinforcement in the drop panel near the spandrel; #3 bars with 90 degree hooks on the ends were arranged throughout the remainder of the drop panel.

In addition to the steel reinforcement, structural steel members were placed within the column slab joint. Because the centerline of the forces and reactions was 15-1/2 in. from the center of the columns, structural steel was required to carry the torsion produced by the eccentricity of the load and to stiffen the connection. A 6X6X1/2 structural tube, 19 in. long, was embedded in the concrete slab perpendicular to the column and passed about 4 in. into the column, as shown in Fig. 3.10. An 8X18.75 channel section, 28 in. in length, was welded to the tube and was oriented vertically in the column. Holes were drilled in the tubes, through which the #6 reinforcing bars could pass. The #3 bars were butted against the tube.

3.2.2 Application of Load. Figures 3.11 through 3.15 show the loading frame on the third level and the connection to the lab reaction wall. The orientation of the test specimen with respect to the reaction wall is seen in Fig. 3.11. Schematics in Figs. 3.12 and 3.13 and the photo in Fig. 3.14 show the loading frame, which consists of two 6X4 structural tubes connected by 6X6 tubes. The centerhole rams, each with a capacity of about 200 kips and 10 in. travel, are arranged so that two rams apply

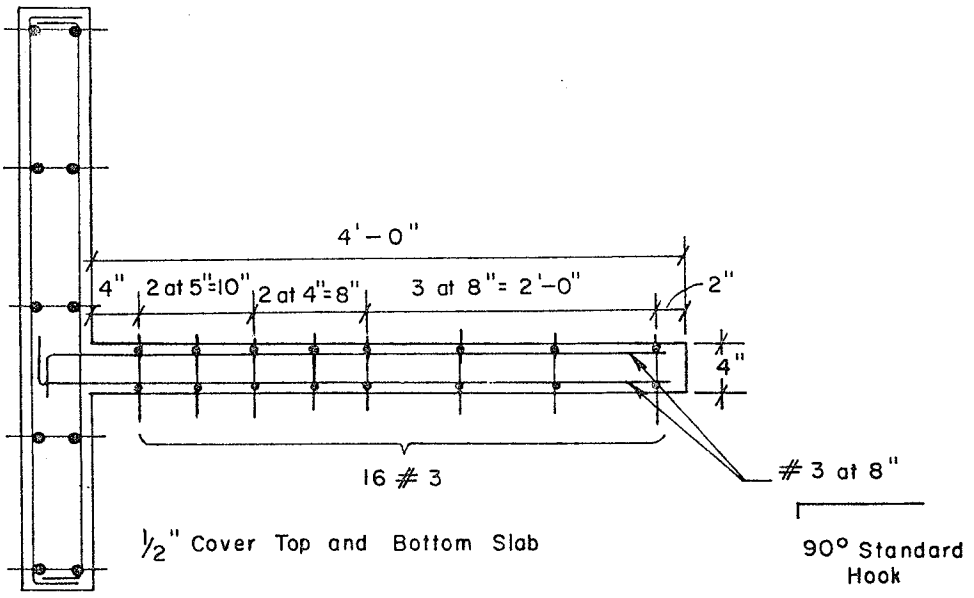

SECTION A-A

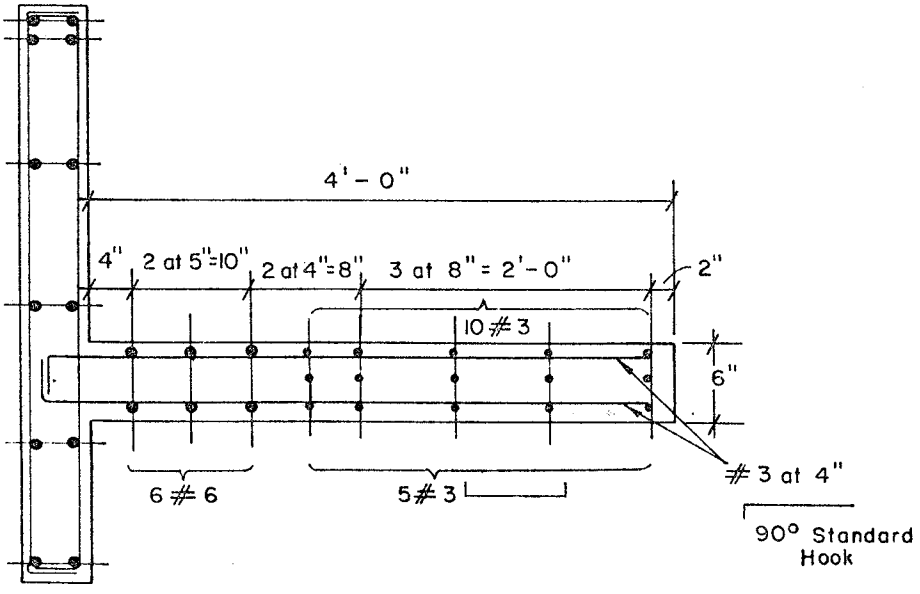

SECTION B - B

Fig. 3.9 Slab Reinforcement

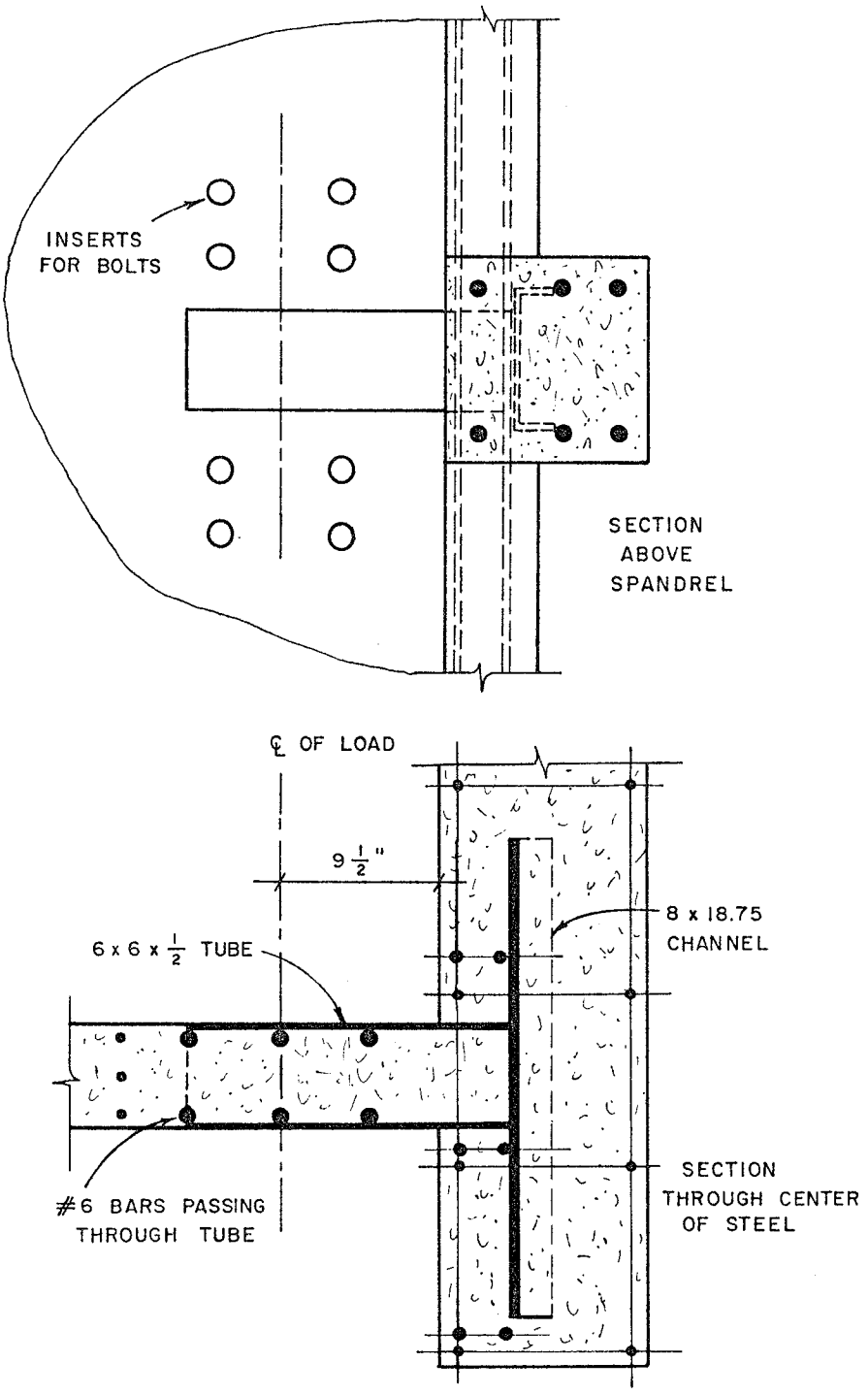

Fig. 3.10 Structural Steel in Column-Slab Joint

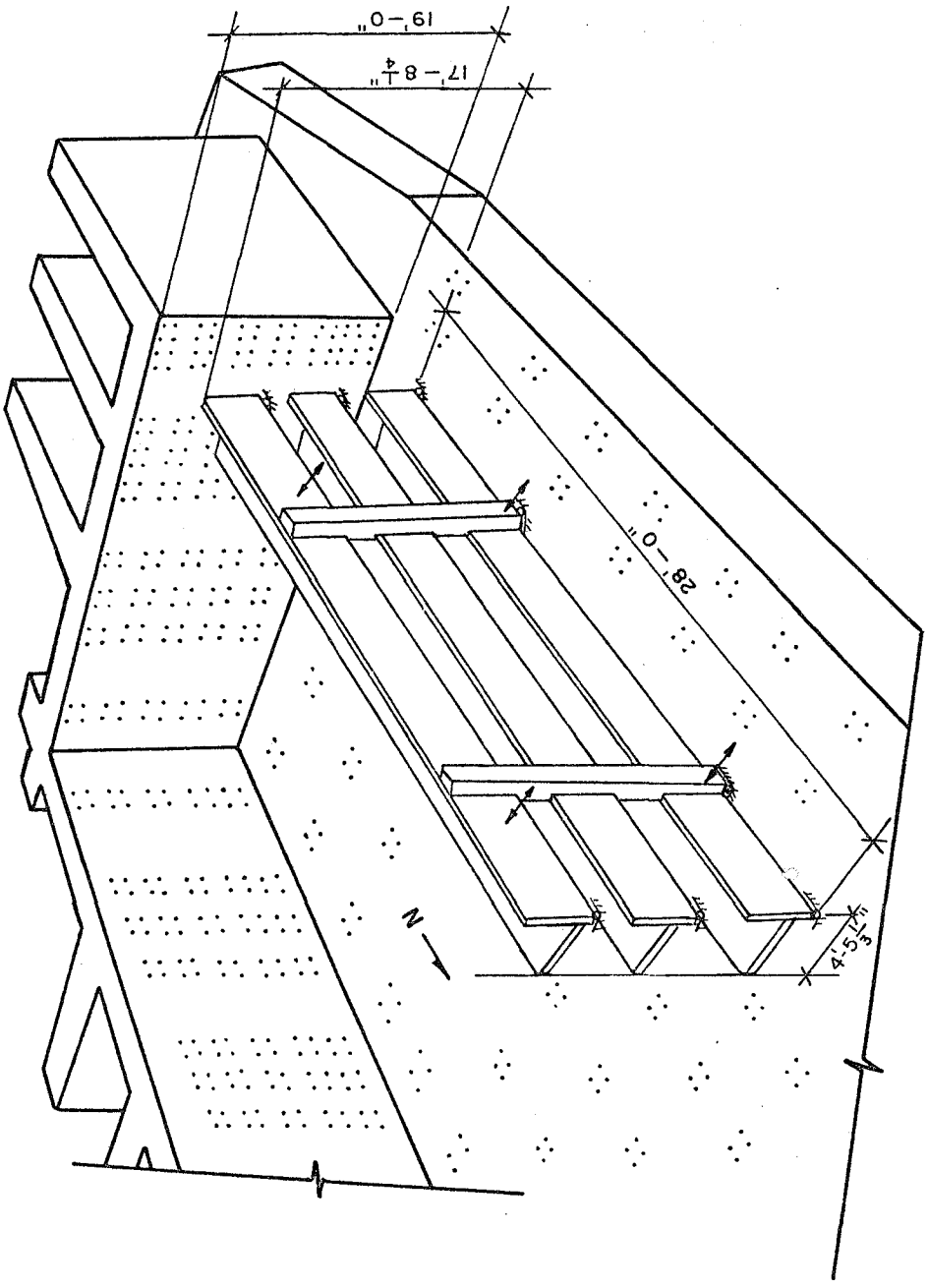

Fig. 3.11 Orientation of Specimen to Reaction Wall

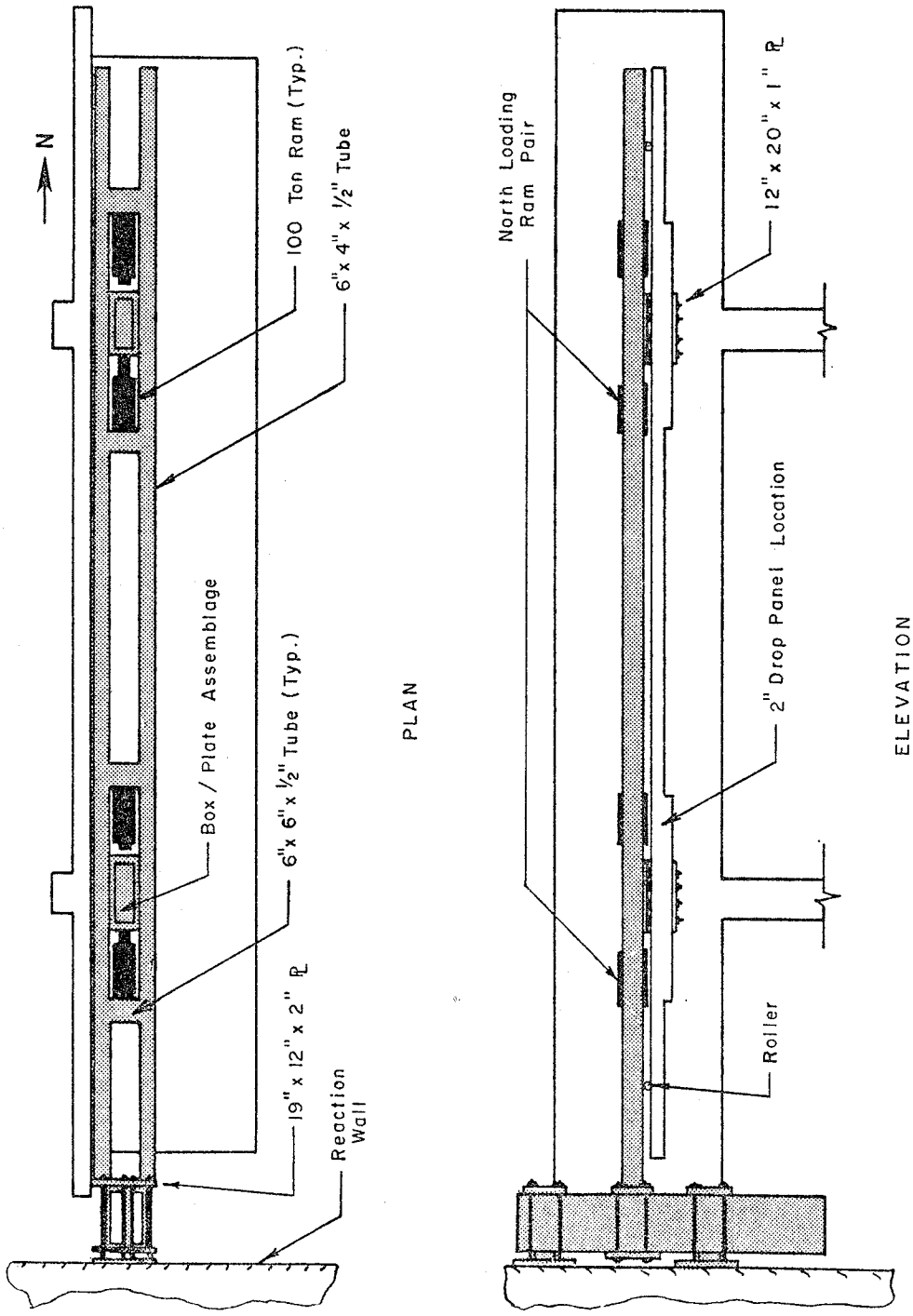

Fig. 3.12 Loading frame

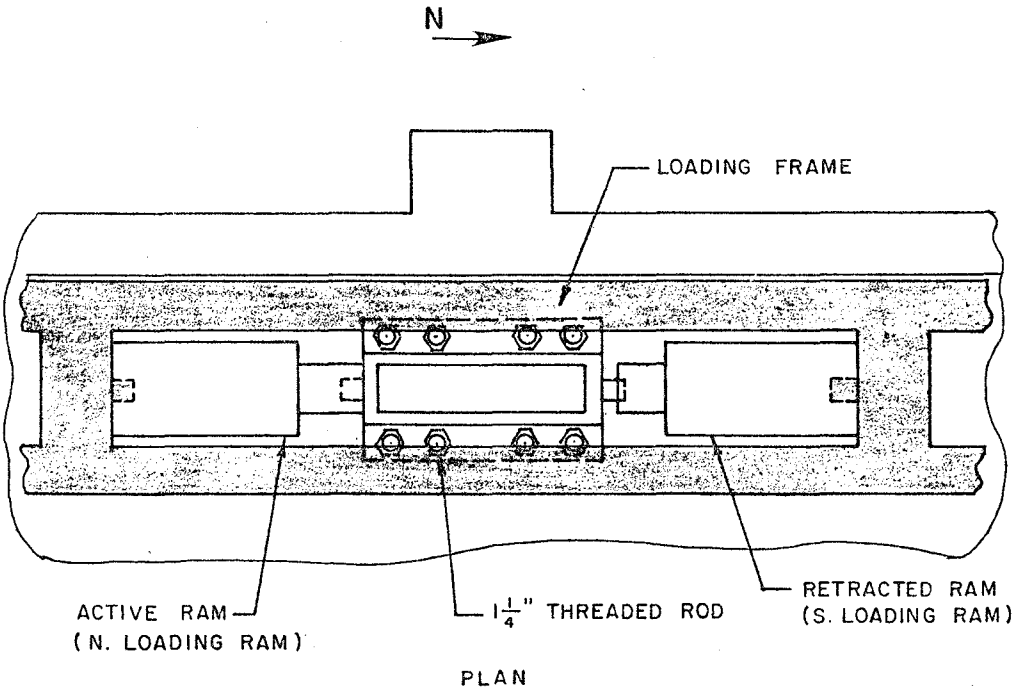

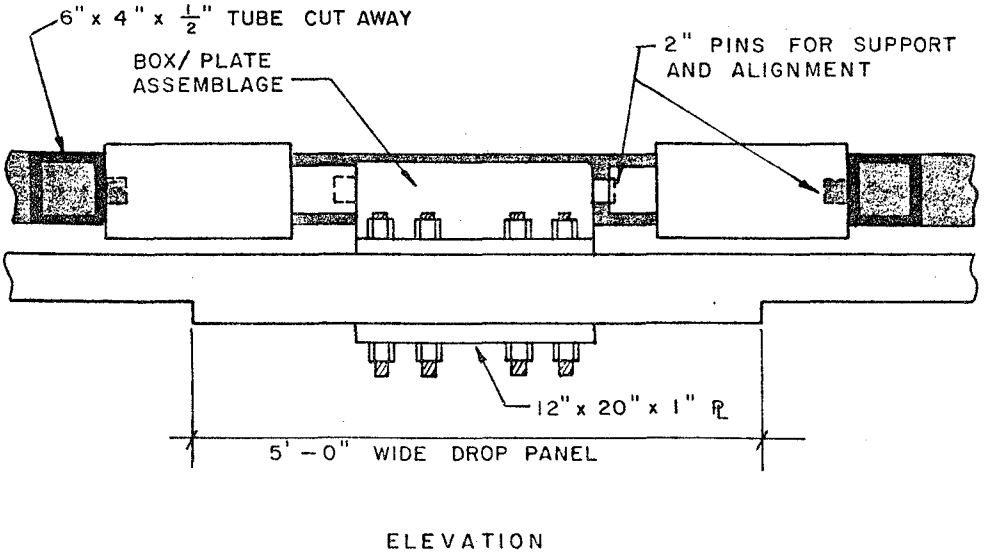

Fig. 3.13 Close-up of Loading Frame at Column

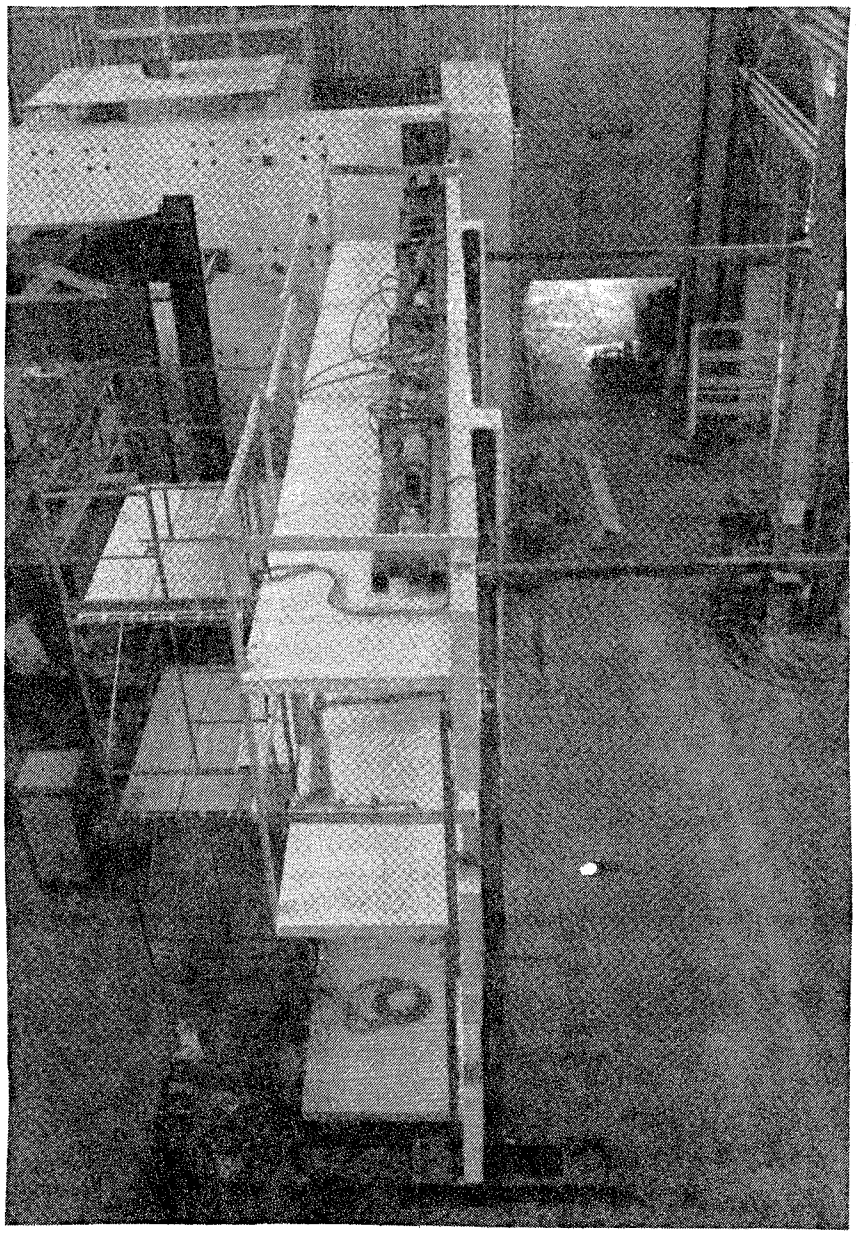

Fig. 3.14 Loading frame at third level slab

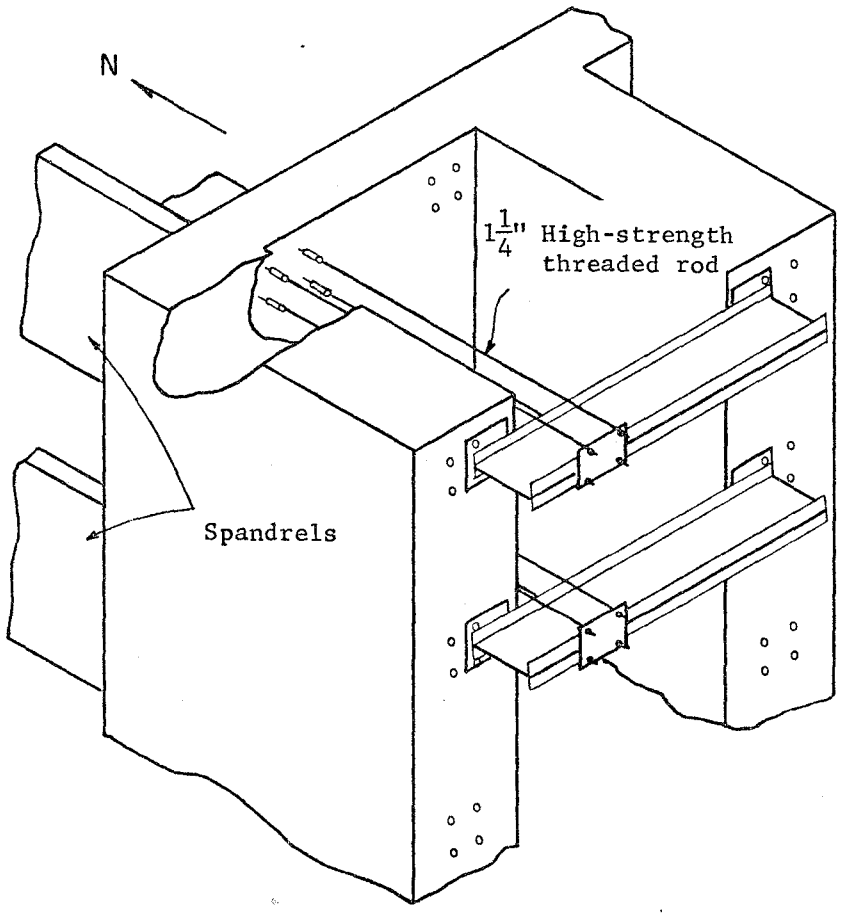

Fig. 3.15 Loading Frame Tension Tie Connection to Reaction Wall

load in the north direction (one at each column), and the other two rams in the south direction.

Load was transferred to the slab through a 1-1/4 in. steel plate grouted to the concrete and held by eight 1-1/4 in. high-strength bolts. Each bolt was stressed to 90 kips to develop sufficient friction between the steel plates and concrete floor slab. A Grade 50 steel box section was welded to each 1-1/4 in. plate, and the rams acted against the box. Figure 3.13 shows the arrangement of plates, rams, and bolts.

The rams were placed in the spaces between the 6X6 tube and the box/plate assembly. Pins welded to the box and tube held the centerhole rams at the correct height and prevented them from slipping during testing. Hydraulic lines ran from the rams to a manifold where the loading directions were controlled by hand operated valves.

The two 6X4 tubes on the third level framed into a pair of 18 in. deep channels fastened to the reaction wall. When the specimen was loaded north, the force was transferred to the wall by bearing. For load in the south direction, eight high-strength threaded rods carried the reaction to the rear of the buttress where the force was applied through bearing to the surface of the buttress. Figure 3.15 shows the tension ties passing through the reaction wall to the rear of the buttresses.

3.2.3 Base Reactions. At the first level, the details at the reaction points were very similar to the loading points at the third level. Two plates were clamped to the slab with eight bolts stressed to 90 kips each. The bottom 1-1/4 in. plates were actually tee sections fabricated of Grade 50 steel with a 2 in. pin passing through each tee.

Figure 3.16 shows the two links (5-1/4 in. by 1-1/2 in. Grade 50 steel bars) pin-connected to the tee and to two C15X40 channels anchored to the reaction floor. The links were instrumented to permit measurement of the reactions. The links prevented development of vertical reactions at the reaction points. The channels were grouted to the floor for a better friction surface, and eight bolts at each column were stressed to 50 kips each in order to transfer the load to the lab floor through friction.

3.2.4 Vertical Reactions. Vertical movements at the spandrel ends were restrained by structural steel struts fastened to the reaction floor. The struts for the bare frame and concrete strengthening tests are shown in Fig. 3.17. Eight inch

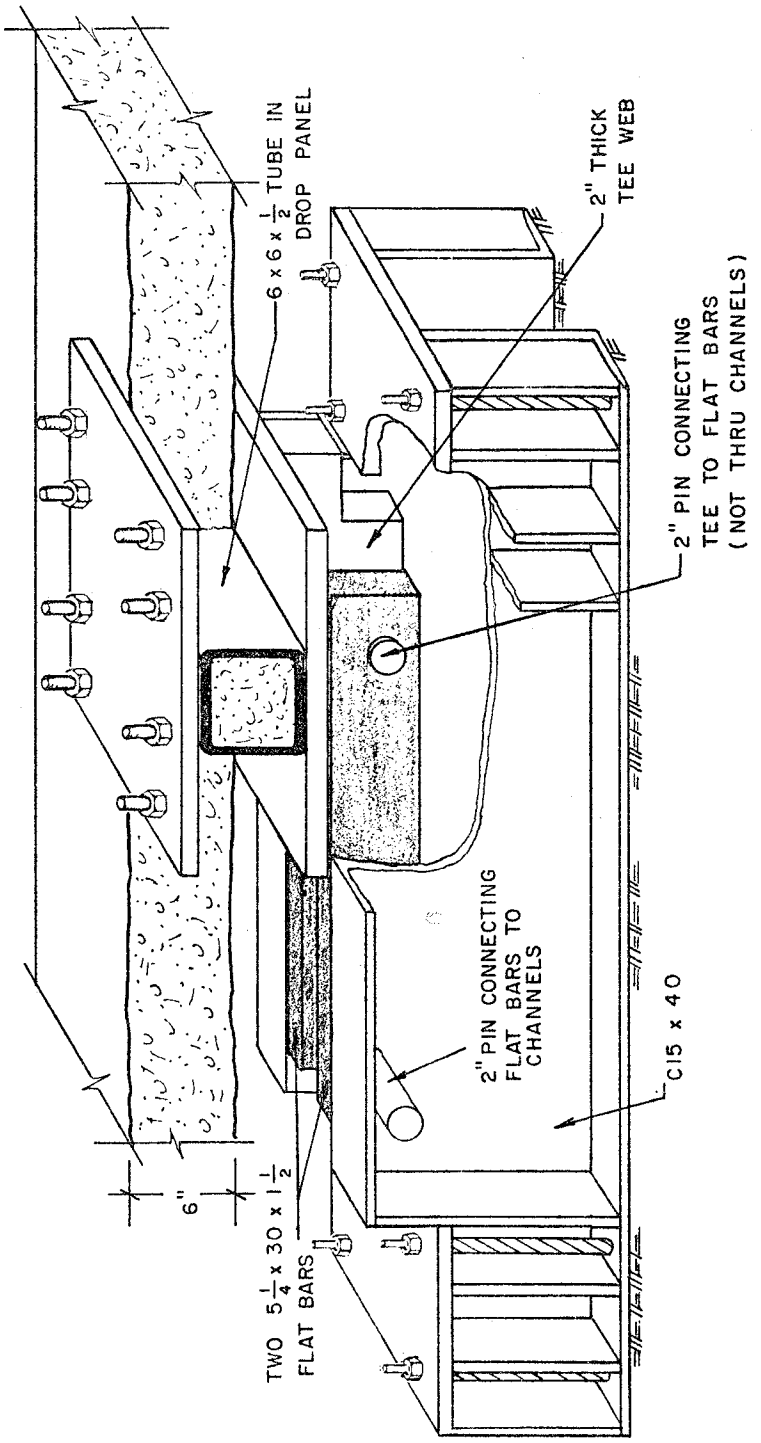

Fig. 3.16 Reaction assembly.

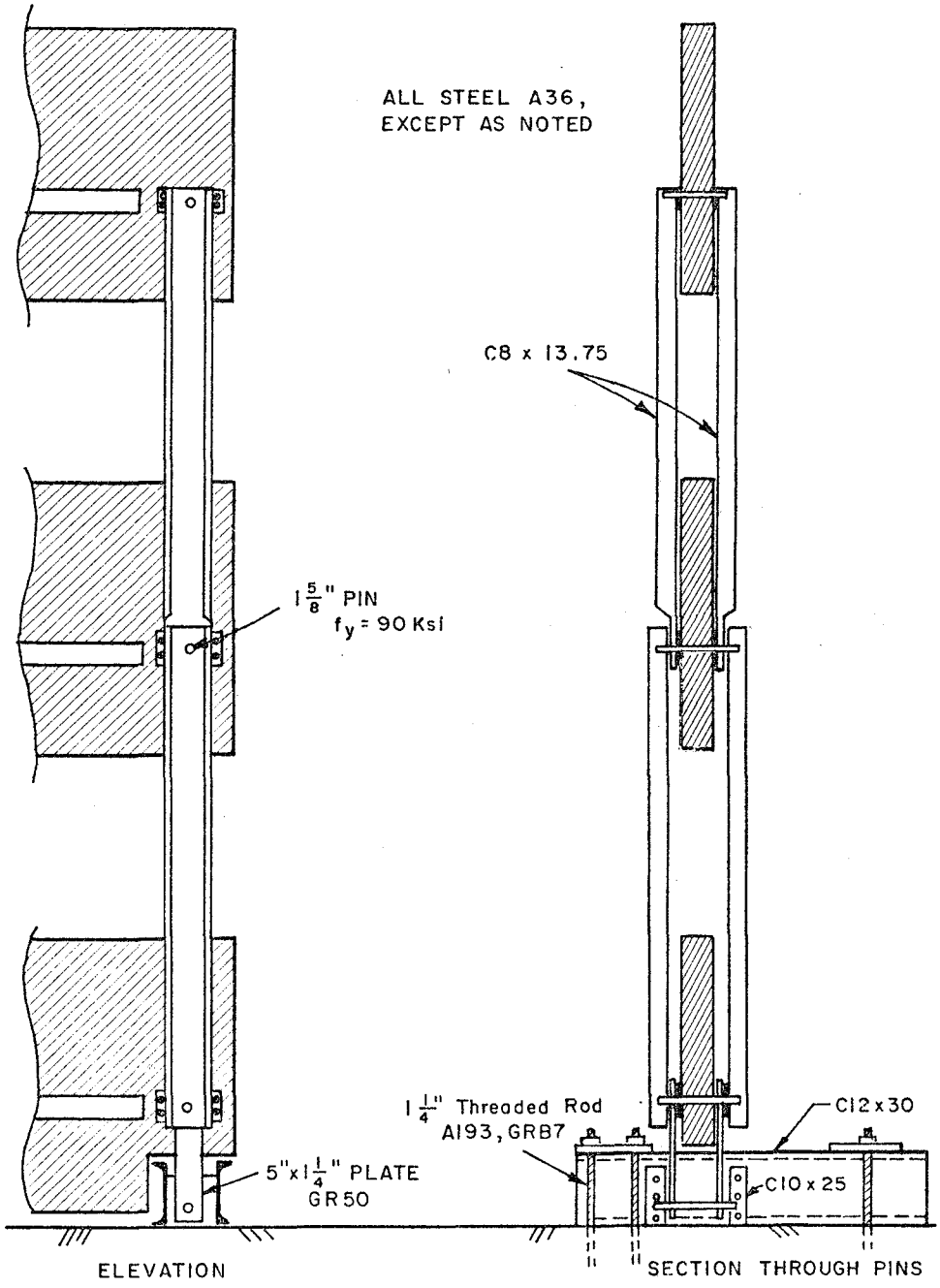

Fig. 3.17 Original Strut Design

deep channel members on each side of the spandrel spanned from floor to floor. Pins at the strut ends passed through the concrete spandrel and two 1/2 in. steel plates. The plates were clamped to the concrete with four 5/8 in. diameter high-strength threaded rods. The rods were stressed to 20 kips each with a calibrated wrench to develop the necessary normal force to transfer the vertical reaction from each spandrel through friction. The pins then transferred the load from the plates to the struts through bearing.

Between the reaction floor and the first spandrel, the struts were 5 in. by 1-1/4 in. Grade 50 steel plates. The plates were pinned to an assembly of channels which were bolted to the floor.

The struts, as originally designed and fabricated, were not adequate for the vertical loads expected from the steel strengthened frame. In addition to the increase in forces, steel diagonals framed into the second level spandrel at the same location that the struts were attached, so a revised connection detail had to be designed.

Figure 3.18 shows the modifications made to the original strut design. The outside channel between the first and second level was converted to a box section by welding an 8 in. by 3/4 in. plate to it. At the bottom level, another 5 in. by 1-1/4 in. plate was used and connected to an additional 10 in. channel.

Due to the larger forces created by the bracing on the exterior side, 2 in. pins replaced the 1-5/8 in. pins in order to carry the high shear forces. To reduce the number of holes which had to be redrilled, the 1-5/8 in. pins were retained on the interior side where the forces were smaller. The holes in the spandrel were drilled out to 2 in. and the gap around the smaller pin was filled with hydrostone to prevent rotation of the pin.

To transfer the load from the braces into the struts, the 1/2 in. clamping plates on the exterior of the second spandrel were replaced with 1 in. thick Grade 50 plates to which the inside flanges of the braces and collector tees were welded. At each end, a plate outside the box section was placed on the pin to serve as a gusset plate for the exterior flanges of the two braces and collector framing into it. These plates were cut from a wide flange beam. The modified struts with the braces framing in at the second level may be seen in Fig. 3.19. Three-quarter inch plates were welded in position between the two gusset plates to stiffen the connection and to serve as erection plates. Figure 3.20 is a photograph of the struts with gusset

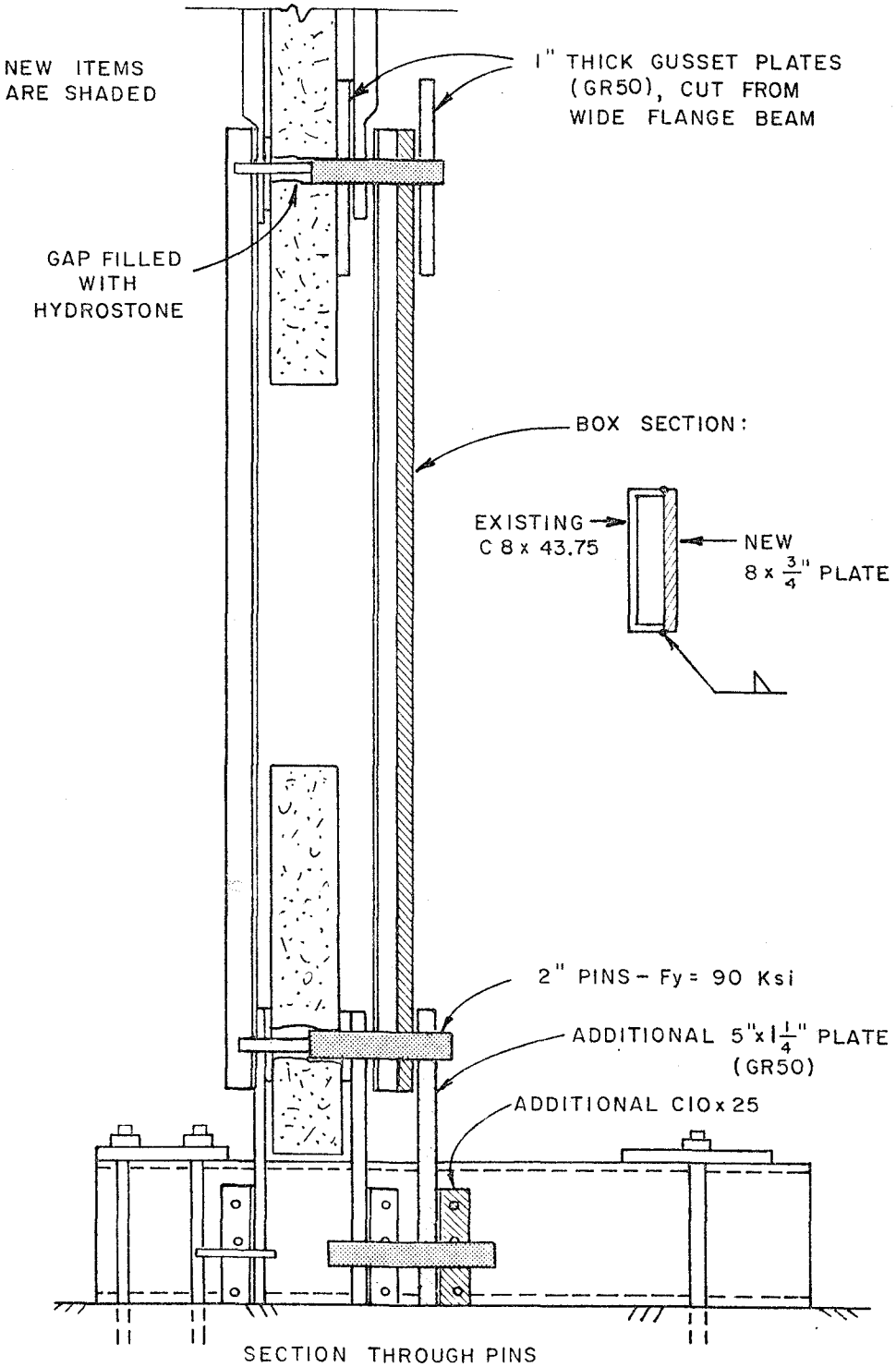

Fig. 3.18 Modifications to Struts

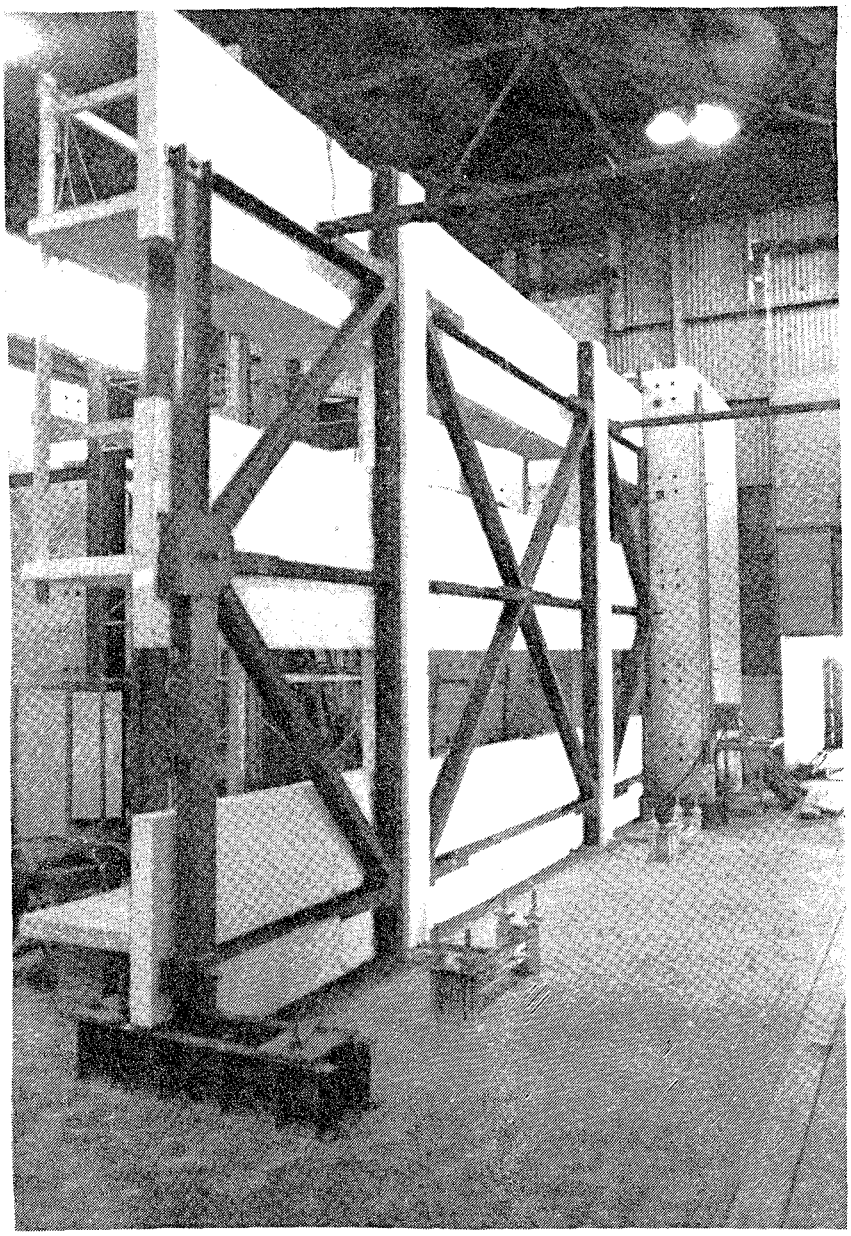

Fig. 3.19 Struts for steel-braced frame

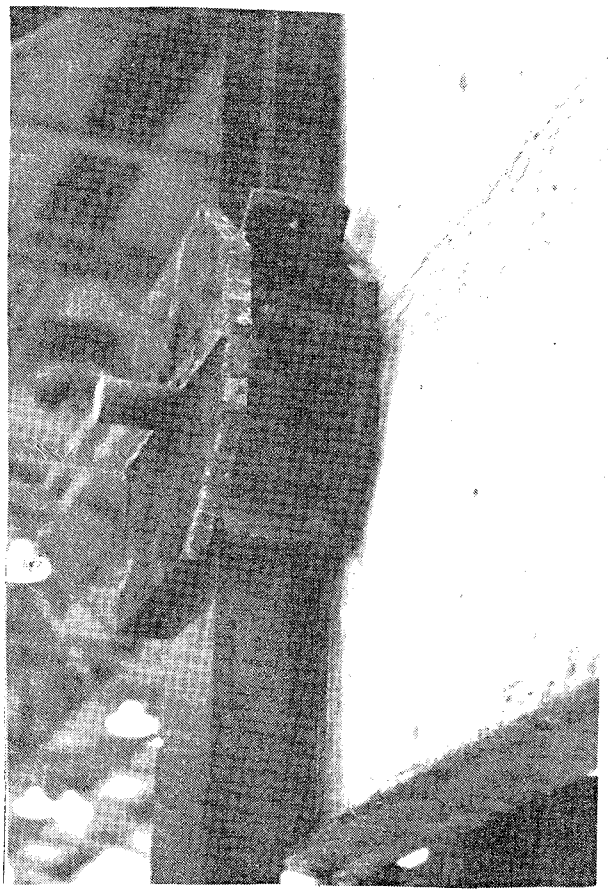

Fig. 3.20 Struts with gusset and erection plates for braces

and erection plates in place before the braces and collectors were hung.

3.2.5 Out-of-Plane Bracing. Out-of-plane bracing was provided at the first and third levels at or near the columns, as was seen in Figs. 2.6 and 3.7. The bracing was designed to provide restraint normal to the plane of the frame only. Near the base, 2 in. diameter pipes were attached to 3/4 in. threaded rods, which had been embedded in the column, and reacted against two 5 in. deep channels. Each end of these channels was welded to a 12 in. channel bolted to the floor. At the top level, two angles welded to form a 3X3 in. box spanned from the frame to the lab walls.

3.3 Fabrication and Erection of Steel Bracing

3.3.1 Preparation of Frame. After testing of the concrete strengthening system was completed, a concrete demolition contractor was hired to make vertical cuts in the piers along the sides of the original column. Horizontal cuts were made at the top and bottom of the spandrels so that the blocks between the spandrels could be removed with a forklift.

The 8 in. deep layer of concrete attached to the spandrel faces was removed by jackhammering as seen in Fig. 3.21. The dowels into the spandrels were torch-cut. Figure 3.22 shows the rough surface resulting from this procedure. There were some places where concrete of the original frame was removed and steel reinforcement was exposed. These bars were later covered with epoxy to prevent buckling. The additional column thickness of 1-1/3 in. resulting from the concrete strengthening was not removed, leaving a column section of about 12 in. by 13-1/3 in.

The areas where steel members were to be placed against the concrete were smoothed with a chipping hammer. The exterior, except where steel members were to be bolted to the concrete, and the interior of the spandrels and columns were whitewashed to provide a surface free of crack markings from the previous test.

3.3.2 Attachment of Tees and Channels. Bolt holes in the channels were drilled 1/8 in. larger than the bolt diameter to allow for easier placement of dowels. The channels were clamped to the concrete columns and were used as templates for drilling the holes in the concrete. The holes were started using a 5/8 in. drill bit. The channels were then removed, and the holes were finished with a 3/4 in. drill bit to a depth of 5-1/2

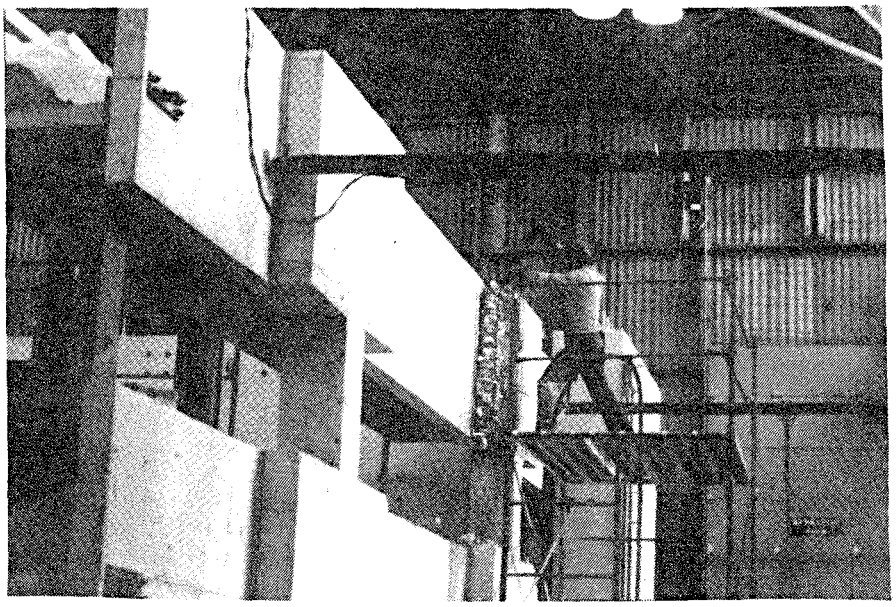

Fig. 3.21 Concrete removal

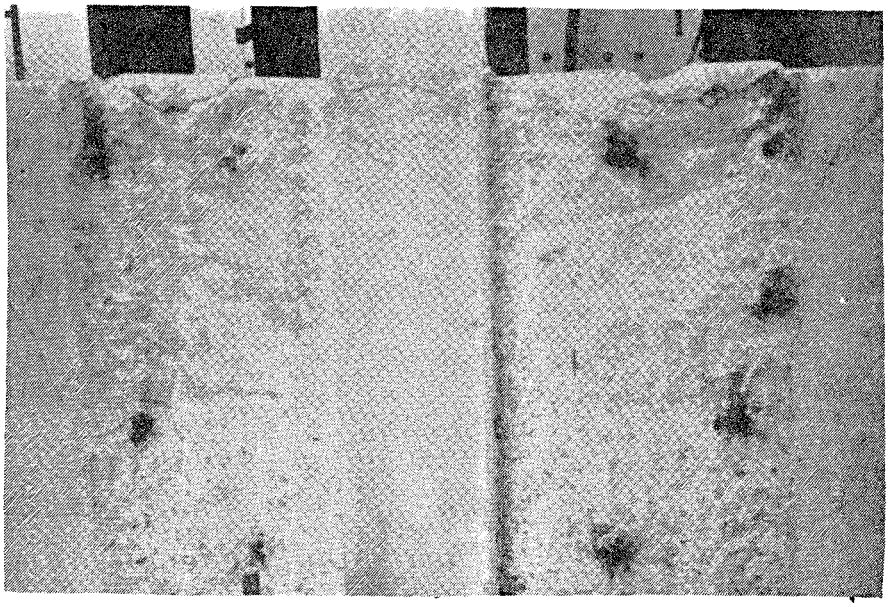

Fig. 3.22 Rough surface around column

in. Holes in the concrete 1/8 in. larger than the dowels are required for epoxy-grouting the threaded bars.

The holes had been placed so that dowels would not coincide with column ties; however, the drill sometimes hit the middle vertical #7 bar, especially in the column splice region. If a hole was at least 3 in. deep before encountering steel, it was considered adequate to accommodate a dowel. There were very few holes less than 3 in. deep in the north column, but in the south column, twelve holes were not deep enough. Therefore, holes were shifted and redrilled in the steel channels. Three holes were still not deep enough, and several near the top of the channels had to be drilled at a slant to avoid steel.

After the channels were used as templates, gusset and erection plates were welded to them. One of the channels was instrumented, and the pair was clamped to the concrete columns in position over the holes. The threaded rod dowels were epoxy-grouted into the concrete. Just before the channels were put in place, the dowel holes in the concrete were prepared by brushing and vacuuming following the recommendations of Luke et al. [19].

A non-sag gel epoxy (Concresive 1411 - Adhesive Engineering Corp.) was used. The epoxy is especially formulated for use in warm environments. The two-component epoxy has a tensile strength of 1500 psi and a compressive yield strength of 8000 psi [20]. Due to the short pot life at temperatures of about 90 degrees, the epoxy operation was performed on one column at a time (about 50 dowels). The two components were measured by weight and mixed with a paddle on a hand drill. The non-sag gel has high viscosity and requires considerable mixing to ensure uniform distribution of the two components. The best indicator of adequate mixing is a uniform color. Two dowels were also placed in a concrete block for testing to assure quality control.

Figure 3.23 shows the epoxy application procedure. A caulk gun was used to apply epoxy directly to the rear of the hole. As the hole filled, the caulk gun was gradually backed out until about 60 percent of the hole was full. The dowel was pushed into the hole and rotated one turn until it bottomed out. Extra epoxy was forced out of the hole and into the annulus between the bolt and hole in the steel section. Where the steel element was not flat against the concrete, extra epoxy was forced into the gap. Any additional epoxy was removed with a spatula.

After three days the control dowels were tested and it was found that yield was developed with no apparent damage to the epoxy. At this stage, nuts and washers were placed and tightened

Fig. 3.23 Epoxy application procedure

with a small wrench. After seven days the bolts were tightened with a torque wrench to a level of 75 ft-lb.

When the channels were in place, exact measurements for the collector tees were made, and the tees were cut to length and drilled. Erection holes at the ends were drilled, and the ends were beveled for welding with a hand-held disk grinder. The tees were positioned using erection bolts, and the same procedure used for the channels was followed to drill the holes in the concrete. The holes were drilled 4-1/2 in. into the spandrels.

The epoxy operation was done for all tees on the same day, but two batches of epoxy were mixed due to the short pot life. The epoxy application procedure and method of tightening was the same as for the column channels.

After the bolts were torqued, the ends of the tees were welded to the channels. The short tee section stiffeners at the ends of the collectors were beveled with a grinder and clamped to the tees fastened to the frame. The ends were welded to the channels and the webs of the two tees were welded together, as shown by Fig. 3.24. At the second level, the tees on the outer spans were welded to the strut gusset plates, and the short tee in the center connection was welded to the original tee only along its web. At this time, the web gusset plates and erection plates in the middle tee connection were welded in place. When all welding of the tees was completed, strain gages were attached to the tees at the third level as will be described later.

3.3.3 Braces. The tips of the flanges were removed from all the W6X9 braces, as pictured in Fig. 3.25. A guide held the torch so that a flange width of 3-1/2 in. remained. Very little warping of the steel member was introduced using this process. Only one brace had a noticeable sway after torching. The cut edges were smoothed with a grinder.

When the channels and tees were in position, the braces were cut to length, with the four middle braces having one end cut at 45 degrees. Each brace was held in place, and a grinder was used for final fitting. Holes for erection bolts were drilled, ends were beveled, and strain gages were attached. All of the braces were hung on the frame with erection bolts and welded at each end. The entire bracing system is shown in Fig. 3.26.

All of the steel members of the bracing system were painted just before testing. A whitewash mixed with black powder paint formed a light gray color which contrasted with the white

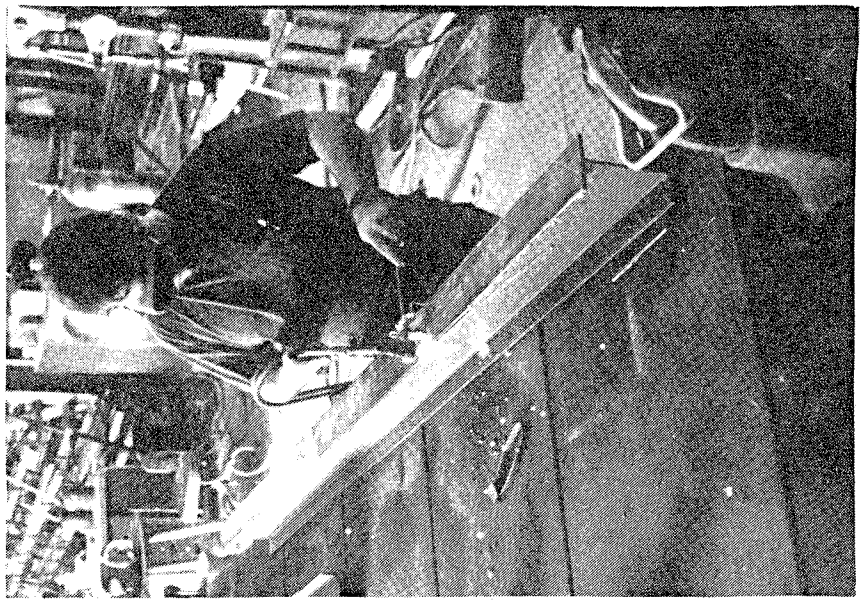

Fig. 3.25 Torch-cutting braces

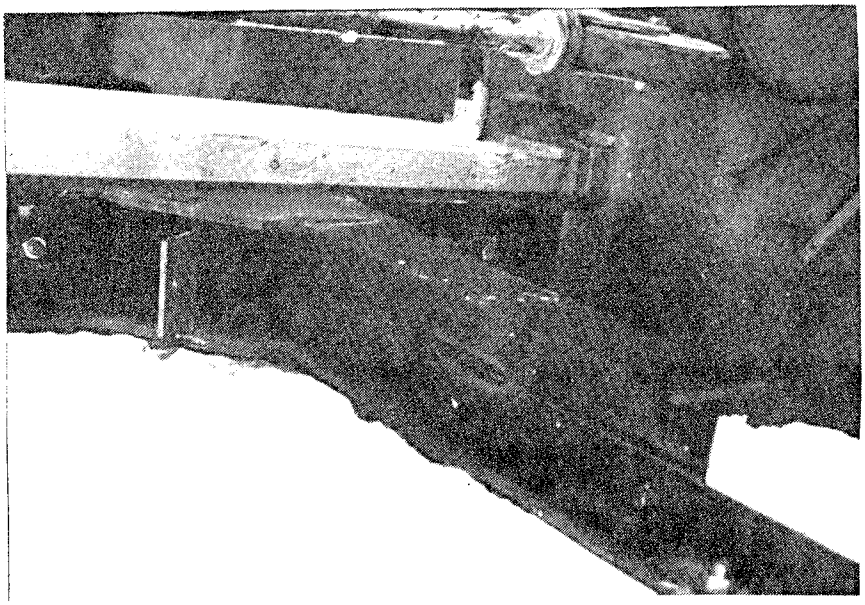

Fig. 3.24 Double tee

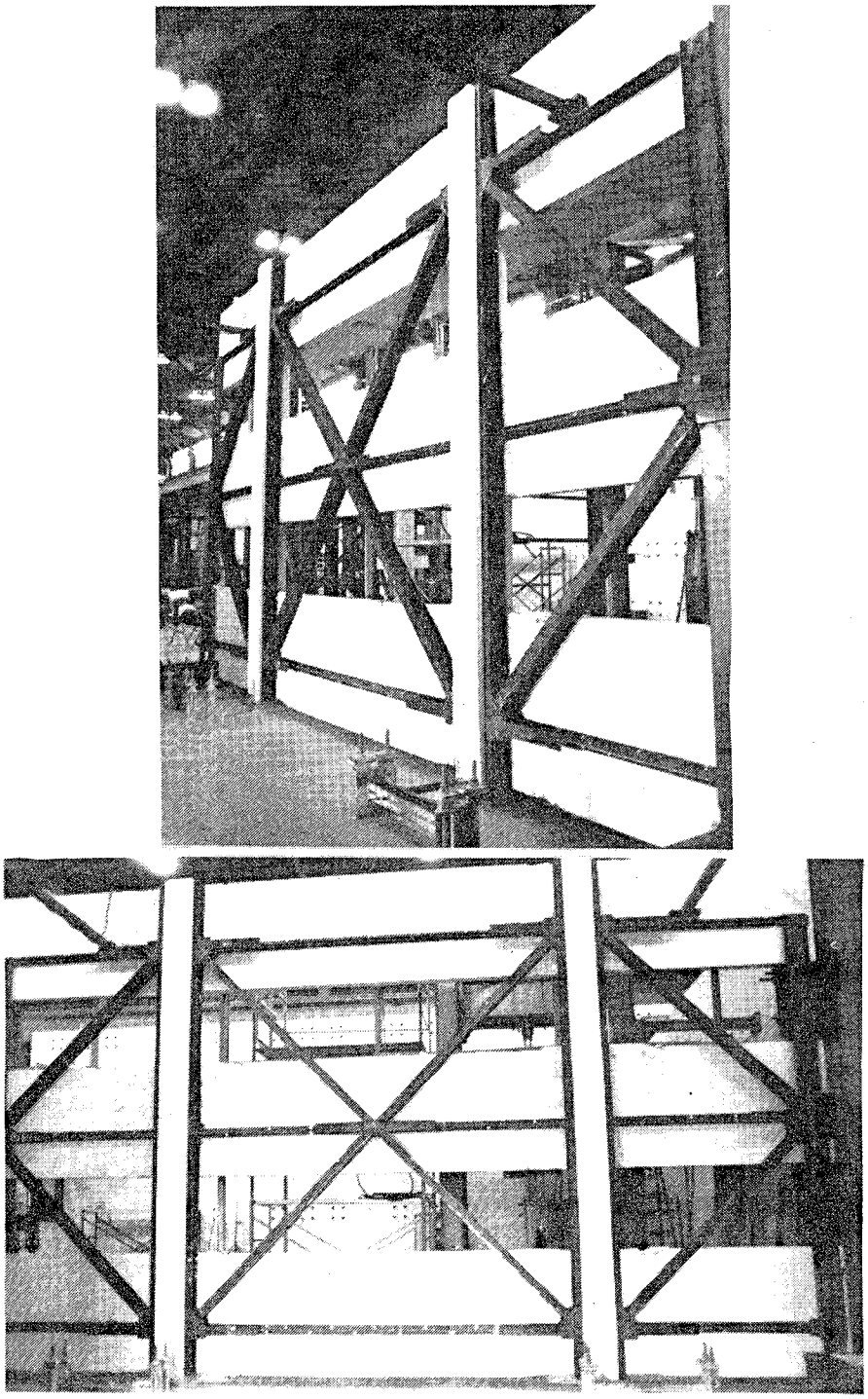

Fig. 3.26 Steel bracing system in place

concrete, and yet was light enough to contrast with the original steel color. The paint indicated steel yielding during the test because it flakes off with the brittle mill scale when the steel beneath is yielding.

3.3.4 Materials. The tees, channels, and wide flange members were Grade 36 steel. Mill reports were obtained from the supplier for the W6X9 braces, which showed an average yield strength of 48.1 ksi.

To verify the figures from the mill reports, tension tests were carried out on samples obtained from extra brace material which came from the same heat. Four coupons were tested (two from the web, two from the flange) following the specifications in ASTM 370-71 [21]. The average static yield values were 48.8 ksi for the web material and 44.5 ksi for the flanges.

Threaded rods and nuts for the dowels were mild steel. High-strength washers were used because their dimensions met clearance requirements on the tees. All welds were formed with either E60-13 or E70-18 electrodes.

3.4 Instrumentation

3.4.1 Loads. The lateral load applied at the third level was measured through use of a pressure transducer. One transducer located at the pump measured the pressure in the hydraulic lines, whether loading the frame north or south. The applied load, then, was the line pressure times the piston area of two rams.

The horizontal reaction forces at the base and the vertical reactions in the end struts were measured by load cells made up of four or eight strain gages. The gages were arranged on the links and struts to increase the sensitivity of the four arm bridge load cells. Each base reaction was measured using the two horizontal links, which had eight strain gages (four on each link) making up the load cell.

The vertical reactions were measured at each level at both ends for a total of six reaction forces. For the original frame test, each pair of struts with eight gages formed a load cell. Only the pairs between the second and third levels were retained as they were for the steel strengthening test. At the bottom level, the plate on the interior of the spandrel at each

end was a load cell in itself, while the two plates on the exterior at each end acted together as a load cell. Thus, the reaction at the bottom at one end was obtained by adding the two load cells. Between the first and second spandrels, a similar arrangement existed, with the box-shaped strut as one load cell, and the single channel on the interior as one load cell.

3.4.2 Displacements. Both global movements of the frame and relative movements between the steel and concrete were measured. Figure 3.27 shows the arrangement of displacement transducers and dial indicators.

Lateral movement of the specimen was monitored at each level by a linear voltage displacement transducer mounted against the reaction wall. At the first and third levels, dial indicators were mounted to serve as checks.

By measuring the lateral displacements of each level, the two interstory drifts and the total drift (first to third level) could be computed. Because displacements were measured relative to the reaction wall, an adjustment had to be made to allow for the movement of the wall. A transit was used to determine the deflection at the top of the wall for each direction of loading. The displacement of the wall was 1 mm at an applied lateral load of 170 kips in the north direction at a load of 130 kips south. With these deflection values and the assumption that the deflected shape of the wall was a cantilever, formulas were determined for adjusting the drifts obtained from the displacement transducers. All values for drift in this thesis have been modified for the movements of the reaction wall unless otherwise noted.

Vertical movements of the spandrels were measured at all three levels at the south end and at the first and second levels of the north end. At the south end, displacement transducers were attached at each level while dial indicators were used to check the results at the first and third levels, as shown in Fig. 3.29. At the north end, only dial indicators mounted on a stand were used to measure vertical displacements.

Displacement transducers were placed in eight locations to indicate the relative movement between the steel and concrete systems, as shown in Figs. 3.27 and 3.28. Two transducers monitored the vertical movement between the steel channel and concrete column at the north end. Vertical and horizontal motions of the center brace-to-tee connection relative to the concrete spandrel were measured. In addition, four transducers were placed on the third level collector to instrument horizontal

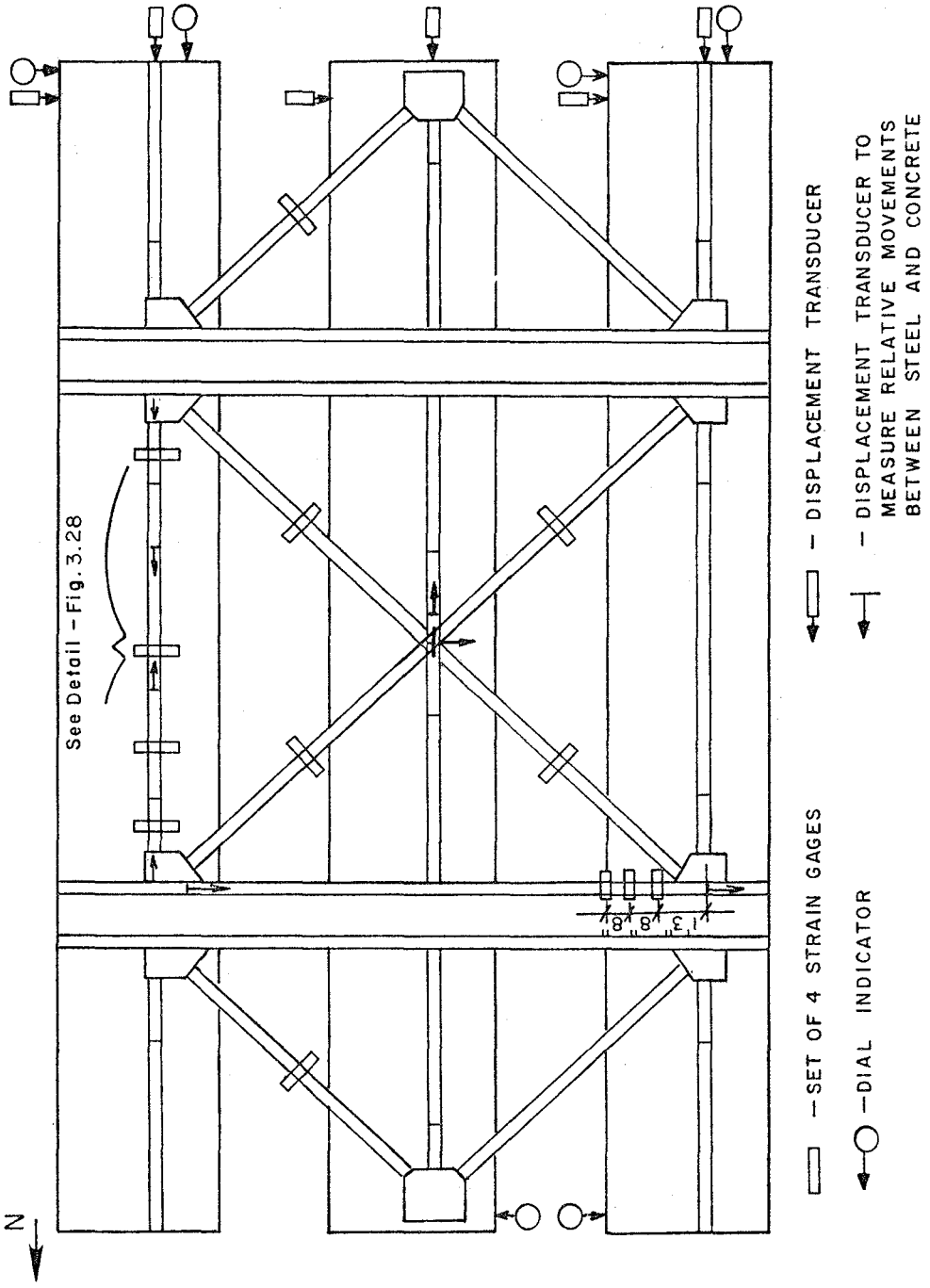

Fig. 3.27 Instrumentation Locations

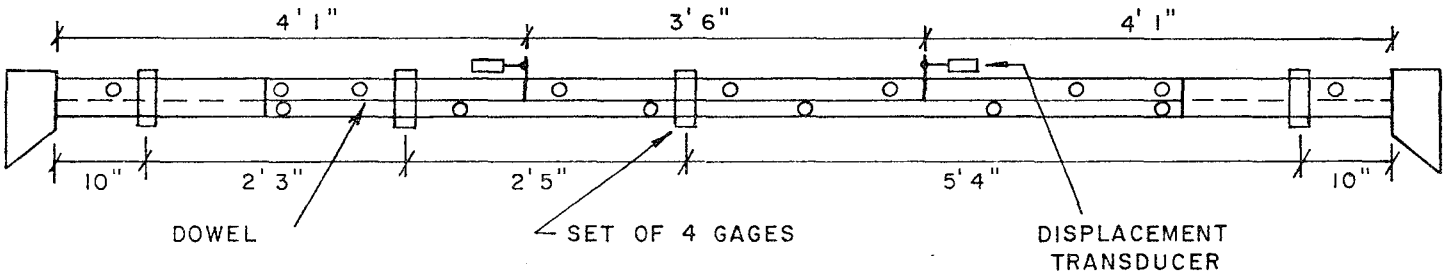

a) Third Level Instrumentation

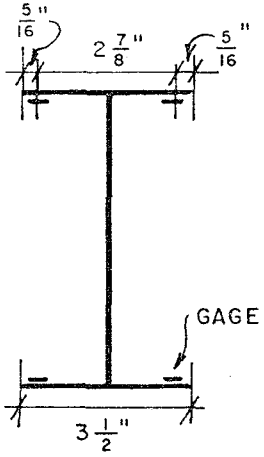

b) Brace Gages

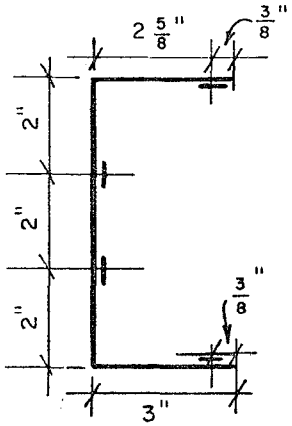

c) Channel Gages

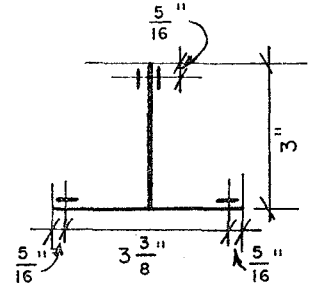

d) Single Tee Gages

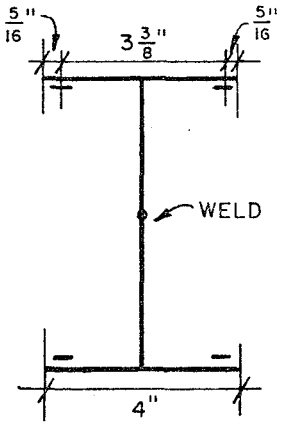

e) Double Tee Gages

Fig. 3.28 Instrumentation Details

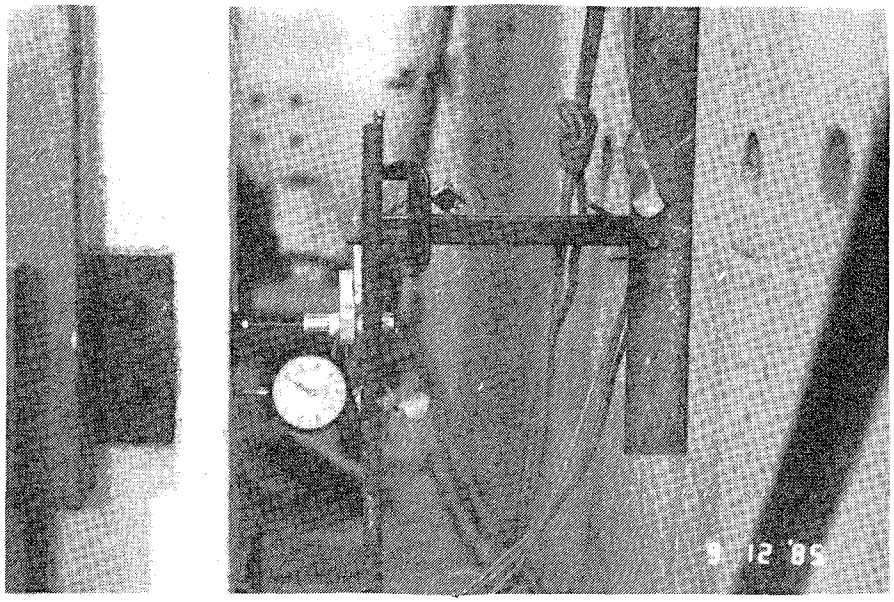

Fig. 3.29 Transducer and dial gage at first level

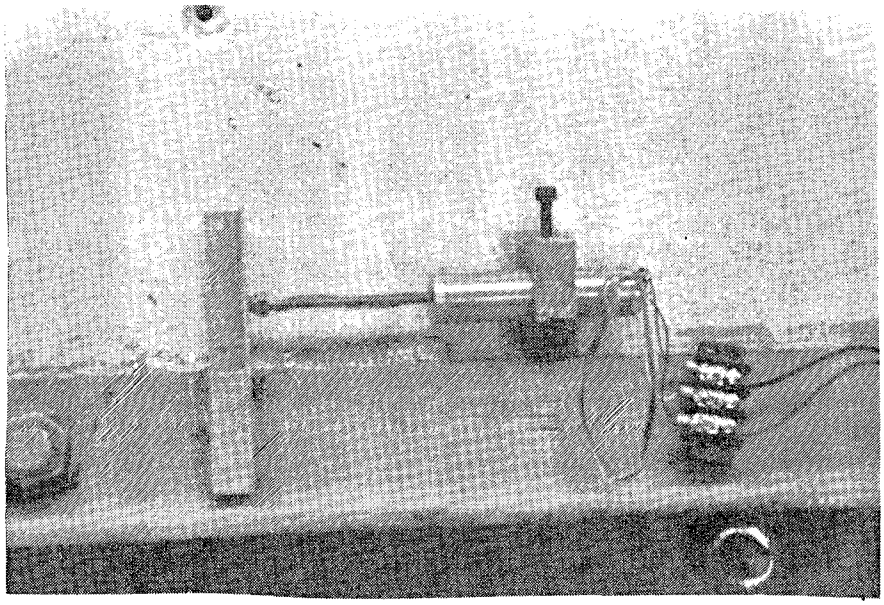

Fig. 3.30 Transducer measuring tee movement

movement. The displacement transducers were mounted using aluminum blocks attached with epoxy, as seen in Fig. 3.30.

3.4.3 Strains. Fifty-two strain gages were mounted on the steel bracing system. Paper-back gages were attached in groups of four at the locations shown in Fig. 3.27. They were arranged as in Fig. 3.28 and were oriented to measure strains along the axis of the member. In this manner, the four strains/stresses were averaged, and, with the member area, the axial load was computed.

The four braces across the top level were each instrumented at their mid-length, as were the two middle ones at the bottom level. The third level collector tee was instrumented at four locations along its length. Different arrangements of the gages were used for the single tee and double tee regions, as was shown in Fig. 3.28. One channel was instrumented at three locations near the bottom of the north column. The gages were placed at midpoints between dowels.

Strain gages on steel reinforcement which were monitored for the steel strengthening test are shown in Fig. 3.31. Since the original intention had been to build a second frame for the steel strengthening scheme, the strain gage locations in the bare frame were selected with the concrete strengthening test in mind. Therefore, there were very few gages in the original columns, and most of the spandrel gages were at the edge of the piers.

3.4.4 Data Acquisition. A data acquisition system was used to scan 72 single-bridge channels and 27 full-bridge channels. The load cells, pressure transducer, displacement transducers, and strain gages were monitored and voltages were converted into engineering units during testing. Readings from dial indicaters were recorded manually at each load stage. An X-Y plotter provided a continuous plot during testing of the applied load versus third story displacement.

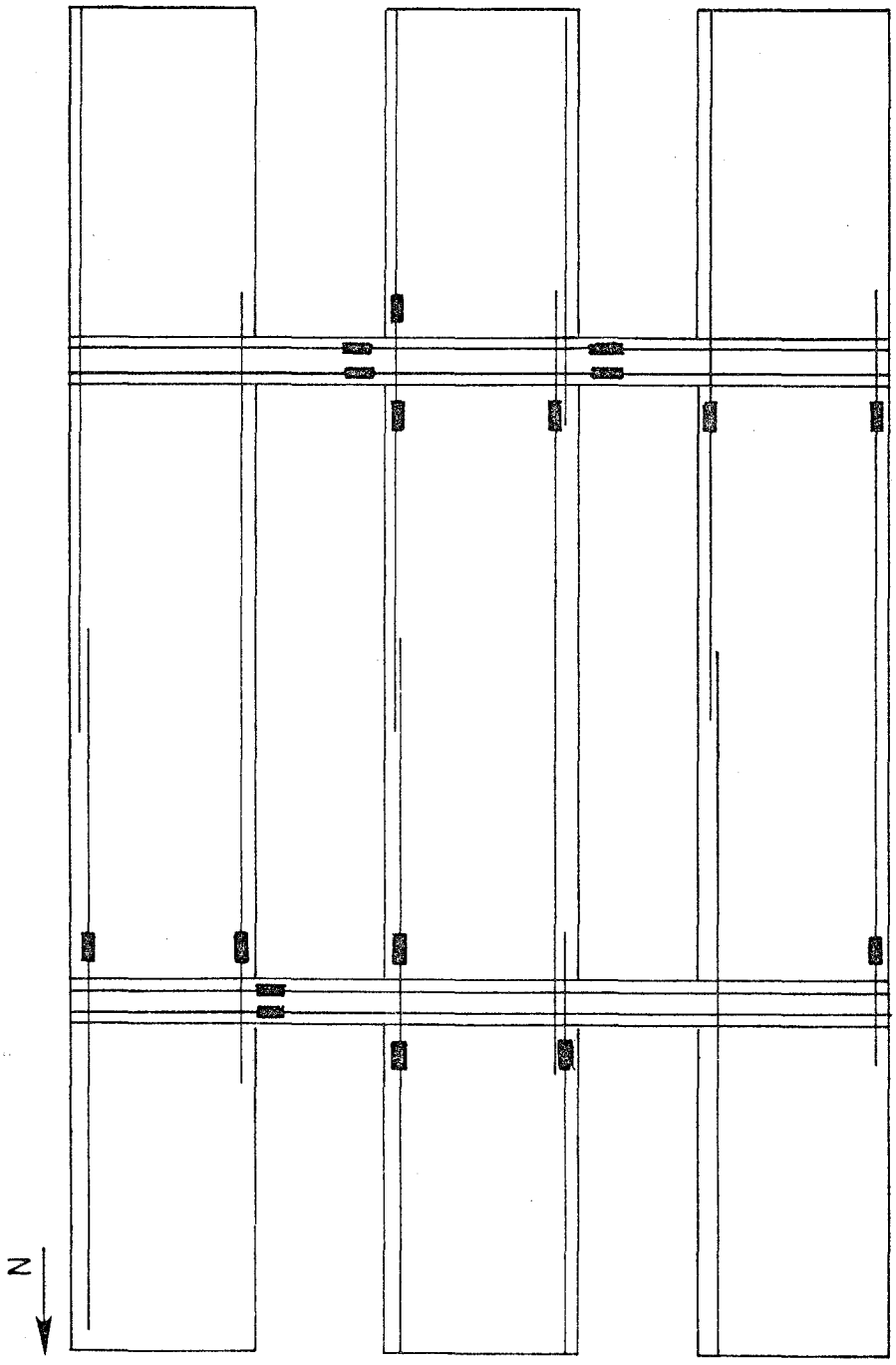

Fig. 3.31 Strain Gages on Steel Reinforcement

CHAPTER 4

BEHAVIOR OF SPECIMEN

4.1 Load/Displacement History

The specimen was subjected to four series of tests. These included two tests at low load and displacement levels on the bare, or original, frame; a test of the specimen strengthened by concrete wingwalls to displacement levels which produced flexural hinging in the spandrel beams; and a test to failure of the frame strengthened by steel bracing. The general testing procedure and the loads and displacements which were applied to the test specimen are described in this section.

4.1.1 Loading Procedure. In each load series the frame was subjected to reversed cyclic loading, with each cycle beginning in the north direction. Normally the frame was cycled three times at a specified lateral load or drift level before it was subjected to larger displacements. For the first portion of a test, each set of three cycles was kept at the same load level in the north and south directions. In subsequent cycles, the peaks were controlled by imposing equal drifts in the two directions. The drift used to determine the peaks was measured between the first and third floors of the model and will be referred to as total drift.

During testing, an X-Y recorder provided a continuous plot of the applied lateral load versus the third level displacement from the reaction wall. An example of the plots, in Fig. 4.1, shows the last three cycles applied to the steel braced frame.

The strengthened frame tests were carried out over a period of three to four days to permit adequate time for recording data and making visual observations of damage. Data were recorded approximately 300 times (load stages) during the test of the steel braced frame. At each load stage, voltages of 96 channels were scanned, converted to engineering units, stored on a permanent disk, and printed at the test site. Dial gage readings were recorded manually, and new cracks were traced with colored markers (different colors for the two directions) and labeled to indicate load stage at which they occurred.

4.1.2 Previous Tests. The purpose of the two bare frame tests was to determine the initial stiffness of the

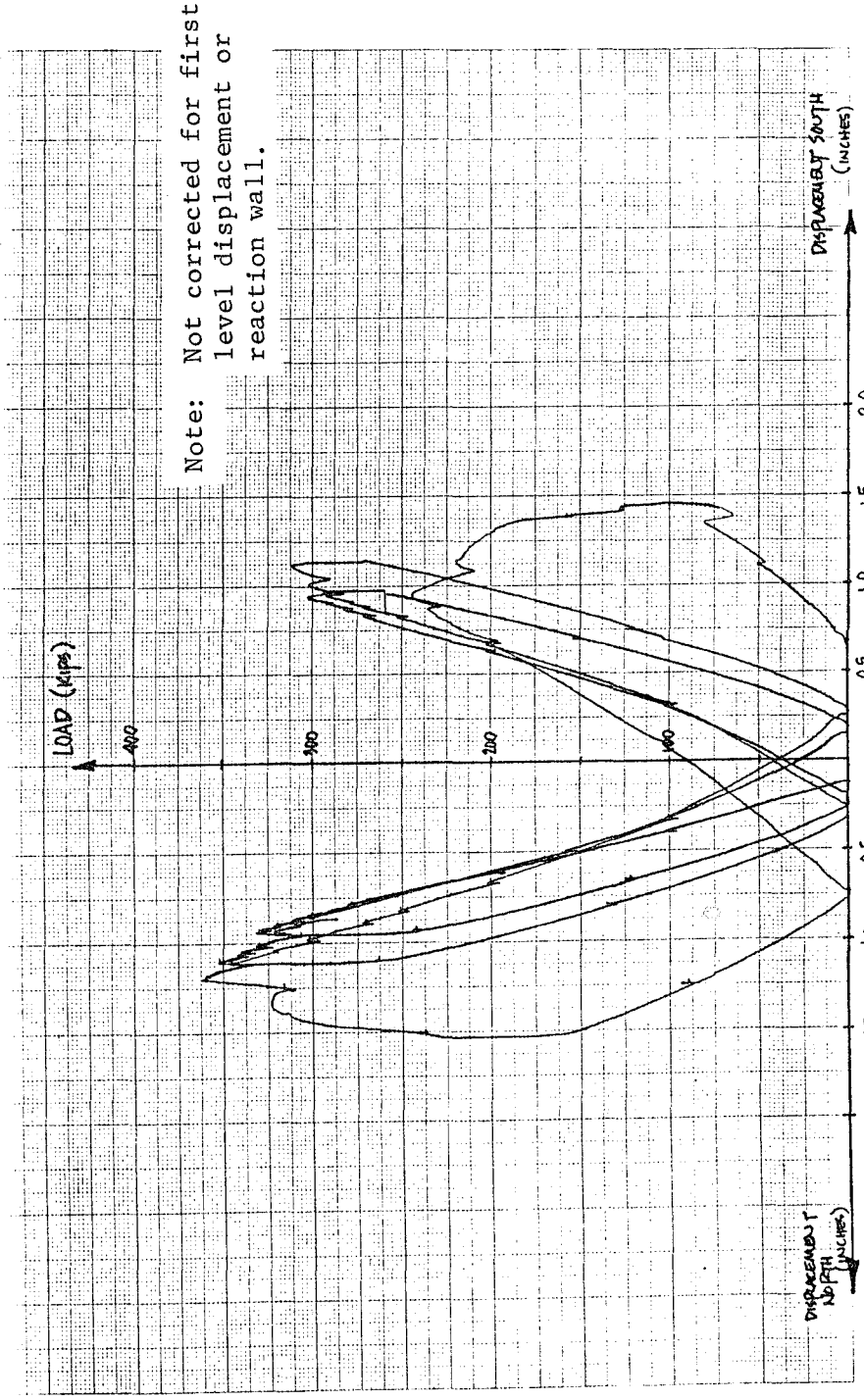

Fig. 4.1 Plot from X-Y Recorder - Final Three Cycles

unstrengthened frame and to check out the instrumentation and loading system. To do this without damaging the columns, maximum lateral load applied was 32 kips which is less than the nominal shear strength of 62 kips for two columns. Both tests consisted of two cycles to 32 kips in each direction. The total drift between the first and third floors was about 0.06 percent, with the frame slightly less stiff during the second test. At this displacement flexural cracks appeared in the spandrels near the corners of the columns, but there were no column shear cracks.

The displacement levels imposed on the concrete strengthened frame are displayed in Fig. 4.2. Four sets of three cycles were performed at increasing drift levels. The last three cycles were at 0.5 percent total drift, with the interstory drifts approximately equal. At this displacement level, there was extensive cracking of the spandrels with hinging near the piers. Some shear cracks in the piers crossed the original column.

4.1.3 Steel Strengthening Test. Figure 4.3 shows the displacement history of the frame strengthened by steel bracing. To check out the instrumentation, two preliminary cycles were performed at low load levels: one to a peak of 30 kips, the other to 60 kips. The frame was then subjected to two sets of cycles controlled by equal loads in the two directions. The peak loads were 90 and 150 kips which corresponded, respectively, to about 0.1 and 0.17 percent total drifts.

The remaining cycles were controlled by drift levels between the first and third story. For cycles exceeding 150 kips, three cycles at a drift level of 0.23 pecent, three cycles at 0.36 percent, and three cycles at increasing displacement levels up to 0.84 percent drift were applied. The interstory drift between the second and third level was over 1 percent in the final cycles. The differences in interstory drift between the two levels will be discussed in Section 4.3.

4.2 Behavior During Test of Steel Braced Frame

Load-displacement curves representing the entire load history are shown in Figs. 4.4 and 4.5. Positive loads and displacements correspond to pushing the frame in the north direction. The two graphs are at different scales. Figure 4.4 displays the first cycles at each load or displacement level except for the final three cycles which are shown in Fig. 4.5. The final three cycles will be referred to as the F1, F2, and F3 cycles. The behavior of the steel-braced frame will be

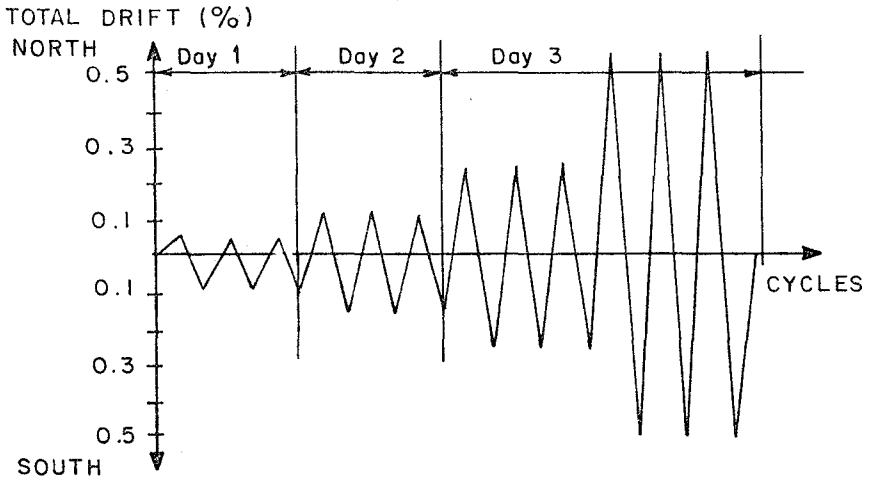

Fig. 4.2 Displacement History - Concrete Test

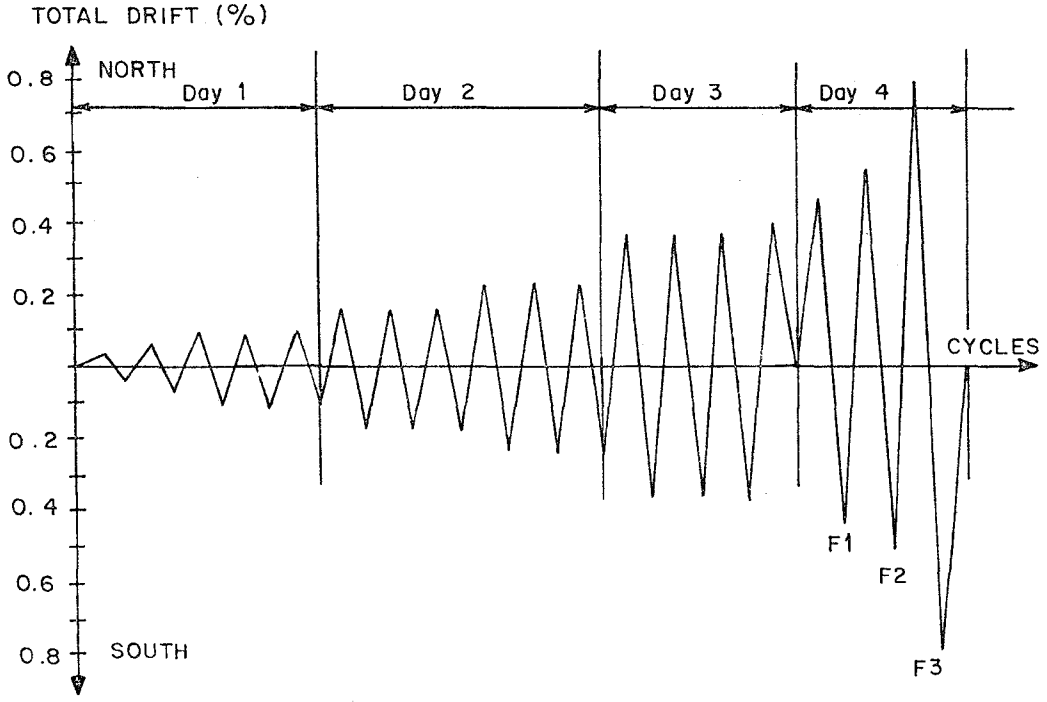

Fig. 4.3 Displacement History - Steel Test

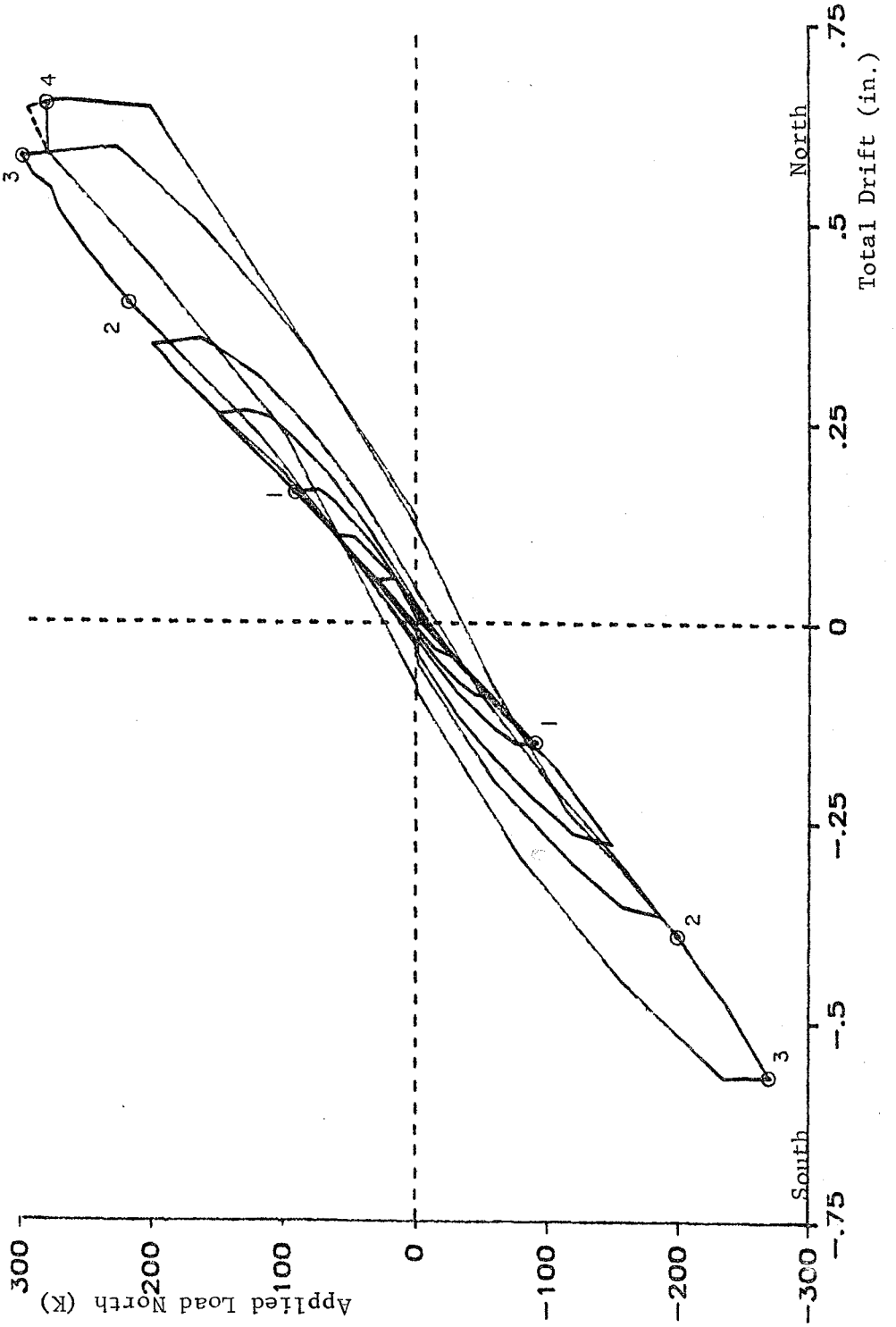

Fig. 4.4 First cycles through 300 kips

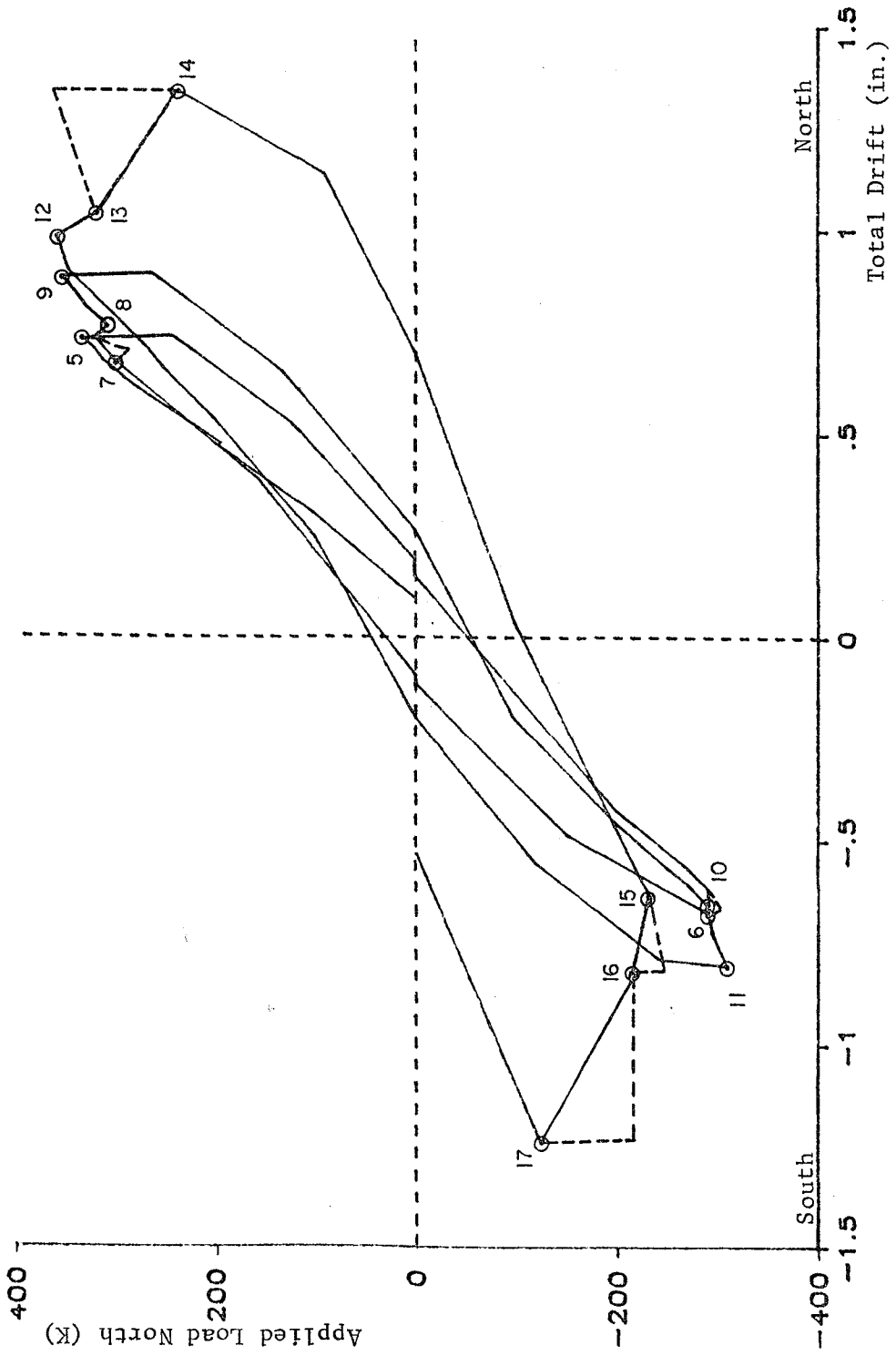

Fig. 4.5 Final three cycles: F1, F2, F3

described using load-drift reference points circled in Figs. 4.4 and 4.5 and the brace notation in Fig. 4.7.

During the preliminary cycles to 30 and 60 kips, cracks from previous tests began to reopen. The most significant cracks were the shear cracks on the slab side of the columns which had formed during the test of the concrete strengthened frame. New cracks did not appear until a load level of 90 kips and 0.1 percent total drift was reached (points labeled 1 in Fig. 4.4). Figure 4.6(a) shows the crack patterns at point 1 in the north column at the second level.

A total drift of 0.25 percent was attained (points labeled 2 in Fig. 4.4) when 220 kips was applied in the north direction and 200 kips in the south direction. A significant increase in column cracking did not occur until 0.4 percent drift was reached at about 300 kips (points labelled 3). Figure 4.6(b) shows the cracking at the same location as Fig. 4.6(a) but at the higher drift level. The new shear cracks in the columns and flexural cracks in the spandrels can be seen.

After the three cycles at 0.4 percent drift, loading to the next drift level commenced. At a lateral load of 295 kips to the north, a brace weld broke, and the load dropped to 280 kips. In Fig. 4.4, the dotted line represents the increase in load to 295 kips and the sudden drop when the weld failed. This is only an estimate of the load-deflection points since a scan of the instrumentation channels was not made until the load leveled off at 280 kips (point 4). The brace-to-gusset plate welds at the bottom of brace B1 (Fig. 4.7) fractured. Upon examination, it was determined that the weld was defective in that full weld penetration had not been obtained. The frame was unloaded, and the connection was rewelded.

After rewelding, loading was started again in the north direction, as shown in Fig. 4.5. When the load reached 330 kips (point 5), part of the weld at the top of brace T2 broke. The welds connecting the interior flange and part of the web to the gusset plates failed leaving the exterior flange to carry the entire brace load. The weld on the outer flanges was able to transfer the load produced by the brace flange yielding in tension. The load was removed, and the connection was rewelded. Loading continued in the south direction up to 300 kips when the weld connecting the web at the bottom of brace T3 failed, reducing the applied lateral load to 290 kips. Data were recorded at this load (point 6). At this time all welds were inspected. The entire middle connection between braces 2 and 3 was rewelded. Nearly all other brace welds were strengthened to ensure that the

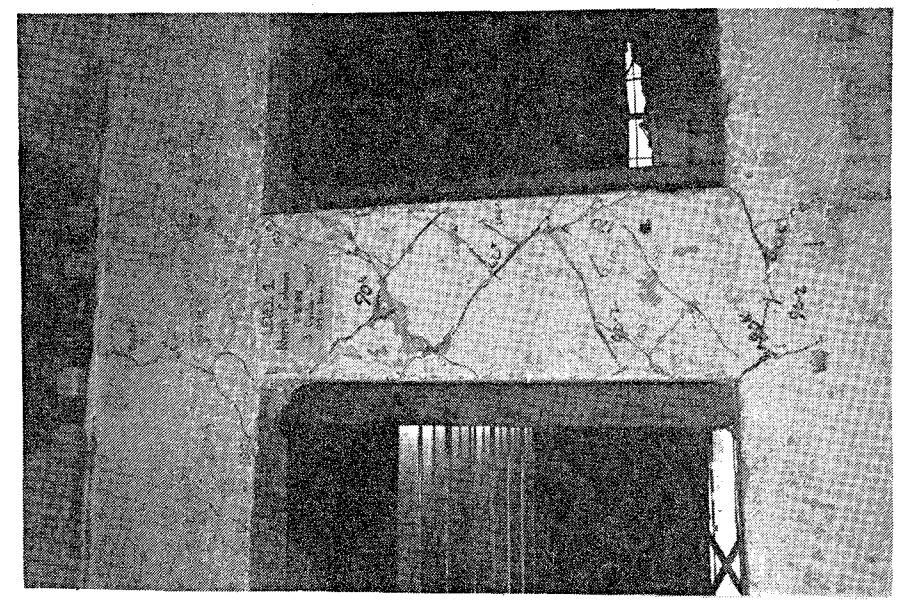

(b) 300 kips

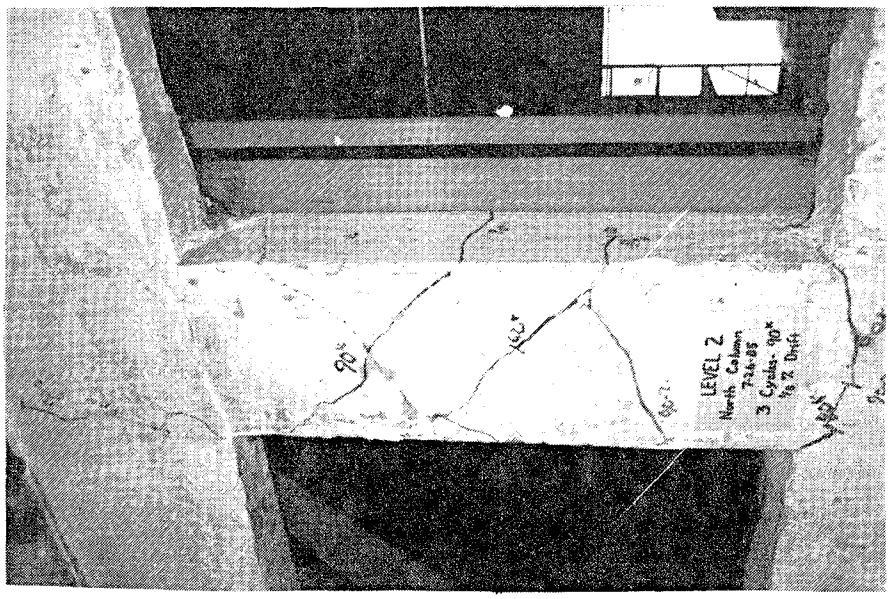

(a) 90 kips

Fig. 4.6 Crack patterns in north column, second level

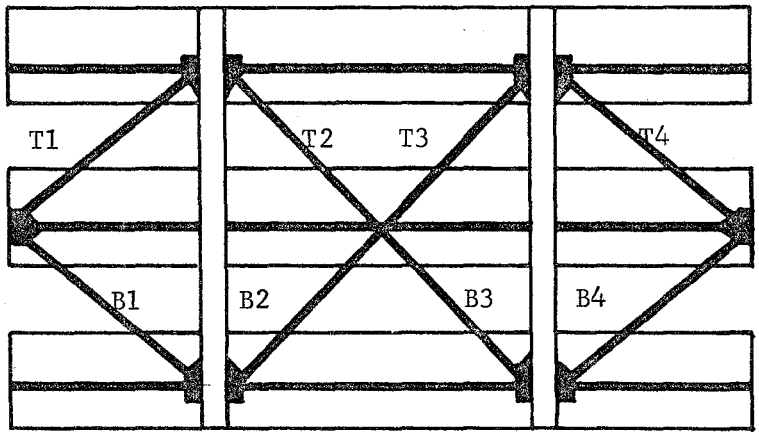

Fig. 4.7 Brace notation

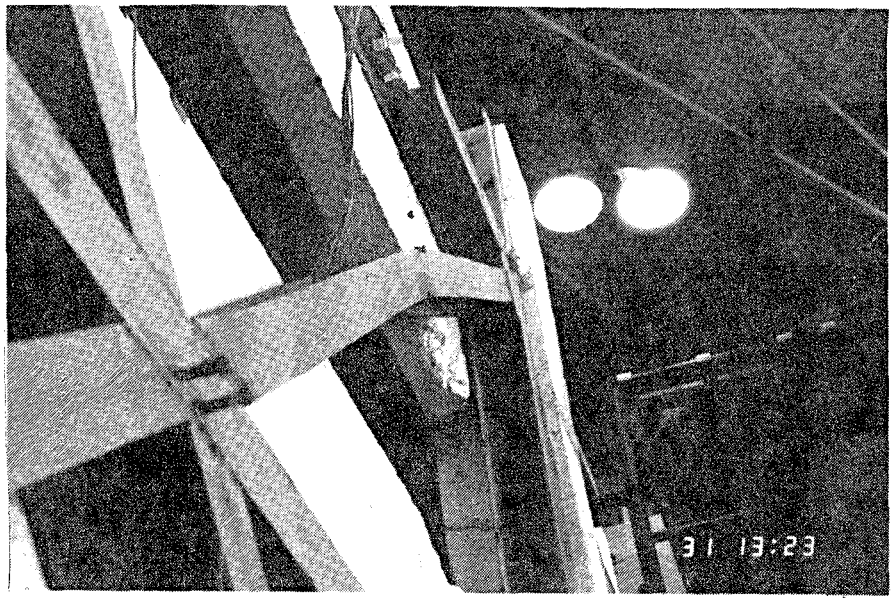

Fig. 4.8 Buckled brace T3

failure mode did not involve the welds.

In the second cycle that 300 kips was attained in the north direction, brace T3 began to bend, although the lateral displacement of the frame was held constant. Point 7 in Fig. 4.5 shows when the brace started to bend, and the dotted line displays the drop in applied load to 285 kips which occurred while the brace buckled.

The applied load was increased to 321 kips, and displacement was maintained while brace T3 continued to deform. The load dropped to 306 kips, and a scan was taken at load-displacement point 8. This displacement represents 0.5 percent interstory drift between the second and third floors. Half percent interstory drift had already been reached in the south direction at point 6.

At the peak load of the second cycle, 352 kips north, brace T3 had buckled as shown in Figs. 4.8 and 4.9 and by point 9. Figure 4.8 displays the buckled shape of brace T3, and Fig. 4.9 is a closer view showing the compression yield lines on the bottom side and the thin diagonal lines on the tension side. The reference lines on the spandrel beam in the bottom left corner of Fig. 4.9 marked the movement of the brace. At this stage brace T1 had compression yield lines in the web but no indication of buckling. The strain gages on the braces showed an average stress of 38 ksi.

During the second loading south, brace T2 began to bend at about 200 kips. At 290 kips (point 10), a weld failed. However, it appeared that the weld failure was caused by the very large strains at the end of the braces developed during the previous buckling failure. The inside flange of the bottom of brace T3 had fractured from the middle connection. Local buckling of the flanges had been produced in the connection area previously when the brace itself was buckling in compression. The concentration of high local deformations led to the weld failure.

Loading continued until the peak of 309 kips was reached which is shown as point 11. At this stage, brace T4 was just beginning to bend, and brace T2 had buckled.

For the third cycle, loading was applied to a level of 357 kips north, when brace T1 buckled for the first time. Figure 4.10 displays the buckled braces, T1 and T3, and also the tension brace T2, which had not straightened completely. None of the braces at the first level showed any movement. When brace T1 buckled, the lateral load dropped to 316 kips producing point 13

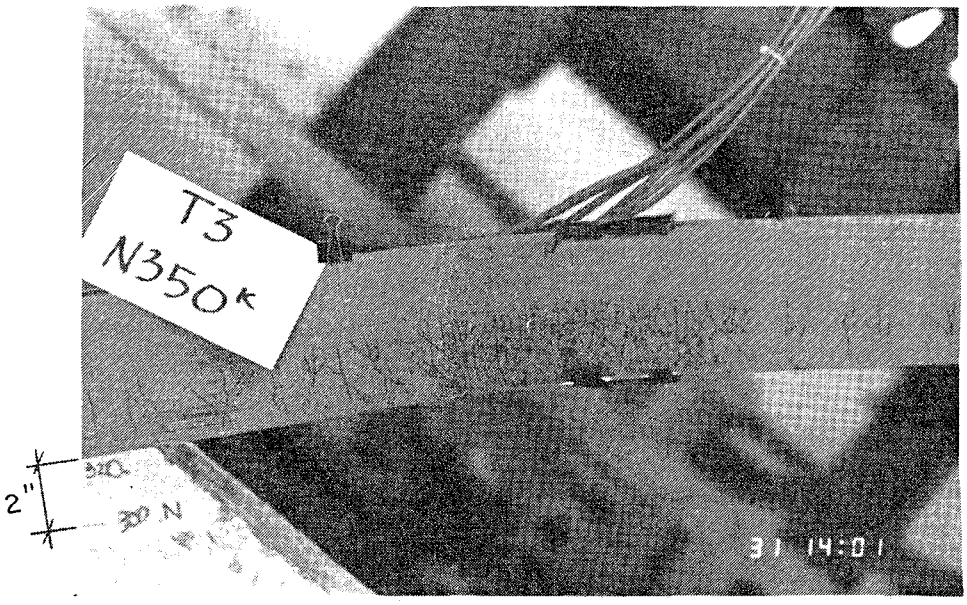

Fig. 4.9 Brace T3 hinge

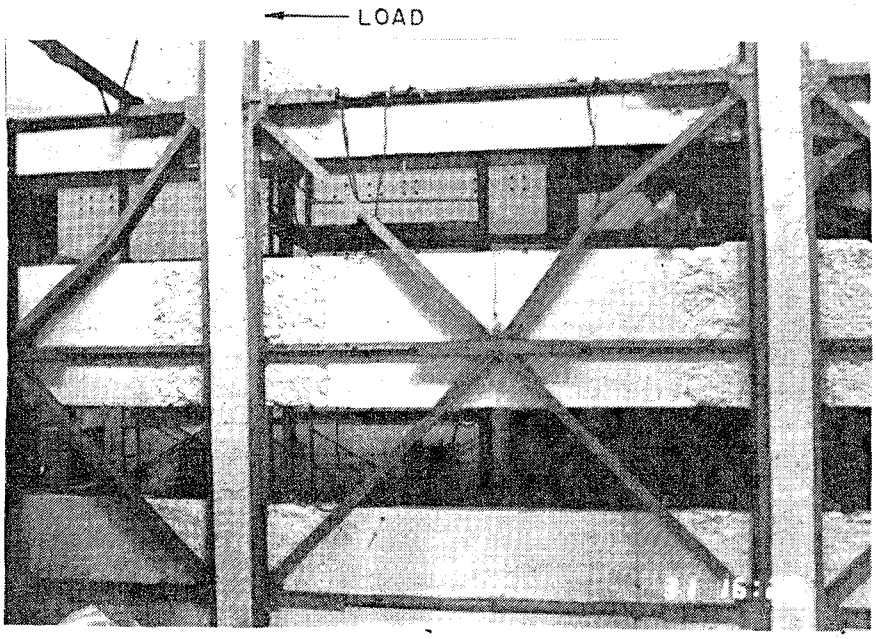

Fig. 4.10 Braces at peak load north

on the curve. At this stage, compression yield lines were noticed on the channels. Figure 4.11 shows yield lines on the north side of the south column near the top of the first sprandrel.

The load was reapplied to a level of about 360 kips (dotted line on Fig. 4.5), when failure at the second level occurred and the load dropped to 237 kips as indicated by point 14. The failure was caused by the complete fracture of the weld at the bottom of brace T2 and shear failure of the columns at the second level. Which occurred first is not certain; however, the dramatic loss in load was traced on the X-Y plotter the instant the weld failed. At this time, the top of the channel on the south side of the south column pulled away from the concrete column. The dowels failed by pulling out cones of concrete from the columns (Fig. 4.12). This occurred in a region where two dowels had been omitted and two were shorter than 5-1/2 in. due to difficulties in drilling holes. In addition, the concrete at this level had the lowest strength (see Fig. 3.1 and Table 3.2). Figure 4.12 also shows the cracks on the exterior of the column and the tension yield lines in the brace.

The slab side of the south column at the second level is pictured in Fig. 4.13. This photo displays the shear failure of the column and the offset at the maximum interstory drift north, which was 1.2 percent.

Figure 4.14 shows the weld failure at the bottom of brace T2. The local buckling caused by high strains at the ends may be seen in the top left corner of the photo.

The frame was unloaded and then loaded in the south direction. Data were scanned at 230 kips (point 15). The lateral load was increased to 245 kips when two welds broke. Load suddenly dropped to 215 kips where a scan was taken (point 16). The bottom of tension brace T3 had fractured further, along with a flange at the top of compression brace T4 which was in tension due to the buckling of the member.

Load was applied for the final time reaching 220 kips before dropping to 125 kips when the bottom welds of both tension braces, T1 and T3, fractured completely. At point 17, the second level interstory drift was 1.3 percent. Around this time, the columns at the second level failed in shear in the south direction. Figure 4.15 shows the wide cracks and exposed reinforcement in the columns at the end of the test.

Figure 4.16 displays the weld failure of brace T1 at the connection to the 1 in. thick gusset plates of the strut

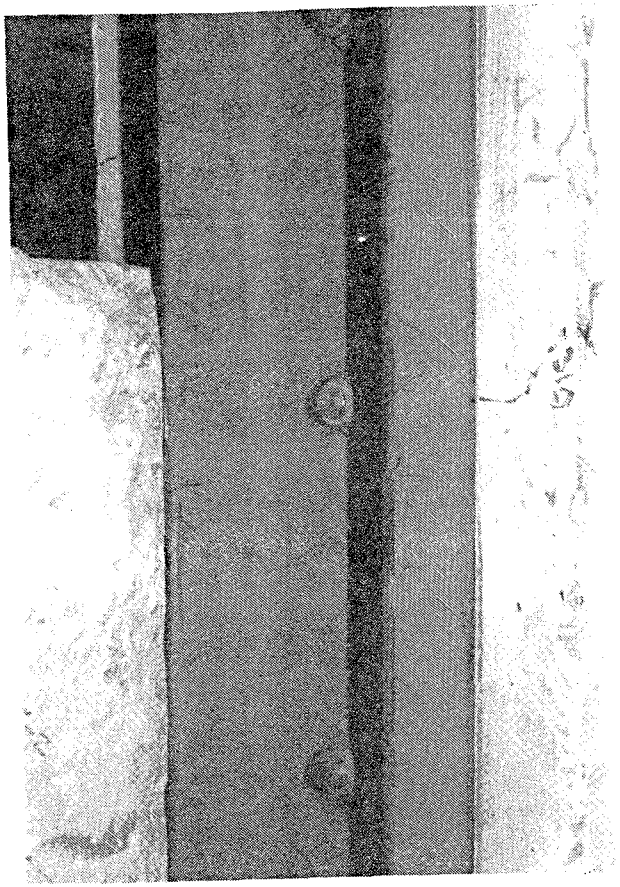

Fig. 4.11 Compression yield lines on channel

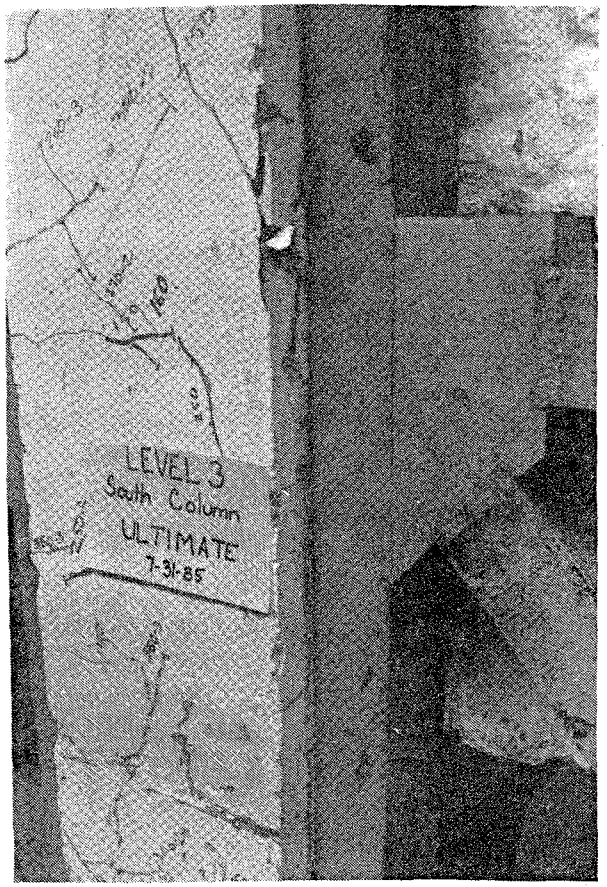

Fig. 4.12 Dowel pullout

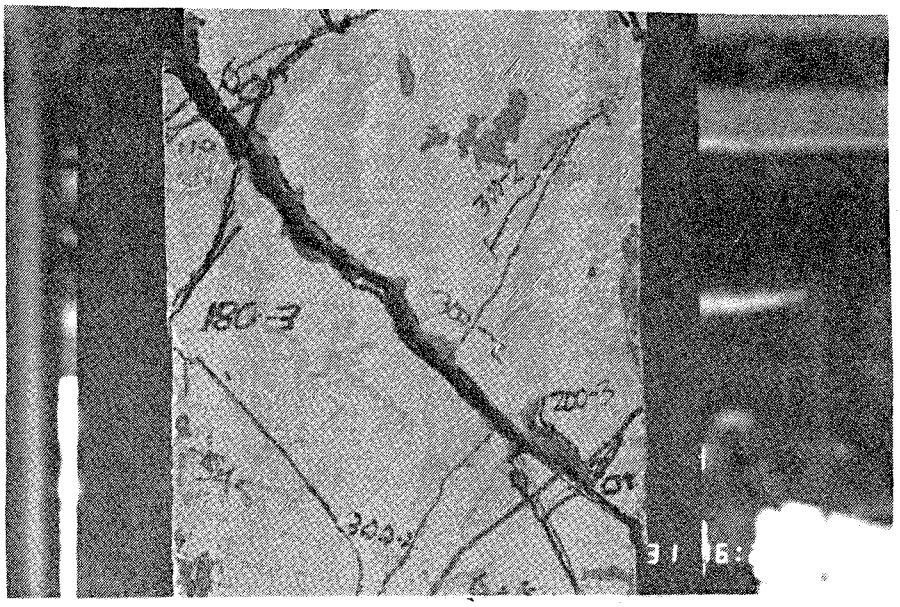

Fig. 4.13 South column at maximum drift north

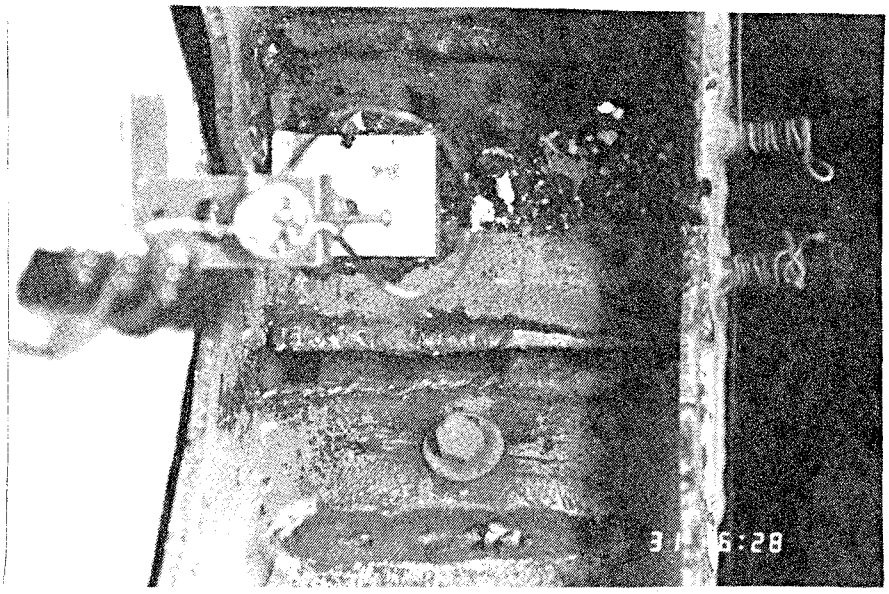

Fig. 4.14 Weld failure at bottom of brace T2

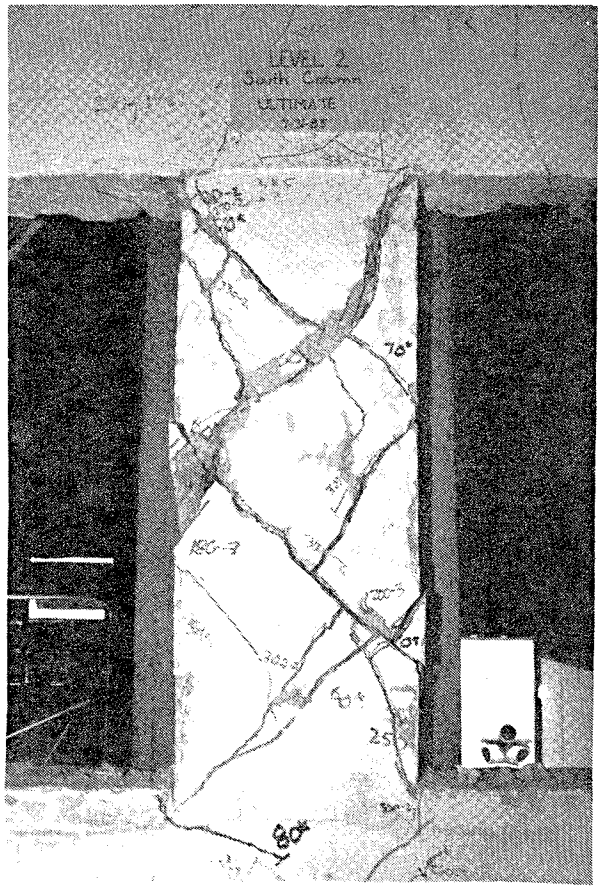

(a) South column

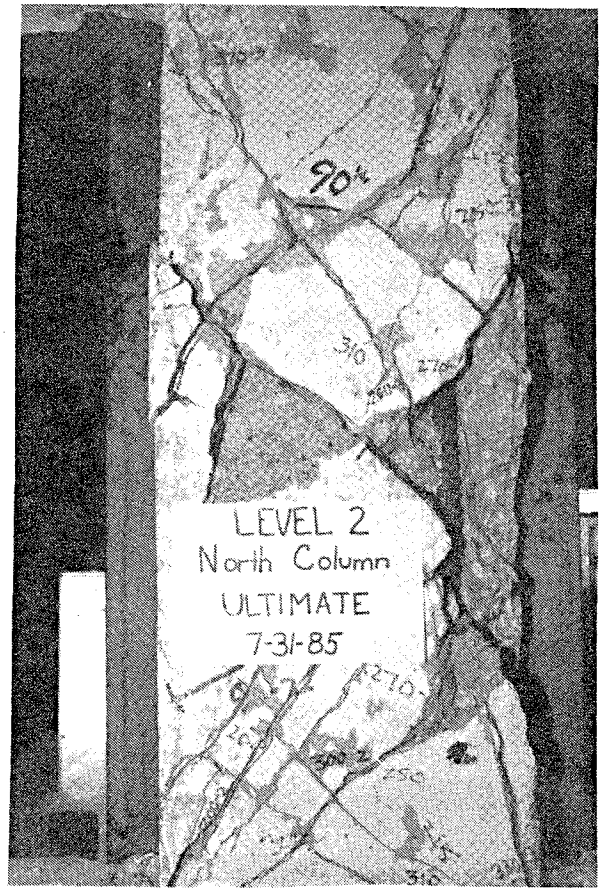

(b) North column

Fig. 4.15 Second level columns at ultimate

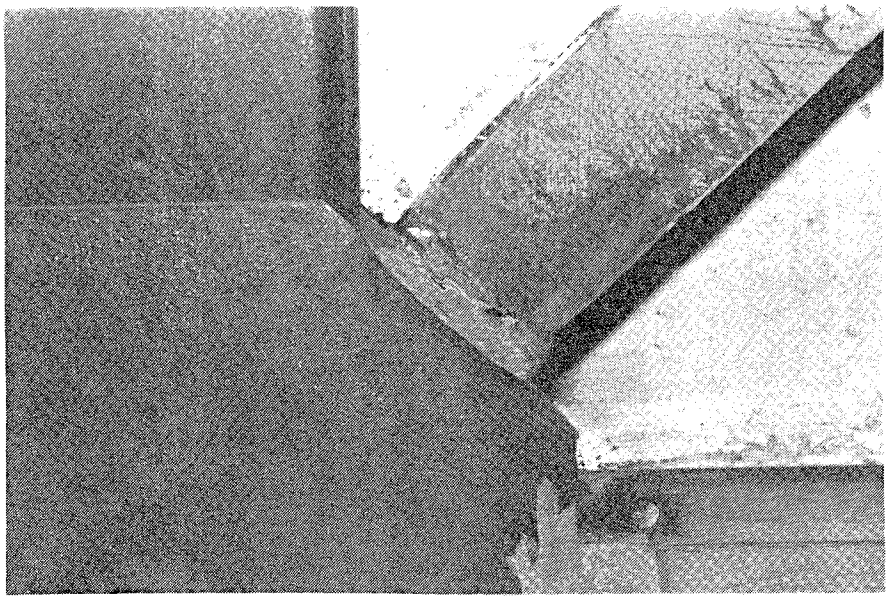

Fig. 4.16 Weld failure at bottom of brace T1

assembly. Part of the fracture surface was through the brace flange rather than through the weld or weld-steel interface. Note the diagonal tension yield lines on the brace and the dark region near the end where all the paint had flaked off the surface.

4.3 Stiffness of Strengthened Frame

4.3.1 Comparison with Bare Frame. The load-deflection curve for the first of the bare frame tests is shown in Fig. 4.17 along with the first cycle load-deflection curve for the steel braced frame. The curves indicate that the strengthened frame had a stiffness about one and a half times that of the original frame. It must be noted that the steel braced frame was initially cracked which reduced its stiffness.

4.3.2 Calculation of Drifts. Drifts were computed from the displacement transducer data as described in Section 3.4.2.1. Table 4.1 shows the drift levels, in percent, for the single-story and two-story drifts. The values at all peak loads are given, except where they are the same in the second and third cycles. The loads near the end of the test which are not necessarily peak loads (because the load dropped before the data could be obtained) are shown in parentheses.

The interstory drifts were about equal at the start, but at load levels exceeding 200 kips there were differences between the drifts in the two directions. In the north direction, the first level was more flexible, while in the south direction, the second level showed less stiffness. As the test progressed, the second level became less and less stiff when the frame was pushed south. In the north direction, the second level did not become the more flexible story until cycle F2, which was when the first brace buckled.

The difference in interstory drifts is obvious from Fig. 4.18 where load-drift curves are compared for the last set of cycles. A maximum drift of about 1 in. occurred in the second story, whereas the largest value for the first level was 0.43 inches. Even without the last cycle (where failure in the second level occurred) the second level drifts were larger than the first, especially in the south direction. Unless otherwise stated, the drift values presented refer to the total two-story drifts.

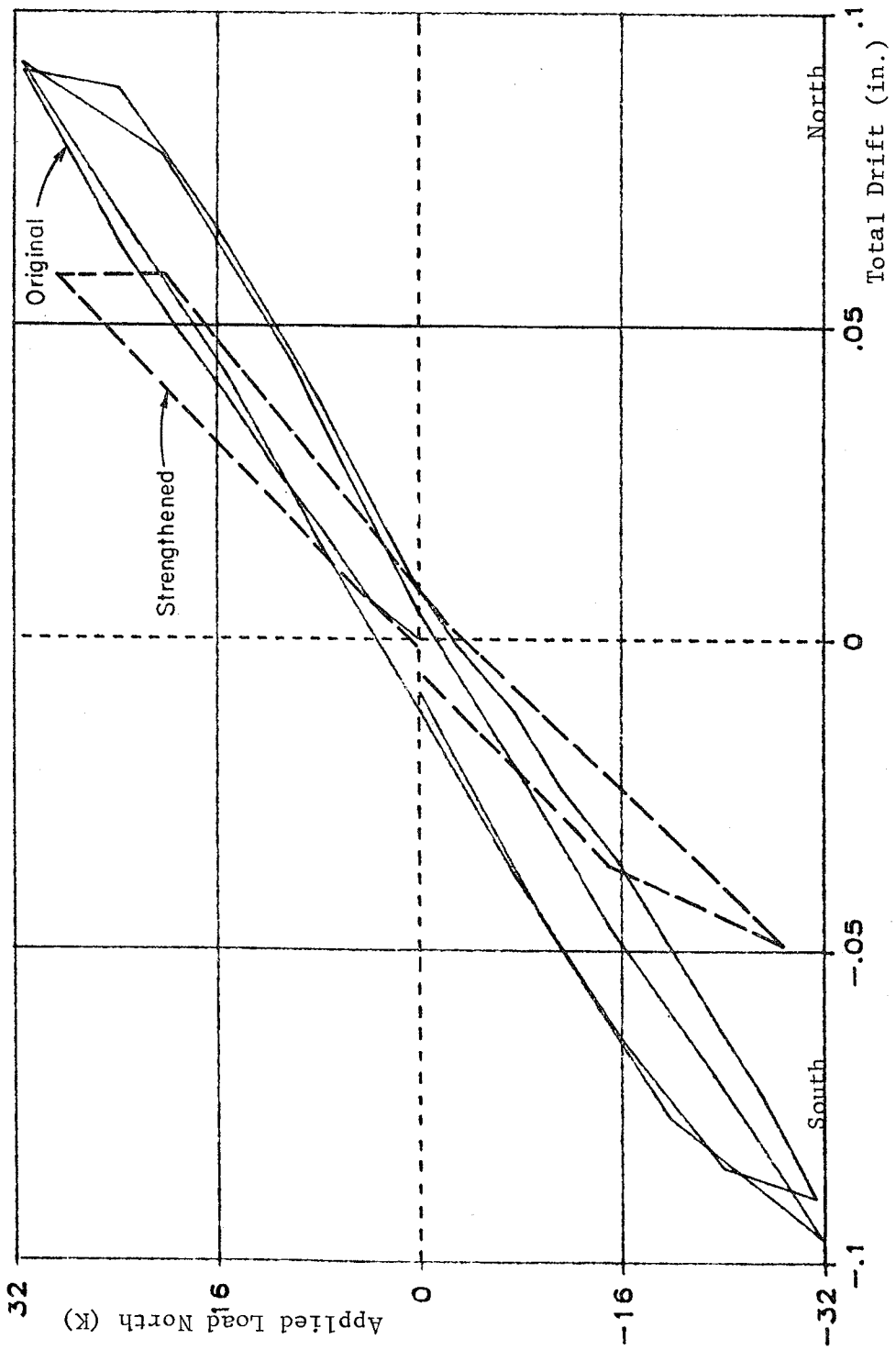

Fig. 4.17 Load-Displacement Curves for Original and Strengthened Frames

Table 4.1 Drifts at Peaks - Steel Test

Load North (kips)	% Drift First Level	% Drift Second Level	% Drift Total
91	0.105	0.100	0.102
150	0.174	0.152	0.163
200	0.228	0.206	0.217
211	0.248	0.217	0.232
199	0.239	0.220	0.230
300	0.380	0.347	0.363
298	0.394	0.334	0.364
286	0.383	0.351	0.367
331	0.476	0.436	0.456
352	0.517	0.586	0.551
357	0.544	0.680	0.612
(316)	0.528	0.773	0.650
(237)	0.492	1.182	0.837
Load South (kips)			
91	0.086	0.103	0.094
150	0.149	0.198	0.173
185	0.205	0.252	0.228
180	0.204	0.254	0.229
270	0.312	0.398	0.355
264	0.310	0.400	0.355
257	0.308	0.401	0.354
(289)	0.342	0.503	0.423
309	0.396	0.613	0.504
(215)	0.296	0.735	0.516
(125)	0.247	1.308	0.778

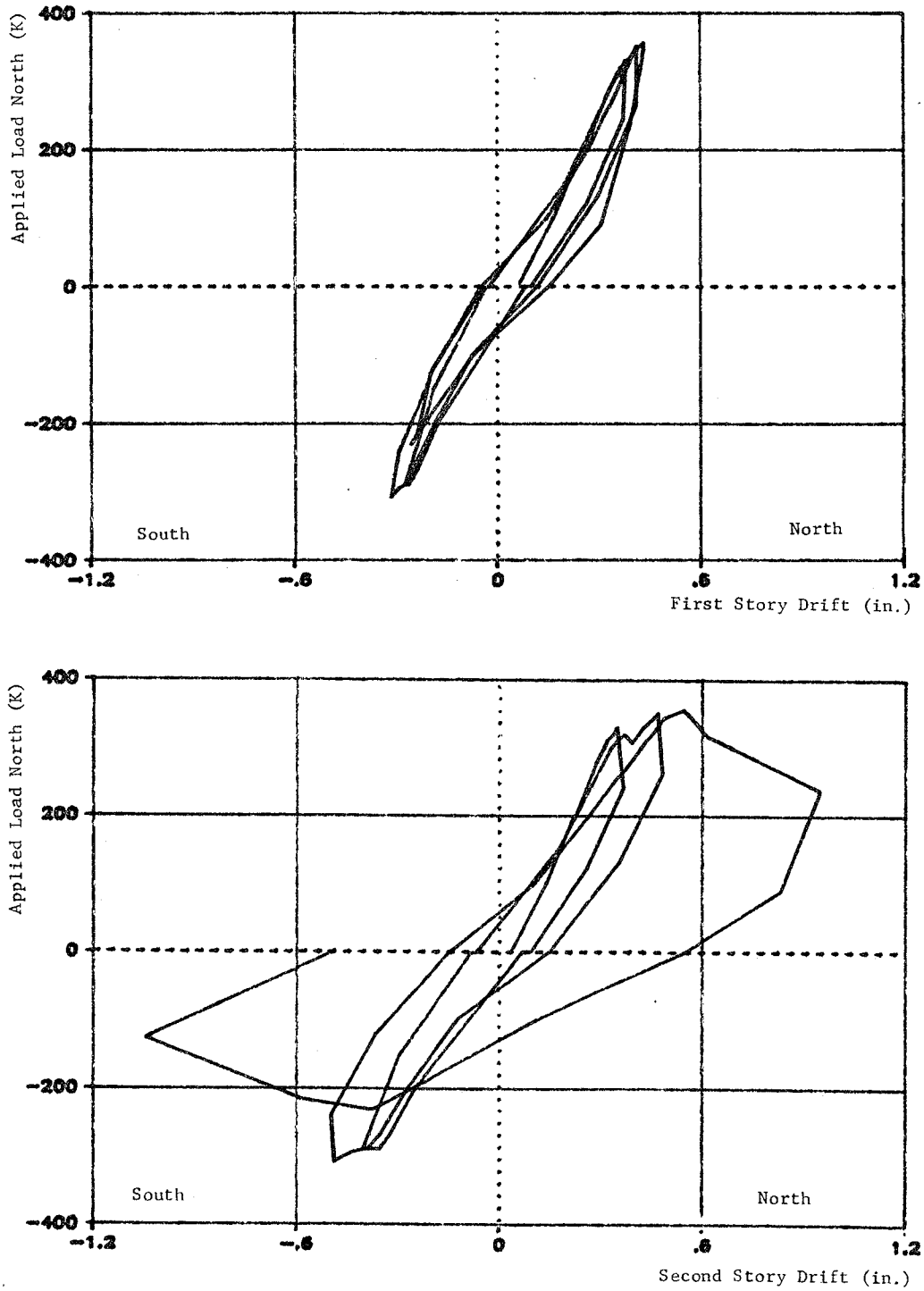

Fig. 4.18 Comparison of Interstory Drifts - Final Three Cycles

4.3.3 Loss of Stiffness. Figure 4.19 is a graph of the first cycles up to a load level of 200 kips. There was no apparent loss of stiffness at this stage. However, the two directions seemed to be behaving differently. Drawing secant stiffness lines to each peak in the north direction would indicate a slight increase in stiffness between 60 and 200 kips. Doing the same in the south direction shows a decrease in stiffness between peaks. The increase in stiffness in the north direction may have been caused by friction between the loading frame and the concrete specimen. When loaded north, the spandrel at the third level came in contact with the end plate on the two structural tubes of the loading frame. The spandrel and the plate moved apart when the frame was pushed south.

At these displacement levels, there was essentially no loss in stiffness during the second and third cycles of a set, as verified by Fig. 4.20. This graph shows all three cycles of the set at 0.23 percent drift. There were only slight decreases in stiffness in the north direction with each cycle.

In subsequent cycles, the loss in stiffness is more apparent. In Fig. 4.21, the three cycles at 0.36 percent drift are overlain with a load-displacement envelope of all previous cycles. Both directions indicate a reduction in stiffness between 200 and 300 kips, and small losses with each new cycle.

The decrease in stiffness was continued into the last set of cycles, as shown in Fig. 4.22. The envelope of previous loads is drawn with the final three cycles. In the north direction, there was a loss in stiffness with each new cycle. In the south direction, the stiffness remained the same for the first cycle, but the frame became more flexible with each of the two remaining cycles. The dramatic loss in stiffness for both directions occurred when the welds failed on the tension braces.

4.4 Discussion of Connections

The connections of the steel bracing system, welded steel-to-steel and dowelled steel-to-concrete connections, had a major effect on the behavior of the frame with respect to lateral capacity, stiffness, and ductility. Specifically, improvements in the design and quality control of the welded brace-to-gusset plate connections and the layout of dowels in the column channels would have transferred the failure mechanism from the connections to the steel members and, thus, would have produced more ductile

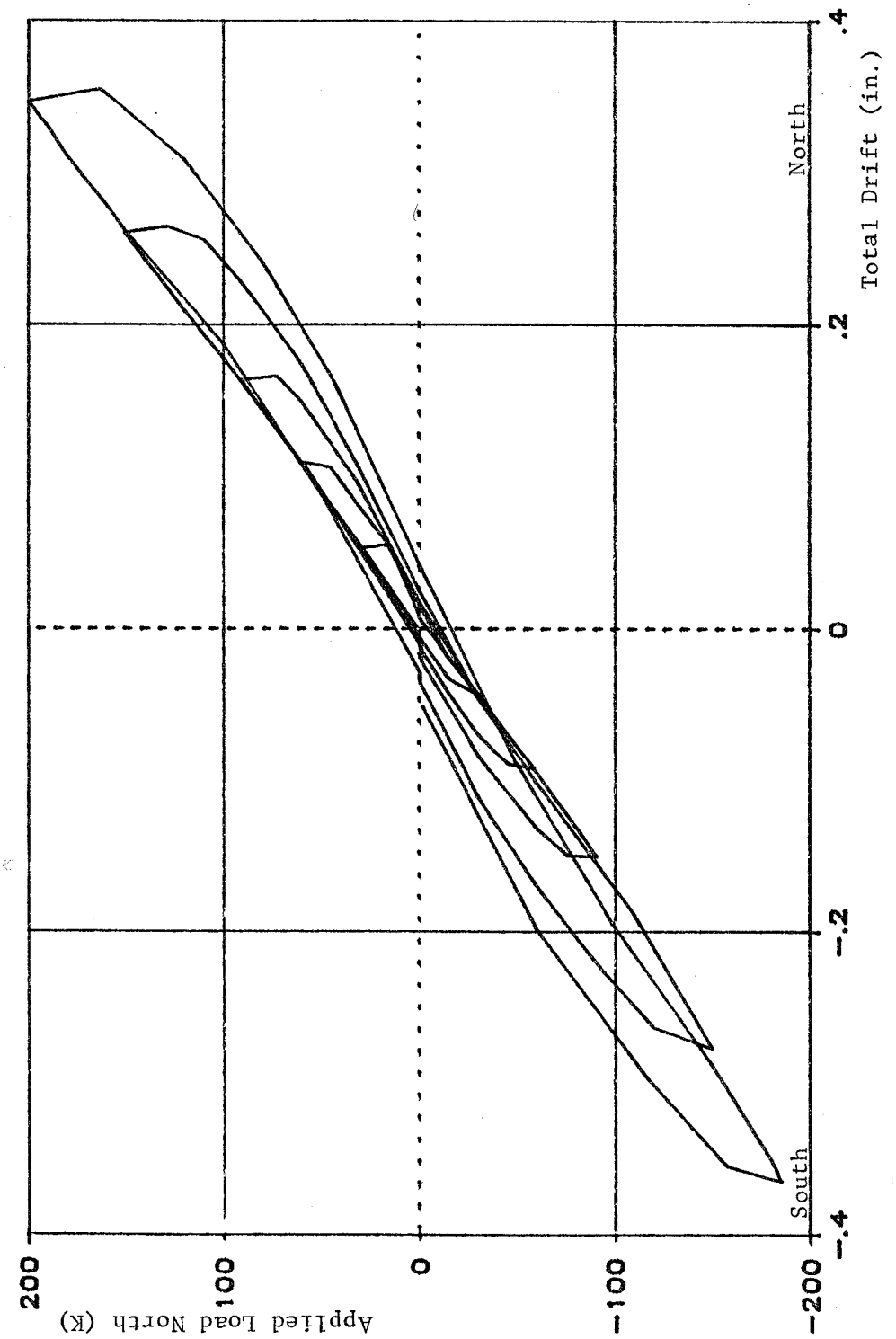

Fig. 4.19 First cycles up to 200 kips

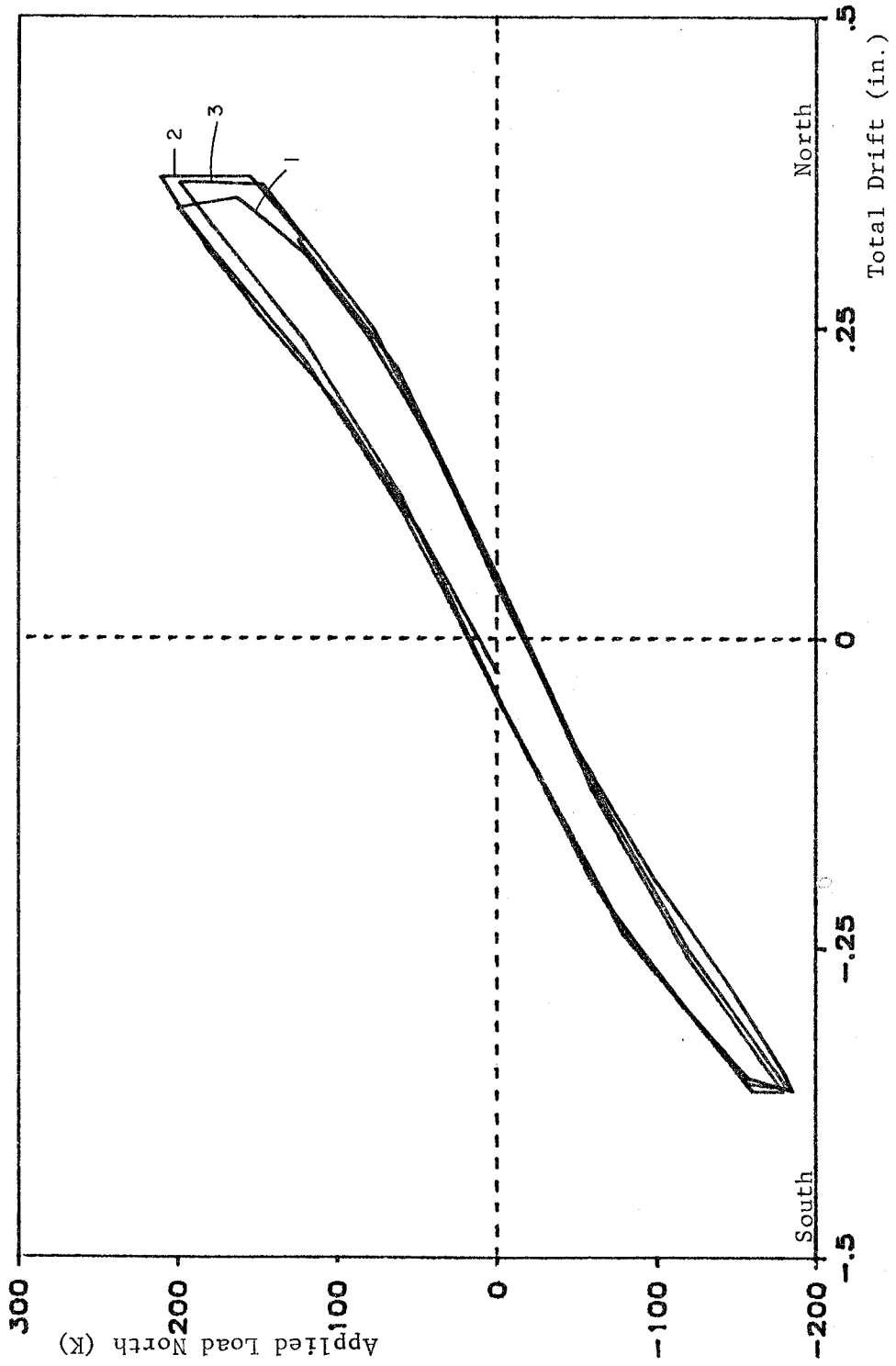

Fig. 4.20 Set of three cycles at 0.23% drift

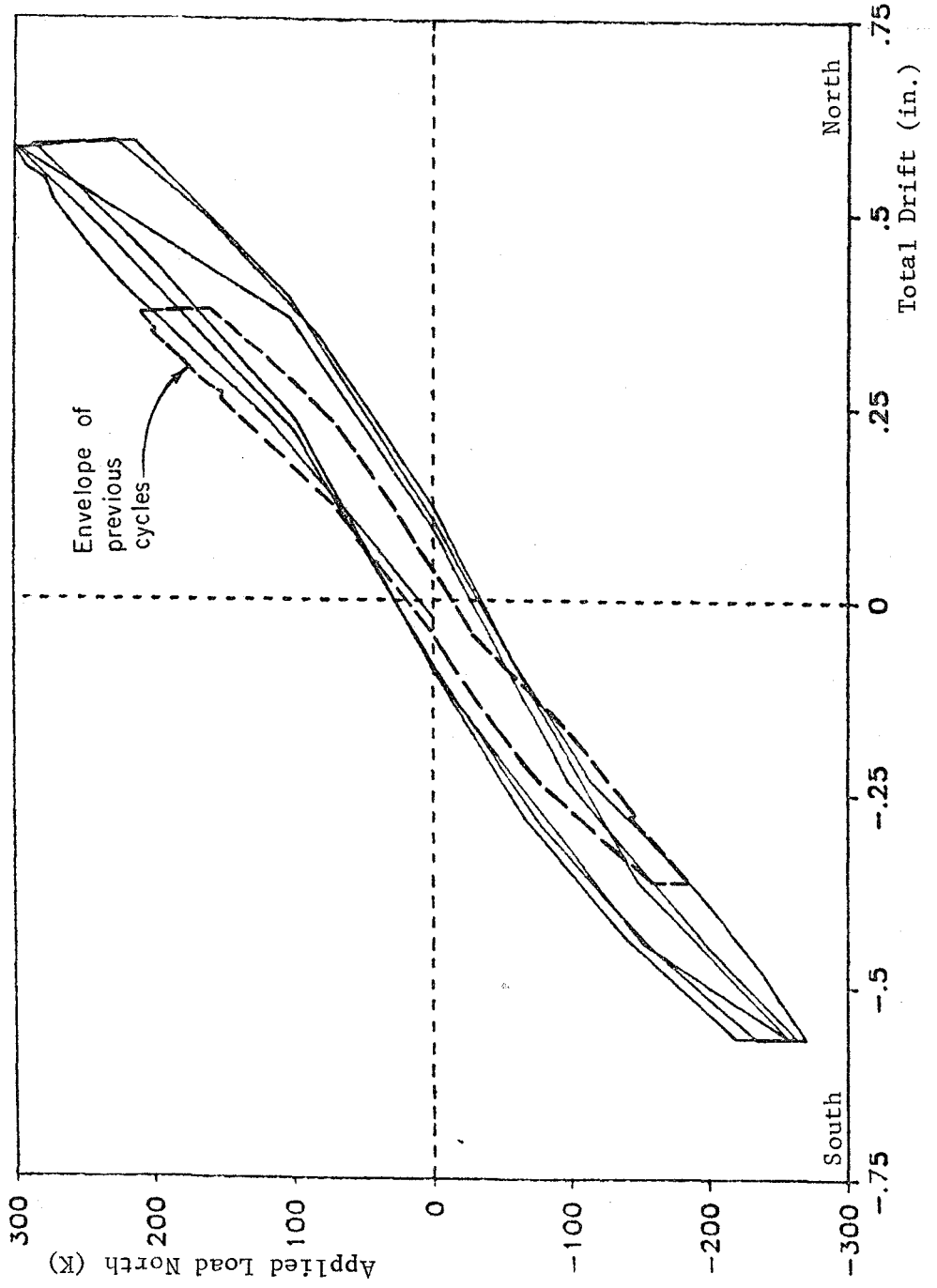

Fig. 4.21 Set of three cycles at 0.36% drift

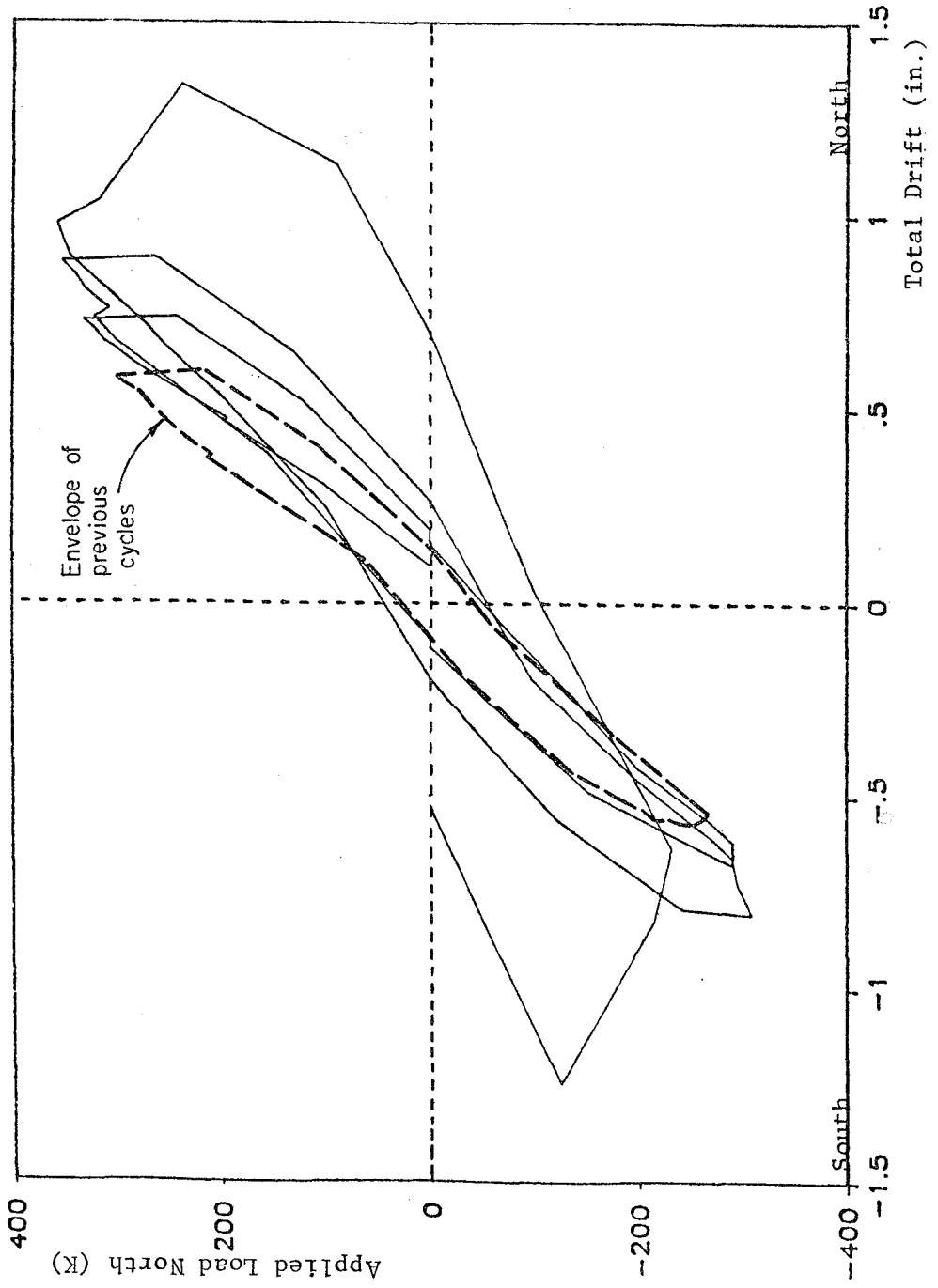

Fig. 4.22 Load-displacement relationships for entire test

behavior.

The brace-to-gusset plate connection design used in the test program will work in actual structures if full penetration is achieved over the entire areas connected. With full penetration of the appropriate weld material, failure should occur as fracture in the steel member before failure of the weld. Full penetration of the welds in the test program was not always achieved because the welding process did not follow all the specifications in the Structural Welding Code of the American Welding Society [22]. For complete joint penetration groove welds made without backing plates, the weld must be formed from both sides (Section 4.6.9), which was not done for the test welds. In addition, clamps or jacks should be used to align members which are over 10 percent out of alignment. The connection as designed provides no room for backing plates or clamps where the flanges are against the concrete spandrels. During the test, it was observed that higher quality welds improved the performance of the entire system. The three welds which were redone during the test allowed larger loads to be carried by the structure.

The design of the welded connections required butt welds and a relatively small weld area. At large loads and displacements, the weld failures were instigated by high secondary stresses due to local yielding and bending of the flanges at the ends of the braces. All of the welds that failed during the last two load cycles were connecting braces which had previously buckled. When the brace was under compression, local buckling occurred near the connections which resulted in permanent deformations and large secondary stresses when the brace was then loaded in tension.

Unless the brace flanges and webs were aligned almost perfectly with the gusset plates, it was impossible to build up a weld connecting the entire end surface of the brace to the gusset plates without clamps. This was especially true for the middle connection where the braces were welded to 1/4 in. web gusset plates and 1/4 in. thick tee flanges. The two-thirds scale braces (flange and web thicknesses of 3/16 in.) magnified the problem of aligning two thin plates and increased the probability of local buckling. Figure 4.23 shows two close-up views of the brace-to-channel connection. Note the very thin brace and collector tee flanges framing into the 1/2 in. gusset plates.

Due to the problems associated with achieving full penetration in the brace-to-gusset welds, design of the connections should be modified. Thicker gusset plates would

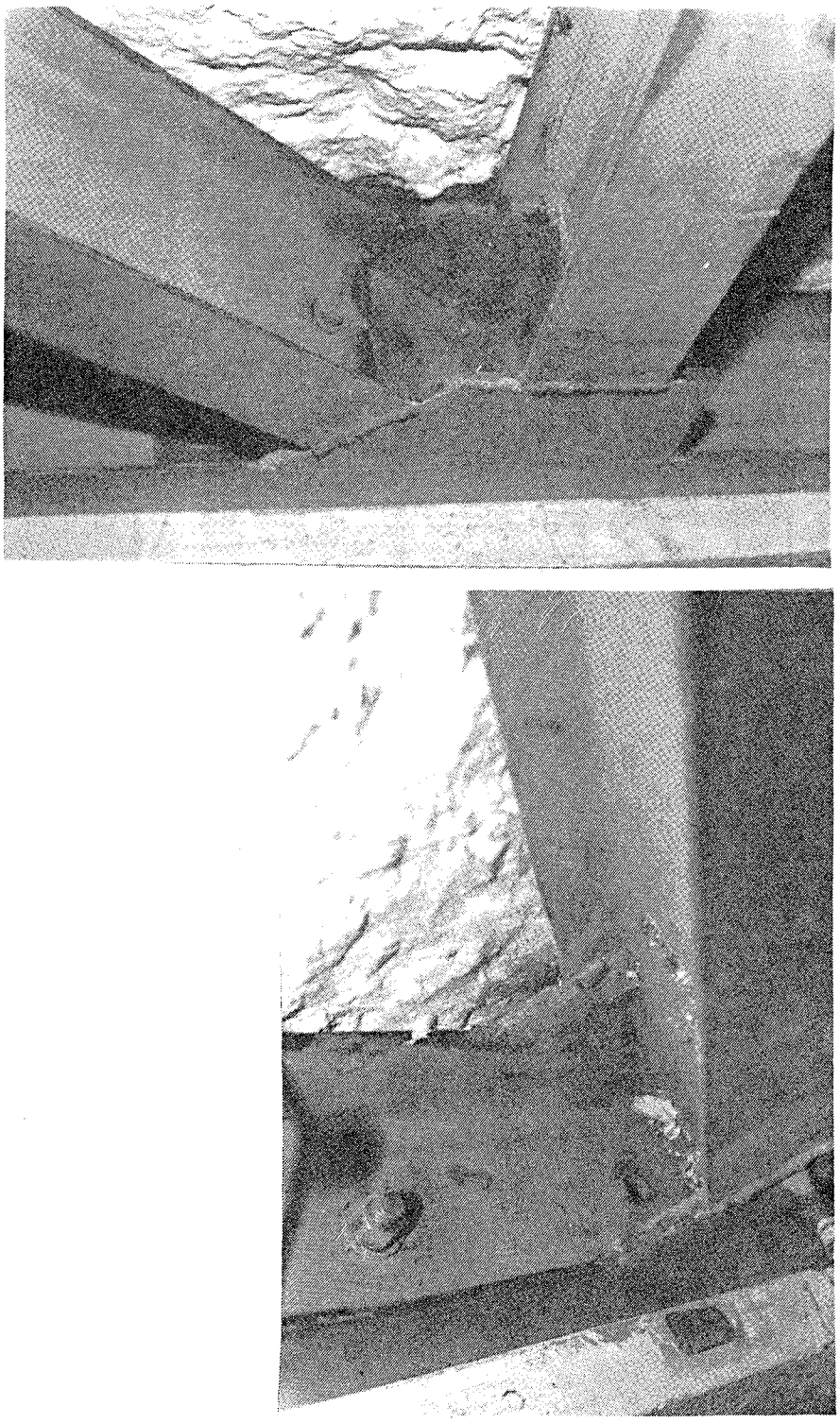

Fig. 4.23 Close-up of welded connection

reduce the alignment problems so that the entire surface at the end of the brace could be welded without the use of clamps. In addition, the concrete surface behind the gusset plates could be chipped to allow room for backing plates. A detail that would ensure that a sufficient portion of the end of the brace is fully penetrated would be to weld a larger area. Figure 4.24(a) shows a connection where the brace is inserted in a slot in the gusset plates and welded around the sides. A disadvantage of this connection is the problem with alignment.

There were even more problems associated with the connection at the intersection of the four braces at the collector tee. The thin web plates and tee flanges and the proximity of plates made it difficult to align and weld. An improved configuration is shown in Fig. 4.24(b) where two octagon-shaped gusset plates connect the flanges of the four braces. Web gusset plates transfer the load between webs and act as stiffeners. The tee on each side is welded to the gusset plates and short tee sections are added as before. All gusset plates should be 1/4 to 1/2 in. thicker than the parts joined. By making the connection stiffer and adding more dowels close to the intersection, better transfer of load between the steel braces and concrete floor slab may be attained. Transfer of load between the four braces attached to the middle connection will be discussed in Chapter 5.

Spacing of the dowels, which was based on the shear capacity of the threaded rods, was satisfactory. It would probably be just as safe and more economical to put fewer dowels in the collector tees, since no problems were observed. For the channel dowels, pullout seemed to be more of a concern than shear capacity of the threaded rods. The largest forces producing separation of the channel from the concrete column were at the brace-to-channel connection, where it was impossible to insert dowels due to interference of the diagonal web gusset plate. Therefore, it would be wise to use a smaller dowel spacing close to the connection.

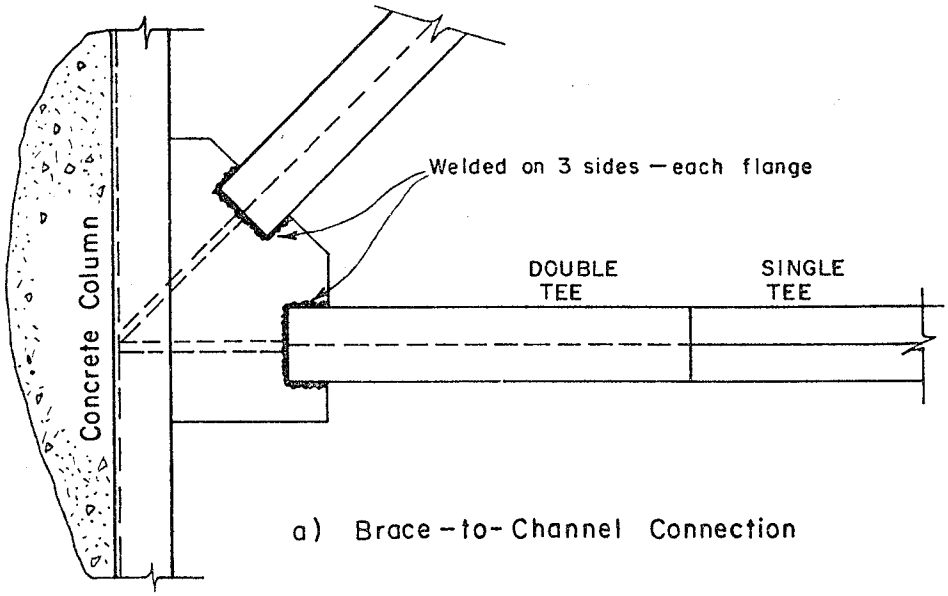

a) Brace-to-Channel Connection

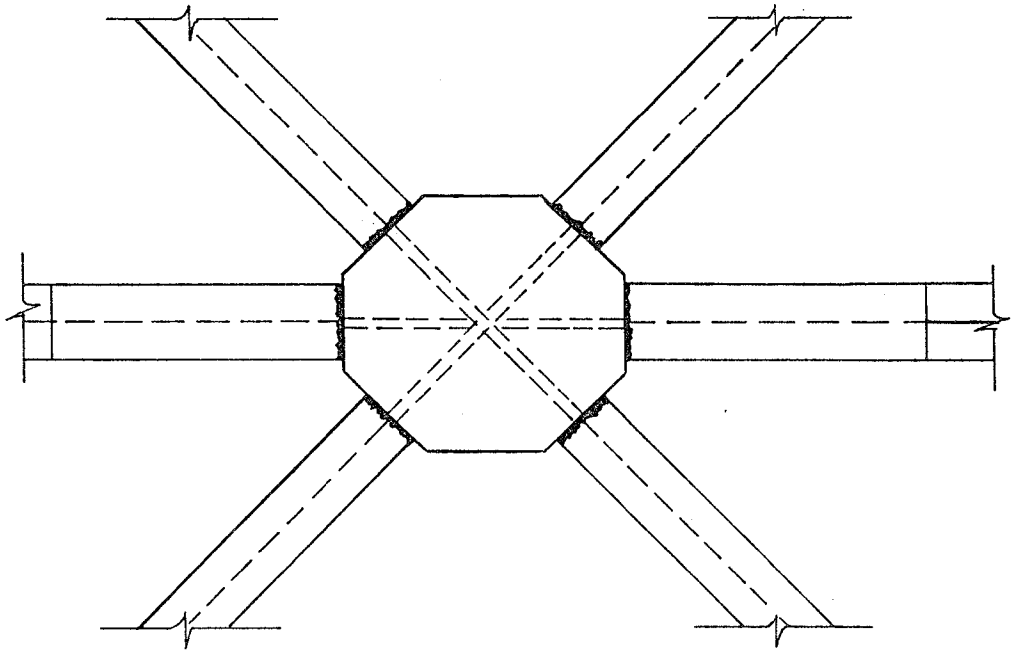

b) Middle Connection

Fig. 4.24 Alternate Connection Designs

CHAPTER 5

DETAILS OF TEST RESULTS

5.1 Behavior of Braces

5.1.1 Strains. Strain gages were attached to six of the diagonal braces in groups of four as was shown in Figs. 3.27 and 3.28. The gages were placed on the inner side of the flanges close to the tips where maximum bending stresses were expected to occur.

The strains measured using each set of four gages were plotted to determine the consistency of readings at a section. Figure 5.1 displays the strains from the four gages on brace B3 for all load cycles on the steel braced frame (brace notation - Fig. 4.7). The four strains were consistent except for the strain measured by gage number 22 during the three cycles to peak lateral loads of 90 kips. Before loading further the bad gage was replaced, and the four strains were consistent for the remainder of the test. The axial force in brace B3 was computed using the four strains for all load stages except those during the three cycles to 90 kips lateral load where the strains from the three good gages were used.

Strains measured in the other braces were very similar to the strains plotted in Fig. 5.1. Two gages on braces at the upper level had to be replaced during the test after inconsistent strains were recorded during the early cycles. In all subsequent cycles, brace axial load was calculated using the average of the four strains.

The arrangement of strain gages on the four flange tips at the mid-length of the brace was chosen so that the initiation of buckling could easily be monitored. Figures 5.2 and 5.3 display the onset of instability in braces T2 and T3.

The strains in brace T2 plotted versus applied lateral load are shown in Fig. 5.2(a) for the portion of cycle F1 (first of the final three cycles - Fig. 4.5) when the frame was pushed south. At 200 kips lateral load, strains at two locations (flanges on same side of web) leveled off while strains at the opposite side began to increase at a faster rate. After 270 kips lateral load, strains in two gages started dropping due to bending of the brace. After reaching the peak load in cycle F1 (290 kips), the frame was unloaded. The strains observed when the frame was loaded south in the next cycle are shown in Fig.

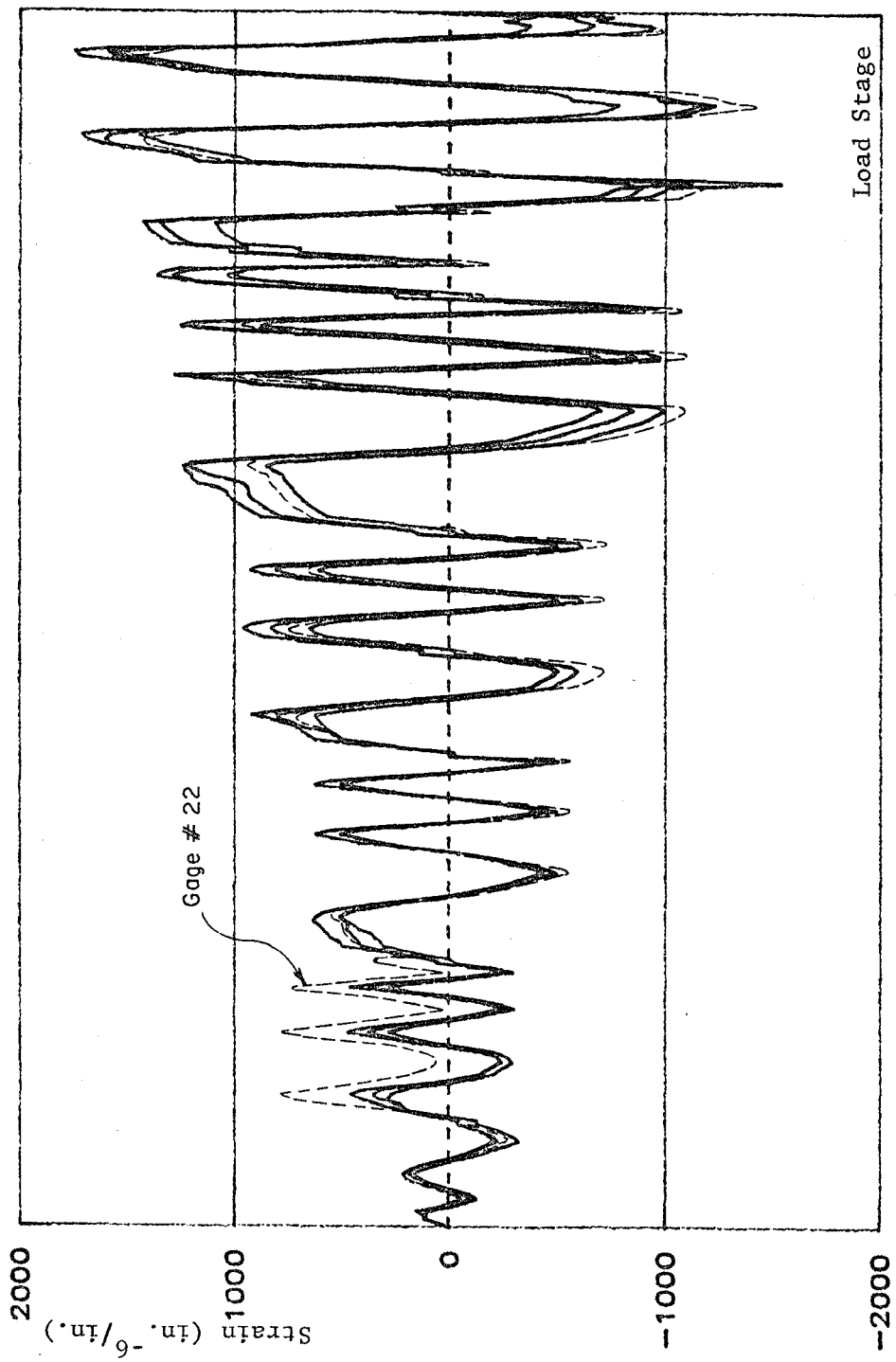

Fig. 5.1 Variation of strains - Brace B3

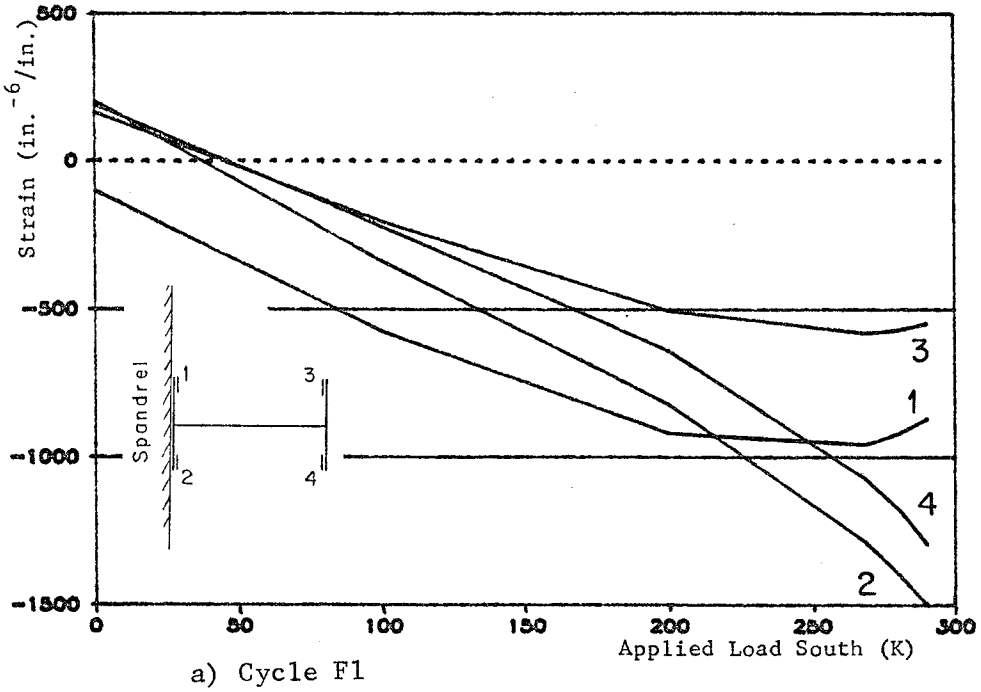

a) Cycle F1

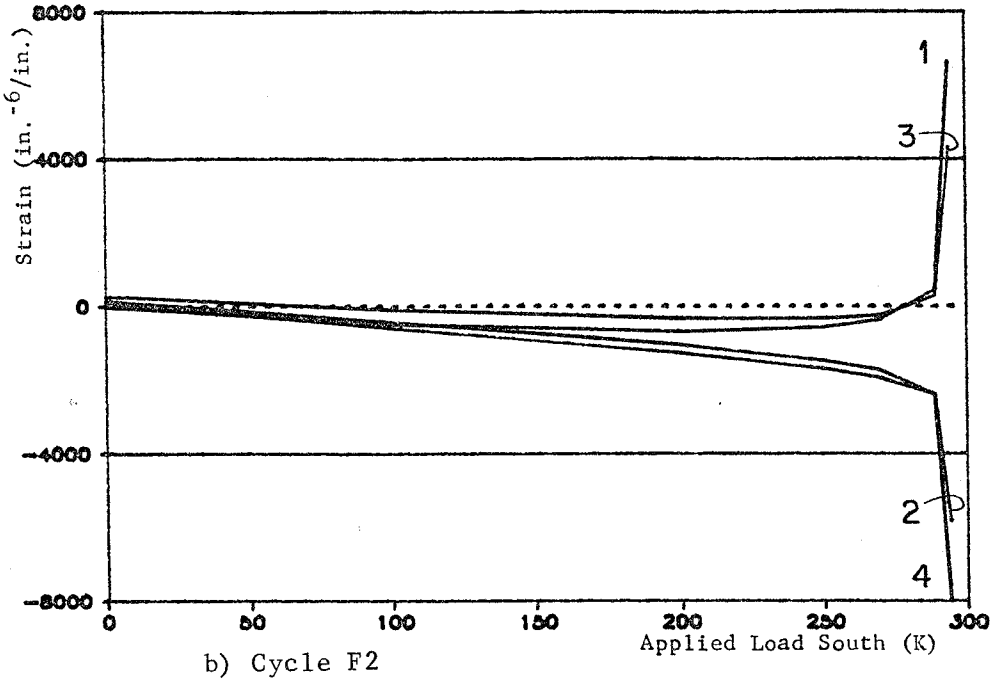

b) Cycle F2

Fig. 5.2 Buckling of Brace T2

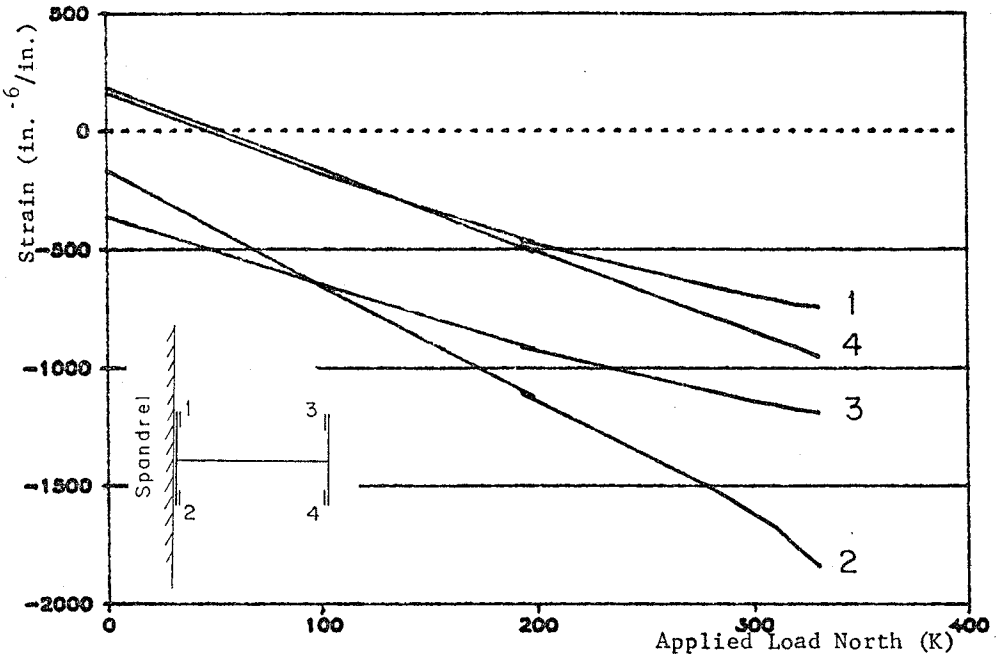

a) Cycle F1

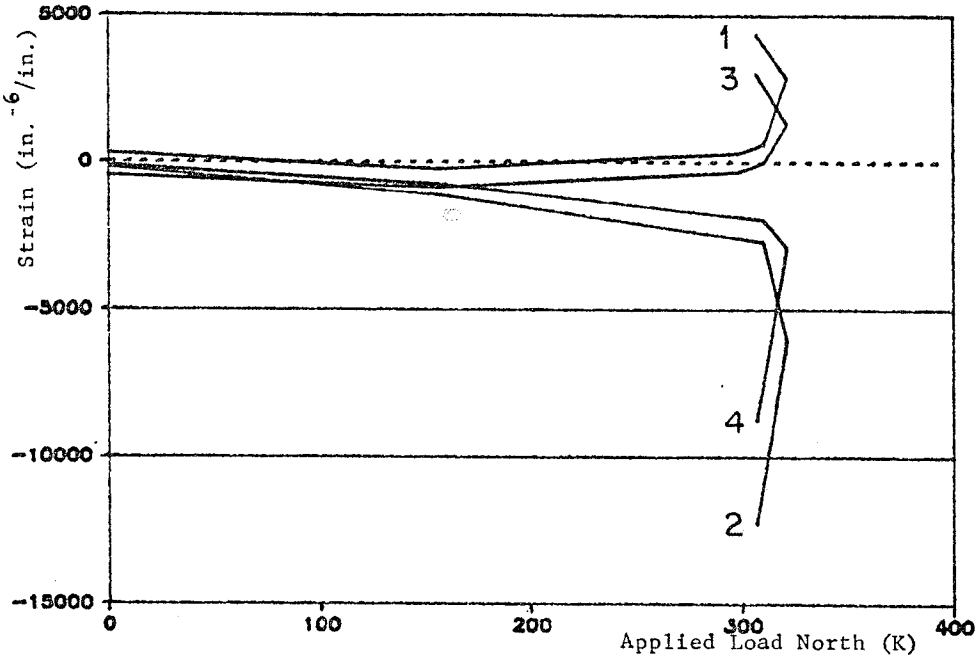

b) Cycle F2

Fig. 5.3 Buckling of Brace T3

5.2(b), which has a different scale than Fig. 5.2(a). The brace buckled before the peak lateral load of 309 kips was reached. At lateral loads in excess of 290 kips, strains were very large indicating general yielding at that location. Observations of the brace clearly indicated that a hinge had formed at the mid-length of the brace.

In Fig. 5.3(a) brace T3 was beginning to show some bending at the north peak of cycle F1 (first of the three final cycles). The graph in Fig. 5.3(b), which is at a different scale than Fig. 5.3(a), shows that the strains began to deviate at an applied load of only 160 kips during cycle F2. At 321 kips, under constant displacement of the frame, brace T3 buckled and the lateral load dropped to 306 kips. The graph is terminated at this level because the gages were no longer reliable.

An example of a complete cycle of a set of four strain readings is shown in Fig. 5.4 for brace T4 during the second of the final three cycles. At the peak lateral load to the south, the brace became unstable, but deformation was not so large that the gages were lost. The arrows show that strain increased at two gages and decreased at the other two during the increase in lateral load to the south from 294 to 309 kips. After this level, the readings from the four gages may not be useful in computing the axial load in the brace due to the localized yielding at the mid-length of the member.

5.1.2 Brace Loads. For all six instrumented braces, the average strain was computed, and from that the average stress, axial load, and horizontal component of the axial load were calculated. The loads were reliable for load stages before brace instability was reached; the axial load carried by a brace could not be determined after buckling.

5.1.2.1 Comparison of Brace Loads. Figures 5.5 to 5.7 display the redistribution of loads between the top four braces. In each graph, the horizontal component of the axial load in the brace is plotted against the applied lateral load. In Fig. 5.5, the loading from zero to 290 kips south during cycle F1 is shown. A scan was taken at 290 kips, just before part of the T3 weld broke and the load dropped to 289 kips where another scan was taken. The horizontal load carried by brace T3 dropped 23 kips while the loads in braces T1, T2 and T4, respectively, increased by 3, 3, and 7 kips. This left 9 kips unaccounted for which may have been carried as shear in the columns.

The portion of cycle F2 is shown in Fig. 5.6 for loading from zero to 356 kips north. When the applied load reached 321 kips, the displacement was held constant while brace T3 buckled

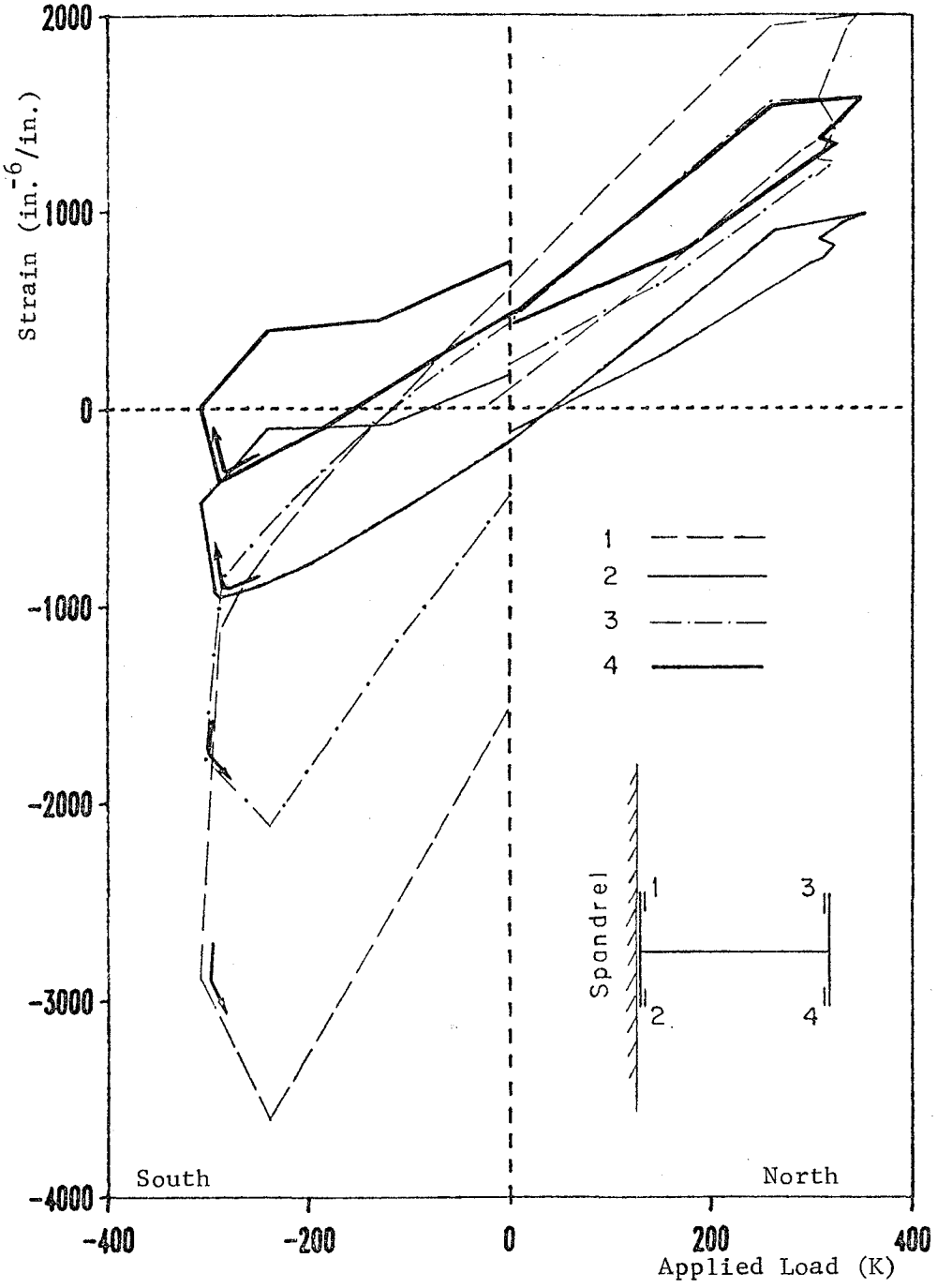

Fig. 5.4 Brace T4 Strains During Cycle F2

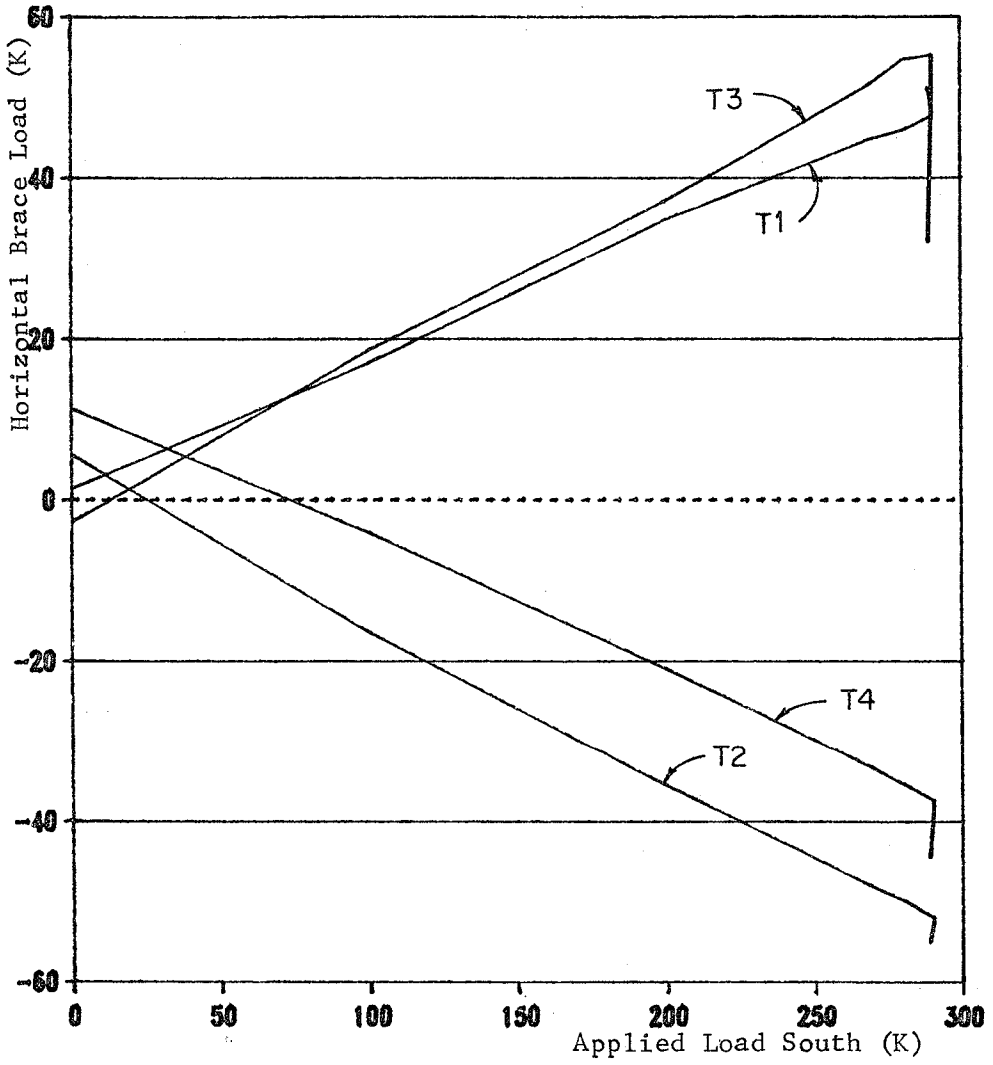

Fig. 5.5 Brace Loads During F1 Cycle - South

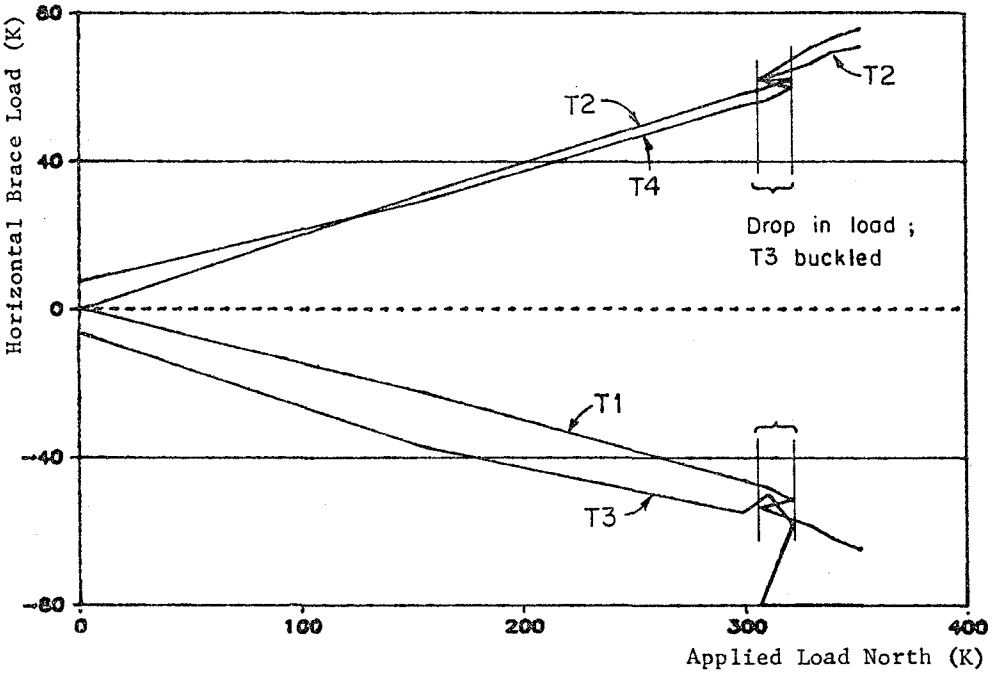

Fig. 5.6 Brace Loads During F2 Cycle - North

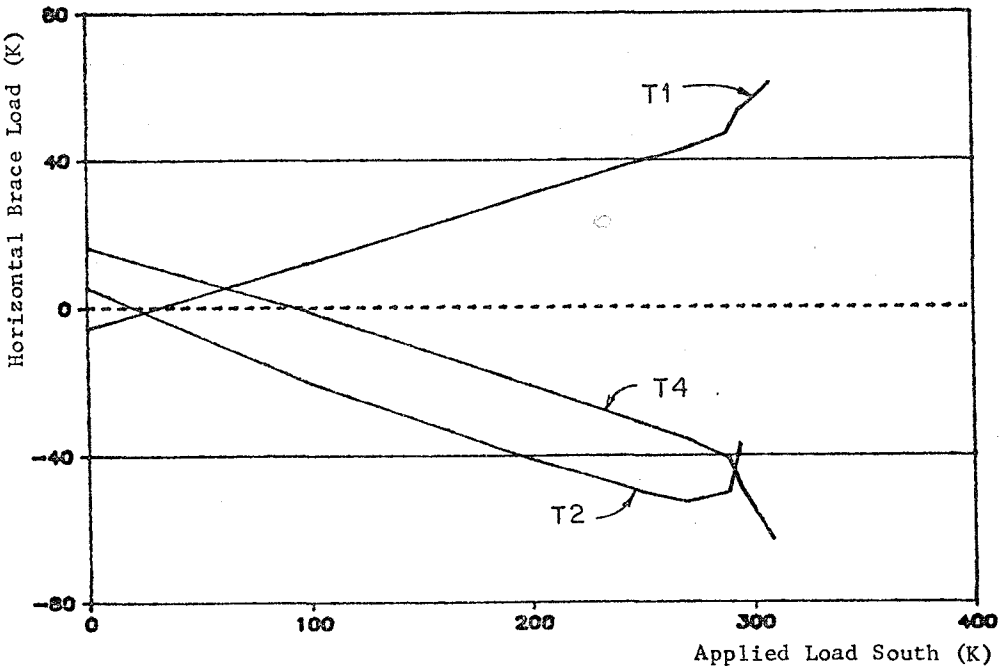

Fig. 5.7 Brace Loads During F2 Cycle - South

and the load dropped to 306 kips. During this step, the horizontal load carried by brace T1 increased by 2 kips, brace T2 stayed the same, and brace T4 picked up 2 kips. The load in brace T3 is plotted, but after about 290 kips the loads are not reliable. Between 321 and 356 kips, brace T4 picked up load at a higher rate than it had before brace T3 buckled, but the slopes for T1 and T2 remained approximately the same.

Figure 5.7 shows the stage at which brace T2 buckled during the F2 cycle south. The axial load in brace T3 is not plotted because it had buckled during the previous load north, and the gages were unreliable. After a lateral load of 290 kips was attained, braces T1 and T4 began picking up axial load at a faster rate, and it is unclear what load brace T2 was carrying.

The loads in the braces were plotted versus the applied load to compare the axial loads in each of the top level braces during the entire test. The loads at the peak of each cycle were plotted as shown in Fig. 5.8. The peaks in the north and south directions were plotted on separate graphs through the second of the final three cycles.

Residual strains increased during cyclic loading. To produce a plot of the increment in axial force versus the increment in applied lateral load, the peak brace loads were adjusted by subtracting the axial force at the previous point of zero applied load. The increment in axial load from zero applied load will be referred to as "adjusted" brace load.

In general, the two graphs indicate that the middle braces (T2, T3) carried higher loads than the outer braces (T1, T4) until the end of the test when the middle braces had buckled. In compression, the middle braces carried about 25 percent more load, while in tension they had about 15 percent more load than the outer braces. In the last load stage shown in the north direction (350 kips), brace T3 had buckled and is not displayed since the load could not be determined. The axial loads in T1, T2 and T4 jumped up at this stage. In the graph for south load peaks, braces T2 and T3 had previously buckled so are not shown in the last load stage (309 kips). The loads in both T1 and T4 showed a large increase between 290 and 309 kips lateral load. the line in the second graph of Fig. 5.8 marks the stage when part of the weld in brace T3 failed. The load in T3 dropped while the other three brace loads increased.

The brace loads were also compared by plotting them versus the interstory drift. This was done due to the differences in drift in the two directions and between the two

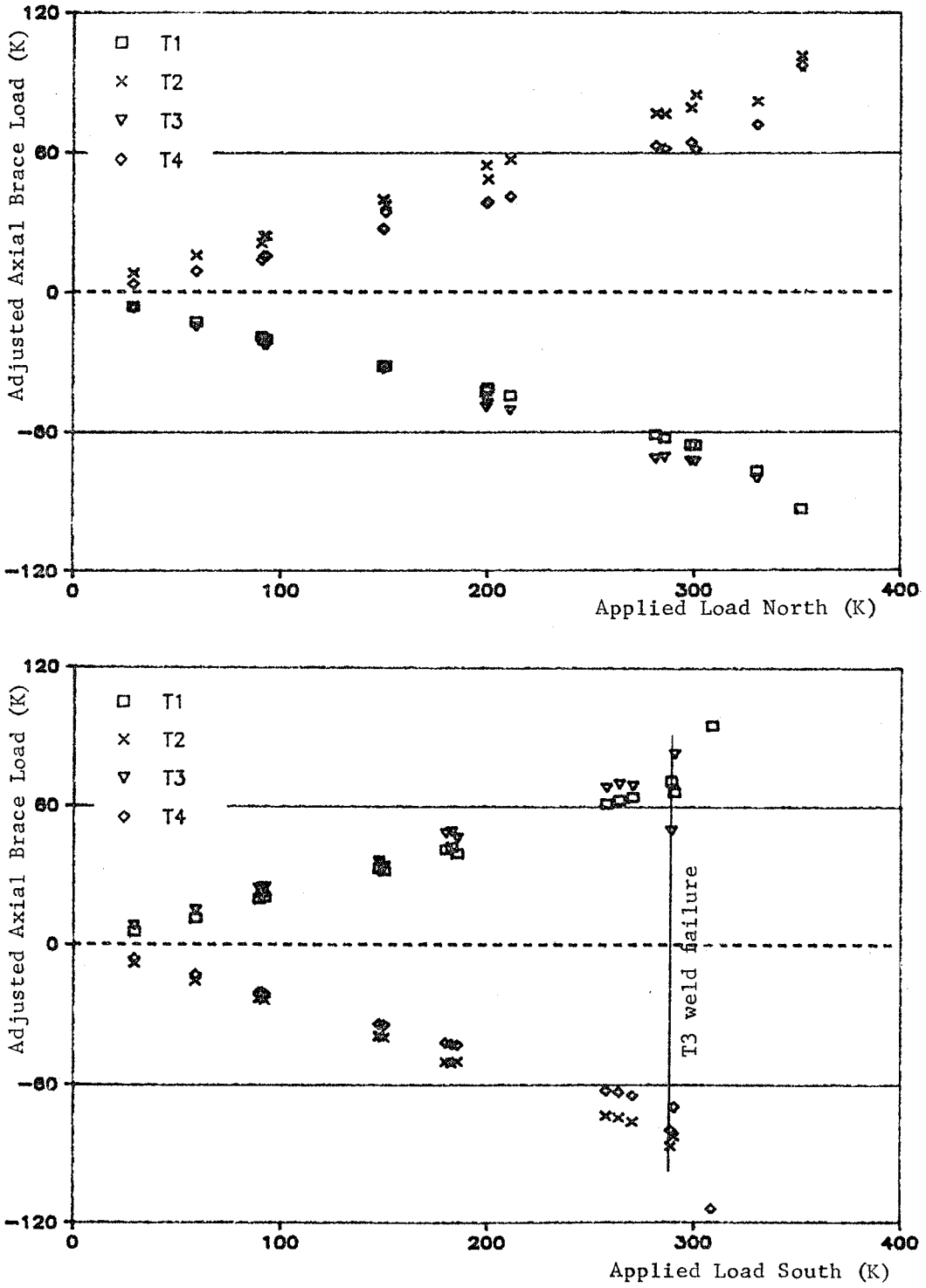

Fig. 5.8 Comparison of Top Brace Loads

stories at a given load. The four middle braces (T2, T3, B2, and B3) are compared in this manner.

Figure 5.9 shows the axial brace load plotted versus the total drift. Although the two interstory drifts were not equal, the graph allows comparisons of the four brace loads at given total drift levels. The pairs of braces (B2-T3, B3-T2), which are continuous across the connection at the second floor level, followed each other closely until the top level braces buckled. In tension the bottom two continued increasing linearly while in compression they tended to increase very little. The vertical line on the graph marks the stage just after the weld on the web of brace T3 failed.

In Fig. 5.10 the same axial loads are plotted but relative to interstory drift. Thus, the B2 and B3 points are plotted versus first story drift, and the top braces are plotted versus second story drift. The load versus drift points for the top and bottom braces were linear initially. At drifts greater than 0.25 inches, differences may be seen between Figs. 5.9 and 5.10. During the cycles when the top compression brace was bending, the axial load in the bottom compression brace was no longer increasing, and when the top brace buckled, the bottom brace load dropped although the drift level was larger. Even though the bottom compression brace was capable of carrying more load, no load was applied to it since the bottom braces are connected to those above at the X-connection at the second floor level.

5.1.2.2 Discussion of Buckling Loads. Buckling loads were predicted using AISC equation (1.5.1) for inelastic buckling without a safety factor [23].

$$P_{cr} = \left[1 - \frac{(KL/r)^2}{2C_c^2} \right] A \times F_y$$

$$\text{where } C_c = \sqrt{2\pi^2 E/F_y}$$

The flange yield strength (F_y) of 44.5 ksi obtained from tension tests was inserted in the above equations to compute buckling loads for two different K values. Rows 1 and 2 of Table 5.1 show the predicted buckling loads using the theoretical K-factor of 0.5 and the suggested design value of 0.65. The outside braces, T1 and T4, were shorter than the middle braces resulting in higher loads.

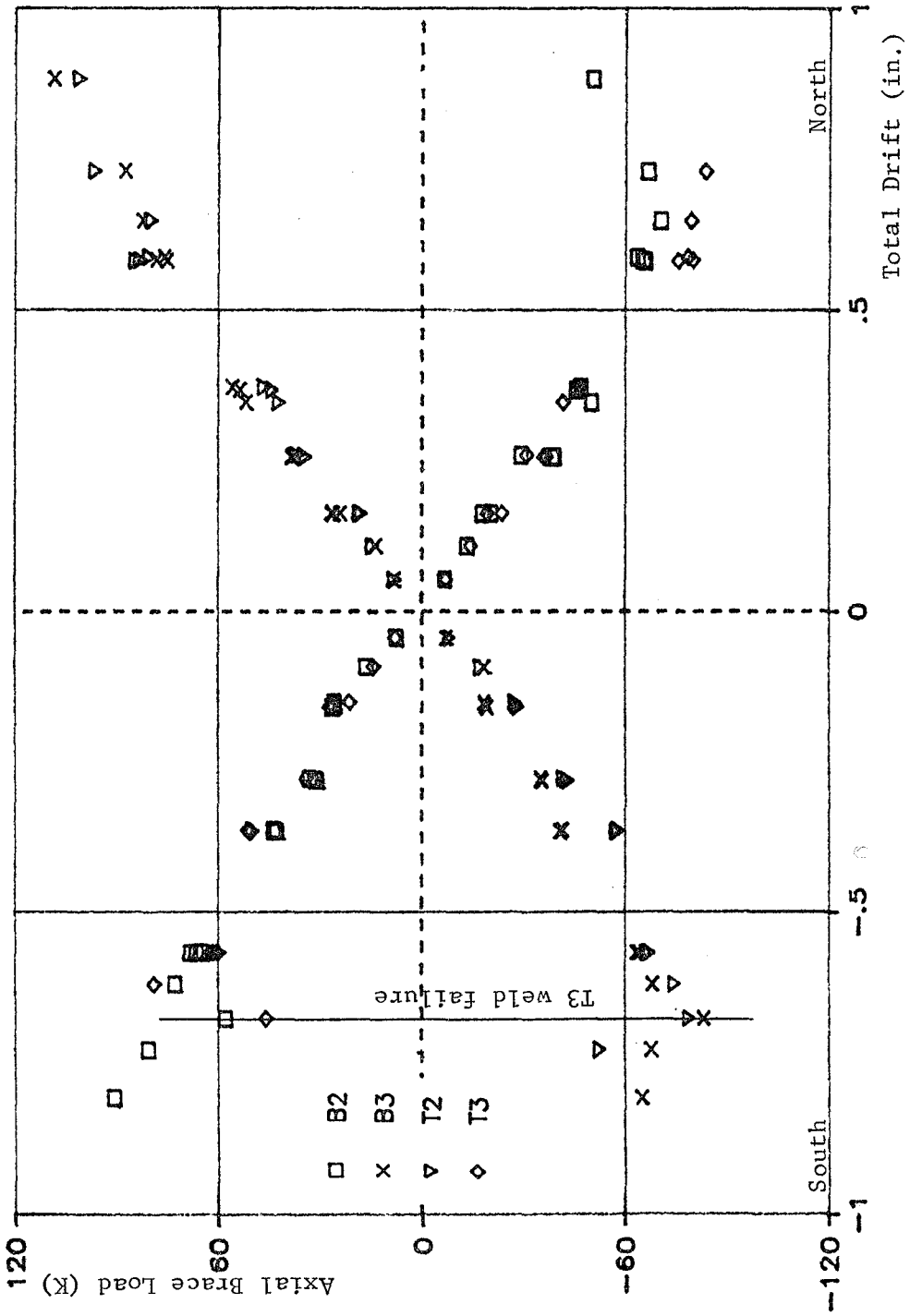

Fig. 5.9 Comparison of top and bottom braces

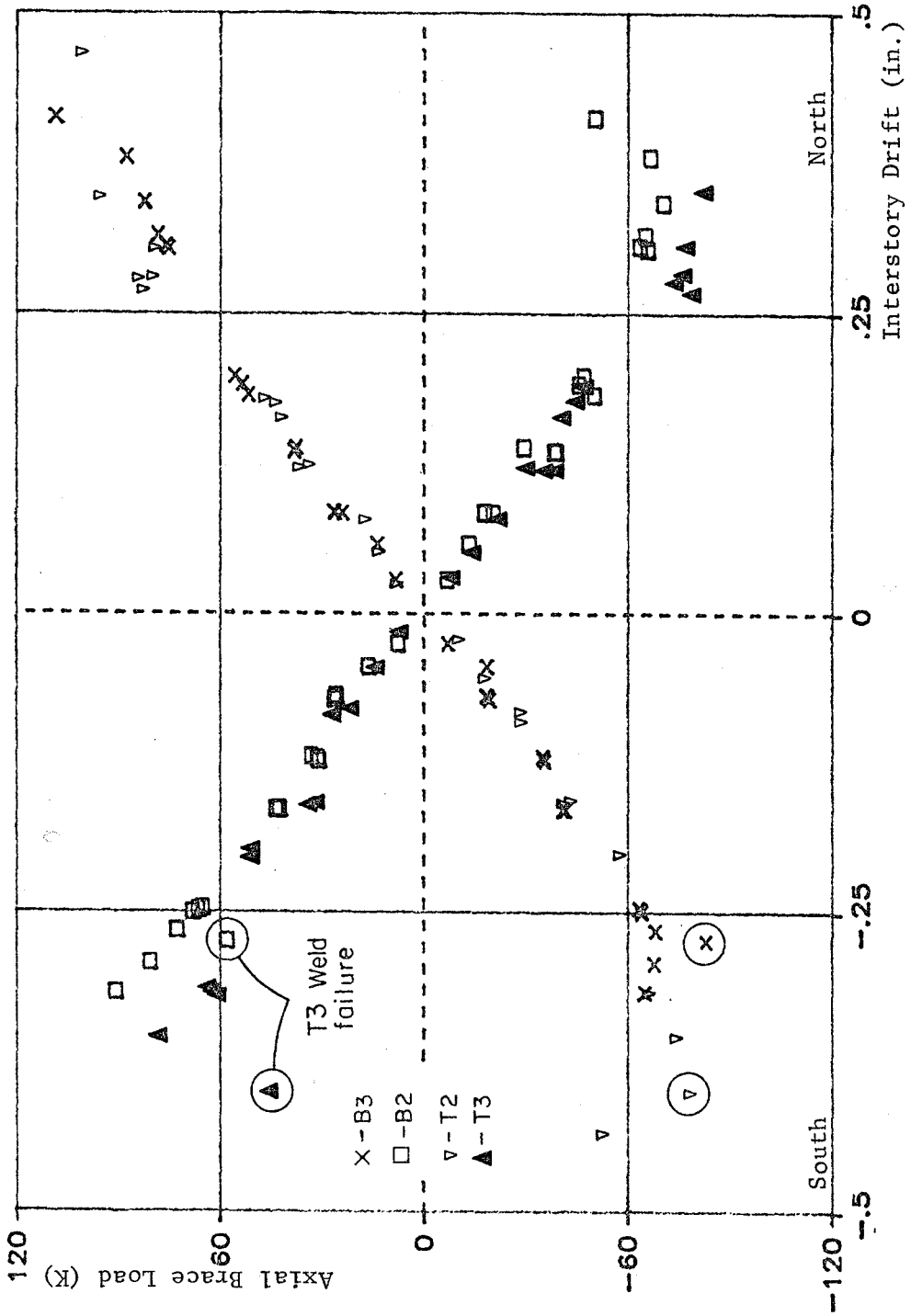

Fig. 5.10 Middle brace loads versus interstory drift

The experimental buckling loads were determined by the maximum compression loads given by the set of four strain gages. The loads (107, 79, 83, and 96 kips) are shown in Table 5.1 and agree well with the predicted buckling loads. The peak loads observed in braces T2 and T3 fall within the range (79 to 91 kips) predicted in rows 1 and 2, while the loads carried by braces T1 and T4 are just above the predicted range of 82 to 93 kips.

The maximum tension loads observed for each top brace are shown in Table 5.1 for two of the final cycles along with the predicted tension load based on the flange and web yield strengths. The strain gage readings were not reliable for the last cycle (F3), nor were they reliable for brace T3 in cycle F2. The table shows that braces T1 and T3 reached larger compression loads than braces T4 and T2, respectively, while braces T2 and T4 attained the highest tension loads. The large loads all correspond to lateral load in the north direction. Several factors could explain this phenomenon. First, the applied lateral load at the peaks was larger loading north than loading south because the frame was stiffer in the north direction. The order of loading may have caused this difference in stiffness. Secondly, the buckling loads for braces which were under compression when the frame was pushed south would have been affected by the previous tension load in the brace during north loading. The Bauschinger effect causes peak compression loads to decrease when tension yielding occurs first.

5.1.3 Total Brace Load. The horizontal components of the axial loads in braces T1, T2, T3 and T4 were summed to give the total shear carried by the braces. In Fig. 5.11 the loads carried by the braces at each peak through cycle F1 are plotted. The brace loads were adjusted as described in Section 5.1.2.1. For this portion of the test, the total brace load varied linearly with the applied lateral load as the line drawn through the points shows. The distance between the brace line and the 45 degree line indicates the shear force in the columns. The load carried by the braces when the frame was pushed south is slightly higher than when loaded north due to the larger drift at the second level.

Figure 5.12 displays the percentage of applied load carried by the braces at the top level. For both directions, the percentage increases only slightly during the test, staying between 60 and 70 percent. For three cycles at a specified drift level, the load carried by the braces also increases with each cycle. Once again, the load carried in the braces when loaded south is higher than when loaded north.

TABLE 5.1 Maximum Loads in Top Braces

(kips)	T1	T2	T3	T4
Predicted Buckling Load (K = 0.65)	82	79	79	82
Predicted Buckling Load (K = 0.5)	93	91	91	93
Maximum Compression Load	107	79	83	96
Predicted Tension Yield Load	112	112	112	112
Max. Tension Load				
Cycle F1	73	97	79	86
Cycle F2	87	101	--	108

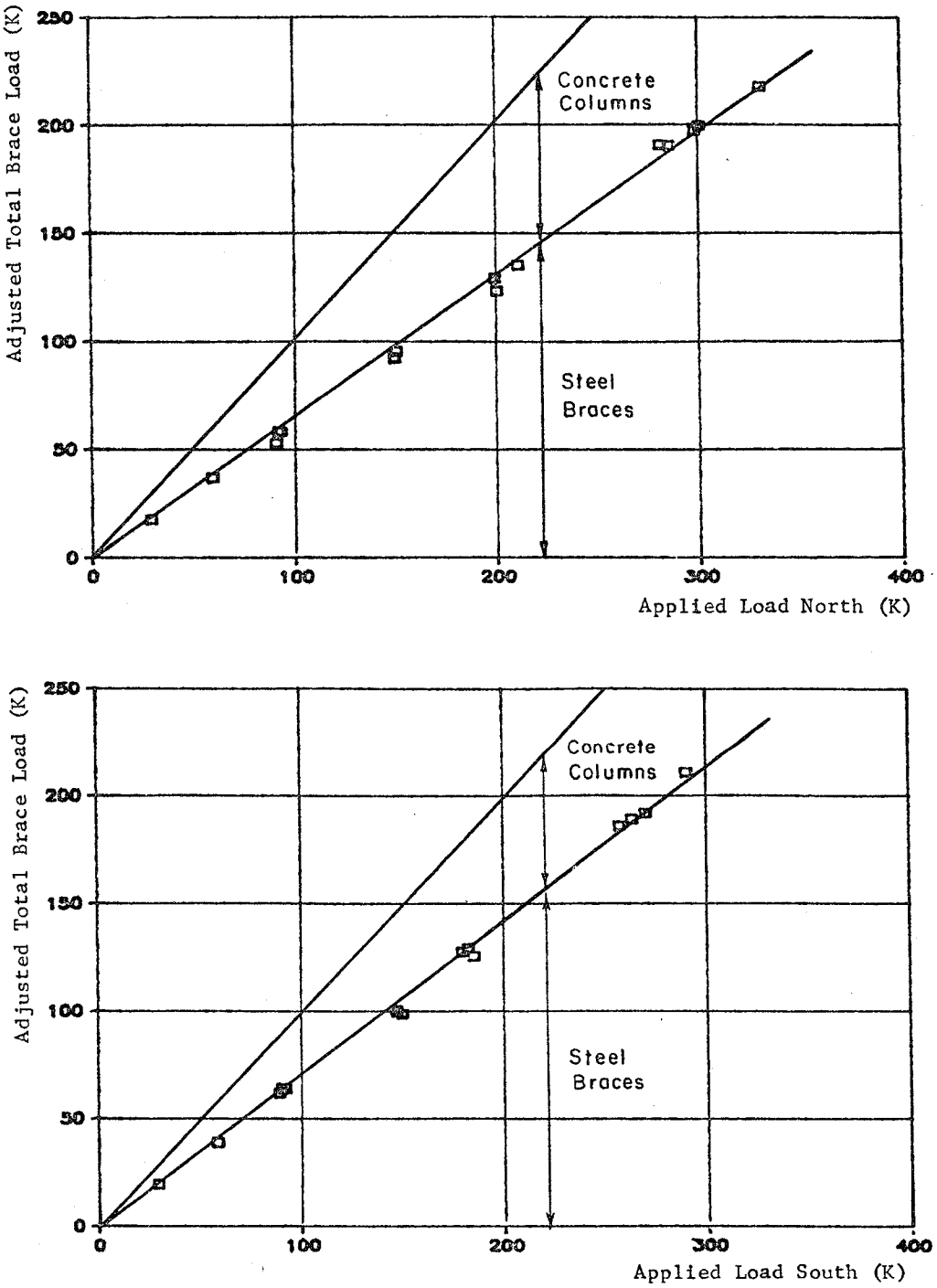

Fig. 5.11 Load Carried by Top Braces

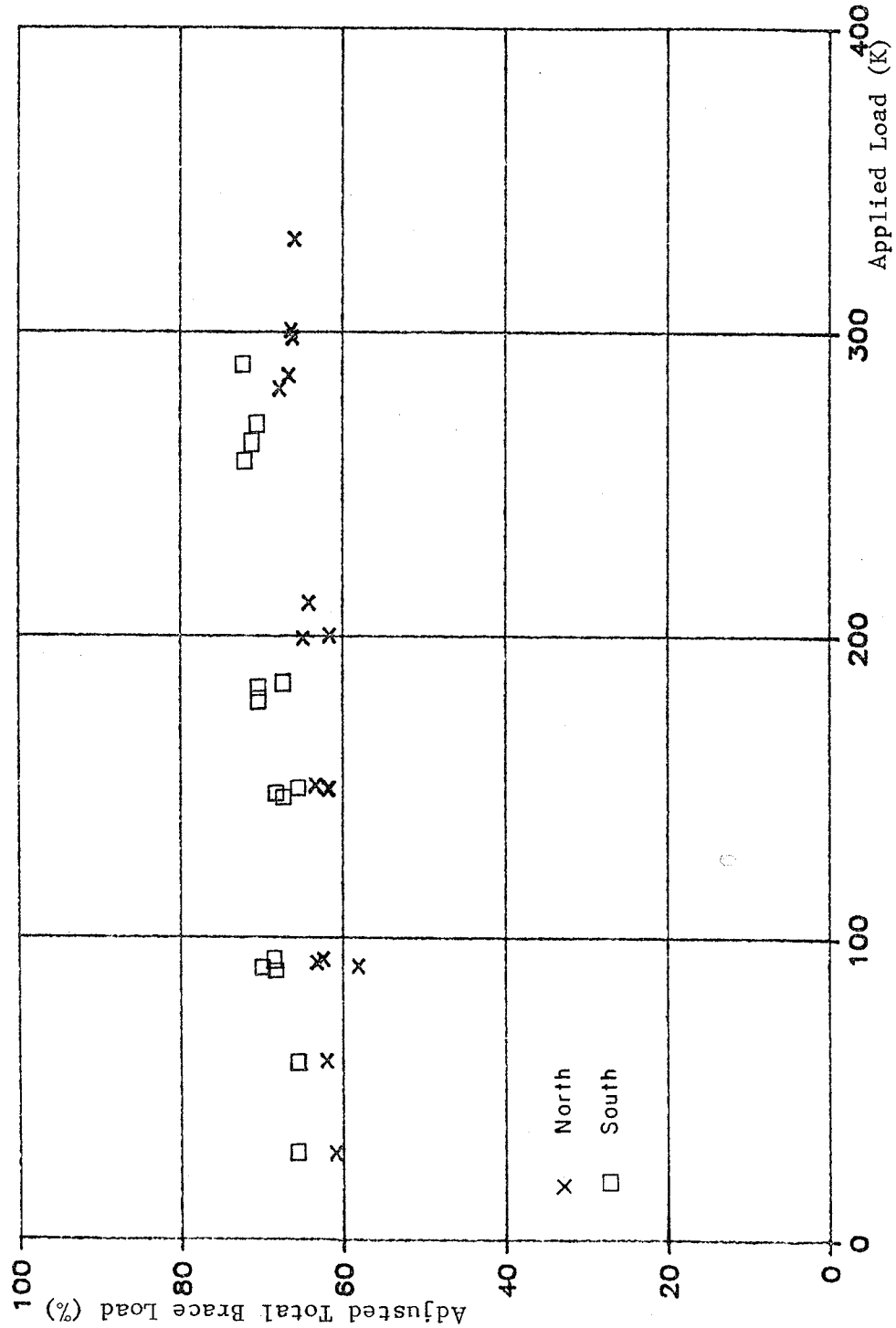

Fig. 5.12 Percent of load carried by braces

The shear force in the columns was estimated by subtracting the total brace load from the applied load, and is plotted in Fig. 5.13. The loads at the peaks are graphed versus the second level interstory drift through cycle F1. The points corresponding to the first, second, and third cycles of each set are marked, making the change in the distribution of load at the same drift level obvious. During the second and third cycles, the columns deteriorate, forcing the braces to carry a larger percent of the load. The largest load carried by shear in the columns before the first brace buckled was 106 kips. The shear force in the columns was more than likely even larger after the braces buckled. The predicted shear capacity of the concrete columns (using the actual concrete strength, the steel reinforcement yield strength, and the actual width of 13-1/3 in. in the ACI equations) was 67 kips. The steel channels increased the shear strength of the columns and, thus, the capacity of the entire system. The strength of the columns with the channels attached will be determined in future tests.

5.2 Steel Collectors and Columns

5.2.1 Collector Tees. The collector tee at the third level was instrumented at four sections as was shown in Figs. 3.27 and 3.28. The single tee had strain gages at locations corresponding approximately to the quarter and mid-length of the member. There was also a set of gages near each end where the extra tee was welded to the outside of the tee forming a "double tee" section.

The variation of strains among the four gages at the south end of the tee are shown in Fig. 5.14. The largest strains were recorded on the bottom portion of the inside flange attached to the spandrel. The next largest strain appeared in the top portion of the inside flange. The two strains in the outside flange were fairly close, but small. The gages at the north end of the collector tee displayed the same pattern. The strains observed in the single tee section were much closer to each other, although the bottom inside flange did show the largest strains.

Figure 5.15 shows the connection region at the end of the tee and the instrumentation location. The drawing emphasizes the many eccentricities involved which could lead to uneven loading of the collector. The dowels in the tees were staggered with the one closest to the end located 6 in. from the gusset plate and 4 in. from the strain gages. The next dowel, which was supposed to be placed through the bottom flange, had been omitted due to the insufficient depth of the hole. The fact that the

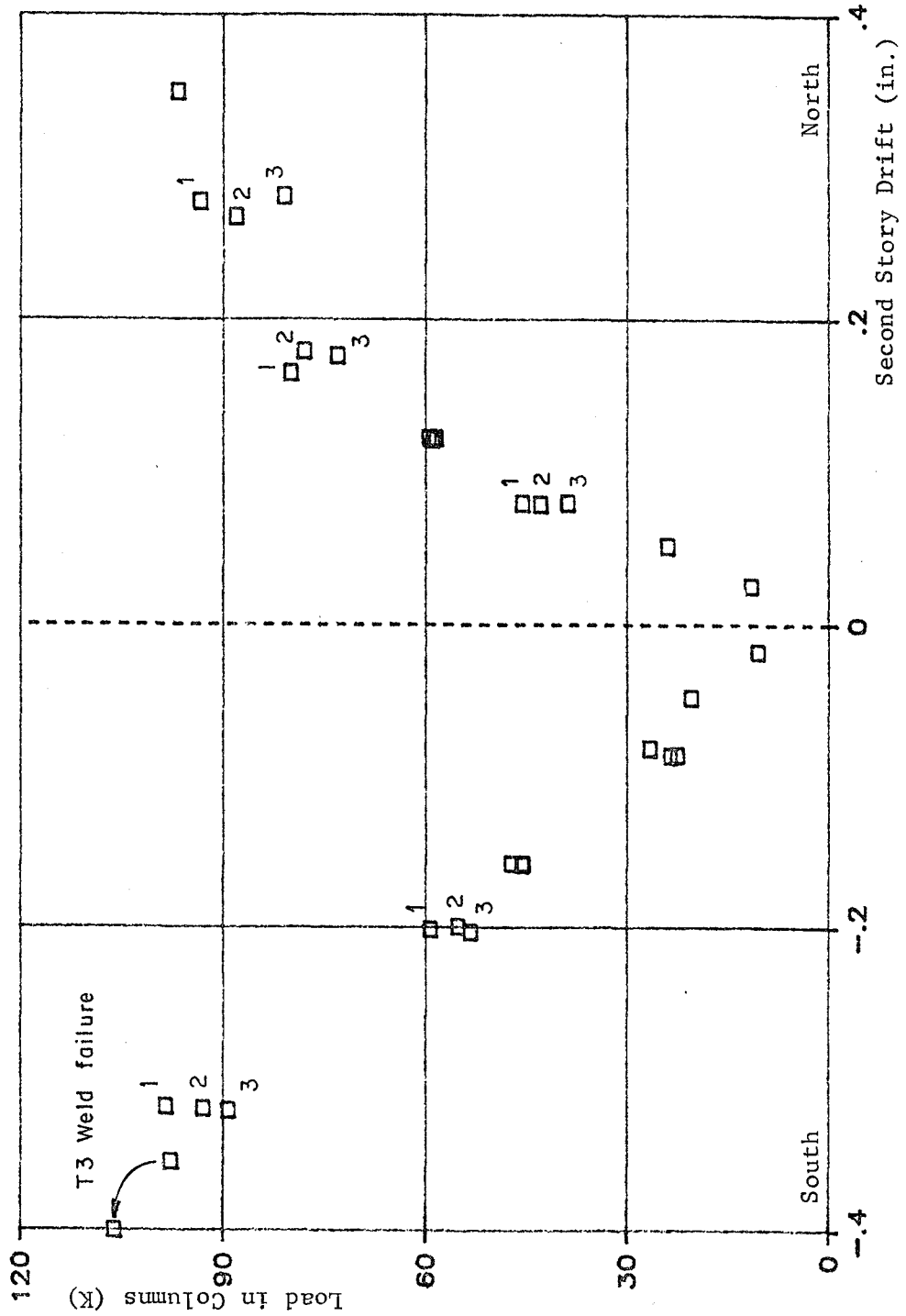

Fig. 5.13 Shear in columns at second level

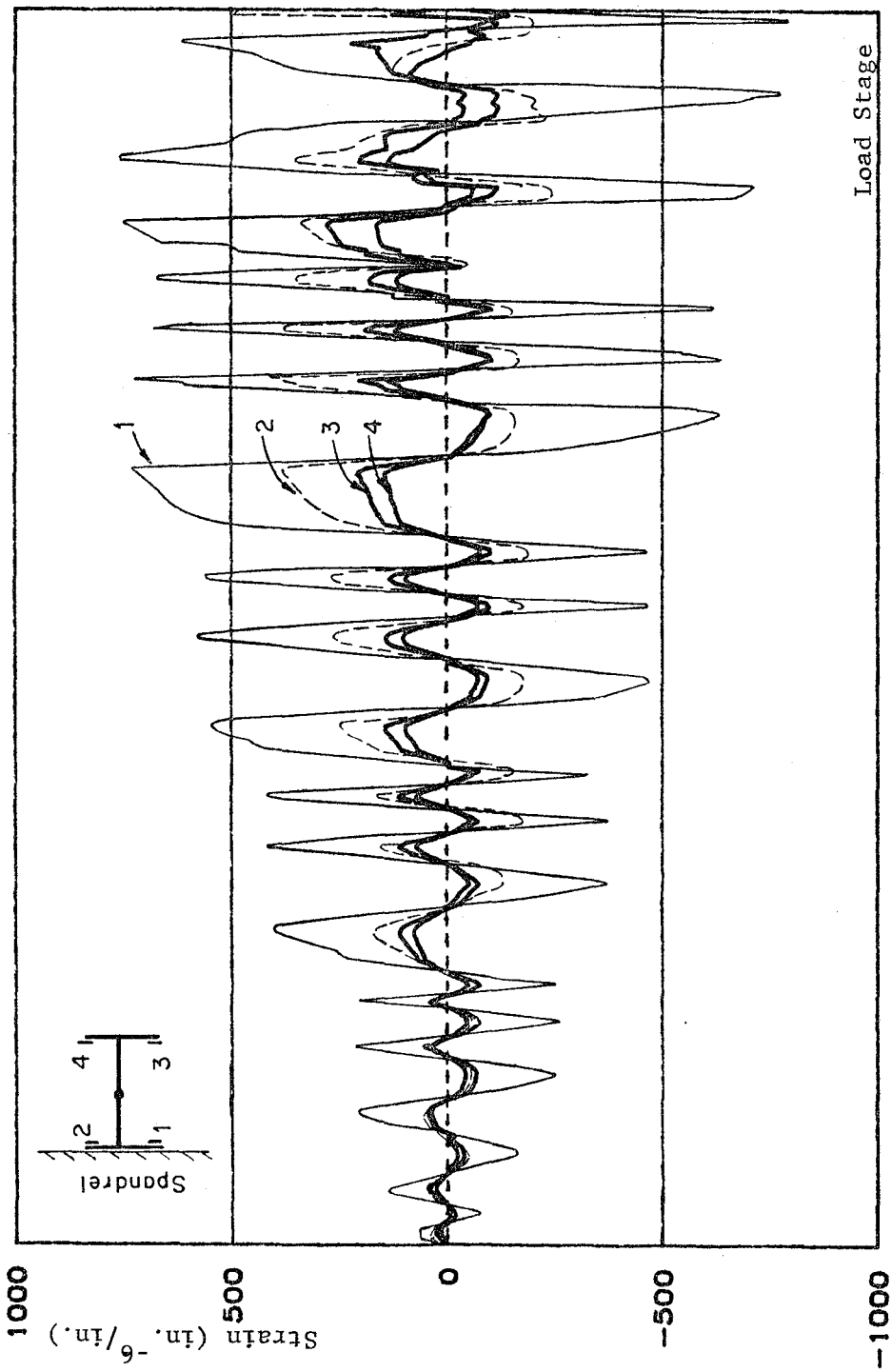

Fig. 5.14 Variation of strains in collector - south end

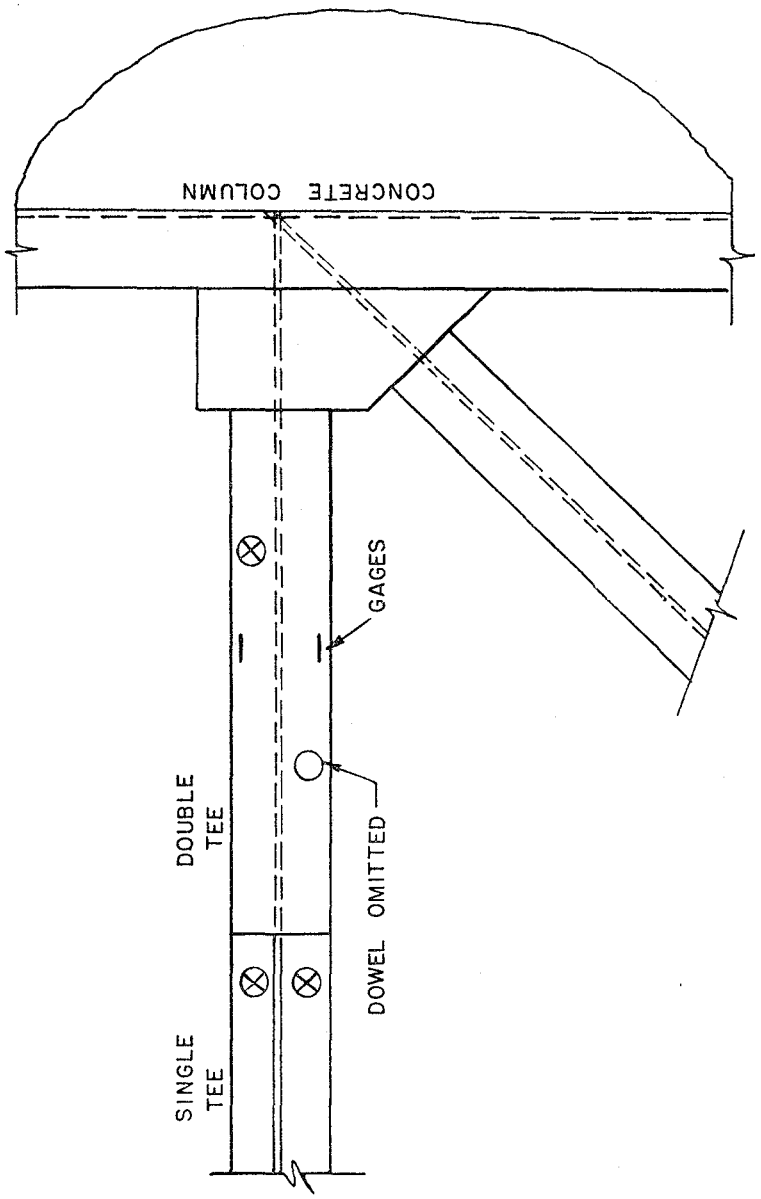

Fig. 5.15 Connection Region at End of Collector

brace frames in from below and not from above could have caused more load in the lower flange tip of the collector. The tee, channel, and wide-flange brace were all 6 in. deep at the connection, but the dowels transferred load to the tee only through the inside flange. Although the collector was not loaded concentrically at its ends, the collector tee load can be obtained by averaging the four strains because the section was symmetric. For the non-symmetric section at the quarter point, the strains were close, so the average was also computed. The four strains measured at the middle of the single tee were not consistent, but the strains were very small, and the average strain produced reasonable loads.

The loads measured at the four locations along the tee are plotted in Figs. 5.16 and 5.17 at varius load stages. The tee loads increased for each new load stage until the last one. On both graphs, the highest lateral load shown (350 kips north, 309 kips south) corresponds to the peak of cycle F2 where the T2 and T3 braces buckled. The lines for these lateral loads are shifted down because the forces at the ends of the collector were not equal due to buckling of the compression brace. For example, in Fig. 5.16 the tension load at the south end of the collector dropped from about 38 kips to 22 kips during the change in lateral load from 300 to 350 kips. Just before 350 kips was reached, brace T3 had buckled and the compression load it carried decreased. The same is true in Fig. 5.17 where the load at the north end dropped when brace T2 buckled.

In Table 5.2 the measured tee load is compared to the load computed using equilibrium of forces at the connection. At the north end of the collector tee, the load should be equal to the horizontal component of the load in brace T2 if no forces were transferred to the concrete at the connection. The loads in the tee and those estimated at both ends are shown in Table 5.2 at the various lateral load peaks. The ratio of the actual load over the computed load ranged from 0.4 to 0.91. Friction and bearing between the steel and the concrete frame and the dowel close to the end probably transferred some of the load from the steel to the concrete between the connection and the gaged section.

5.2.2 Column Channels. Figure 3.27 showed the instrumentation locations for the channel on the south side of the north column. The three gaged sections were 8 in. apart with a dowel between each group of gages. A typical set of strains at a location are shown in Fig. 5.18, for the top set of gages which were just above the spandrel. The strains at the tips of the flanges were much larger than those in the web. The other two instrumented locations showed similar strains although the

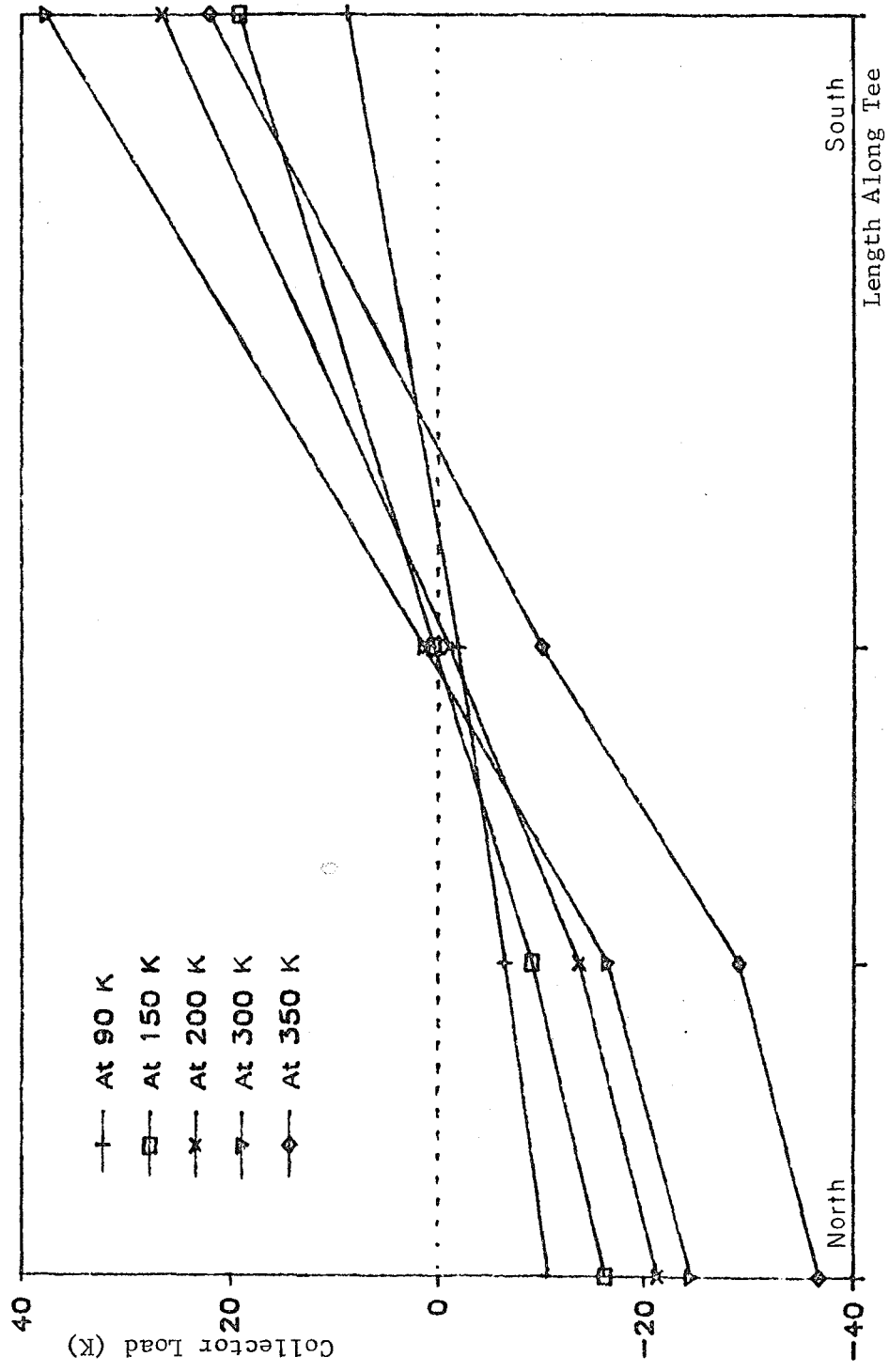

Fig. 5.16 Forces in collector tee at peaks - north load

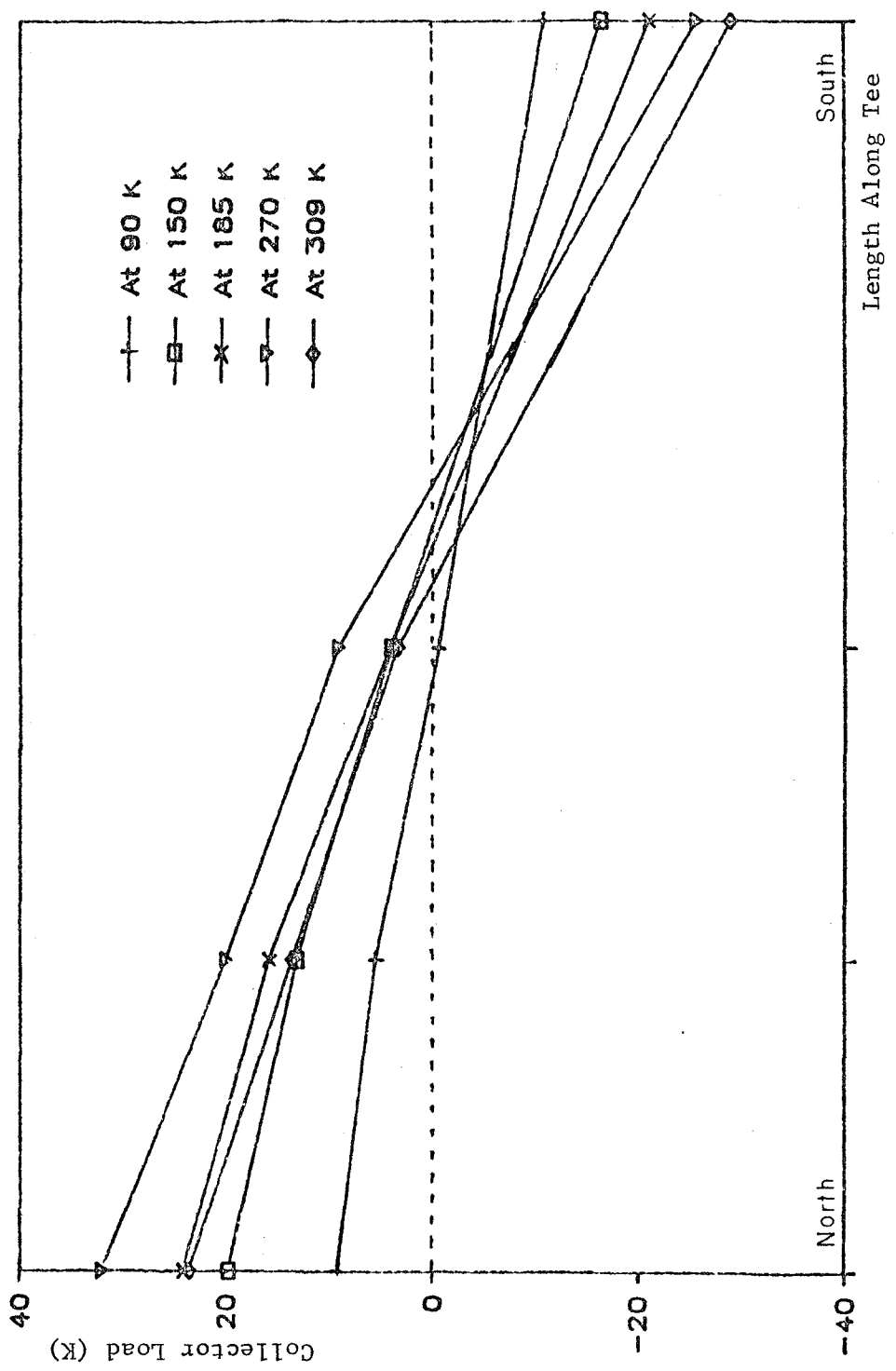

Fig. 5.17 Forces in collector tee at peaks - south load

TABLE 5.2 Forces in Collector Tees (kips)

Applied Load	Tee-North End			Tee-South End		
	Measured*	Computed**	Meas./Comp.	Measured*	Computed**	Meas./Comp.
North						
30	-3.7	-5.8	0.64	3.1	4.9	0.63
60	-6.9	-10.4	0.66	6.4	9.9	0.65
90	-10.7	-12.0	0.89	8.7	16.6	0.52
150	-16.2	-26.0	0.62	19	21.4	0.89
200	-21.3	-29.6	0.72	26.5	29.1	0.91
300	-24.5	-59.2	0.41	37.6	52.7	0.71
330	-27.5	-67.4	0.41	39.4	58.2	0.68
352	-36.7	-70.7	0.52	21.9	(T3 buckled)	--
South						
30	3.9	5.6	0.70	-3	-5.6	0.54
60	7	12.1	0.58	-6.8	-10.1	0.68
90	10.1	22.8	0.44	-11.2	-14.9	0.75
150	19.7	29.0	0.68	-16.6	-31.8	0.52
185	24.1	40.0	0.60	-21.3	-35.1	0.61
270	32	46.1	0.69	-25.8	-43.7	0.59
290	32.2	52.0	0.62	-29.8	-55.2	0.54

*Measured using strain readings

**Computed from equilibrium of forces at connection, ignoring direct transfer to concrete through connection

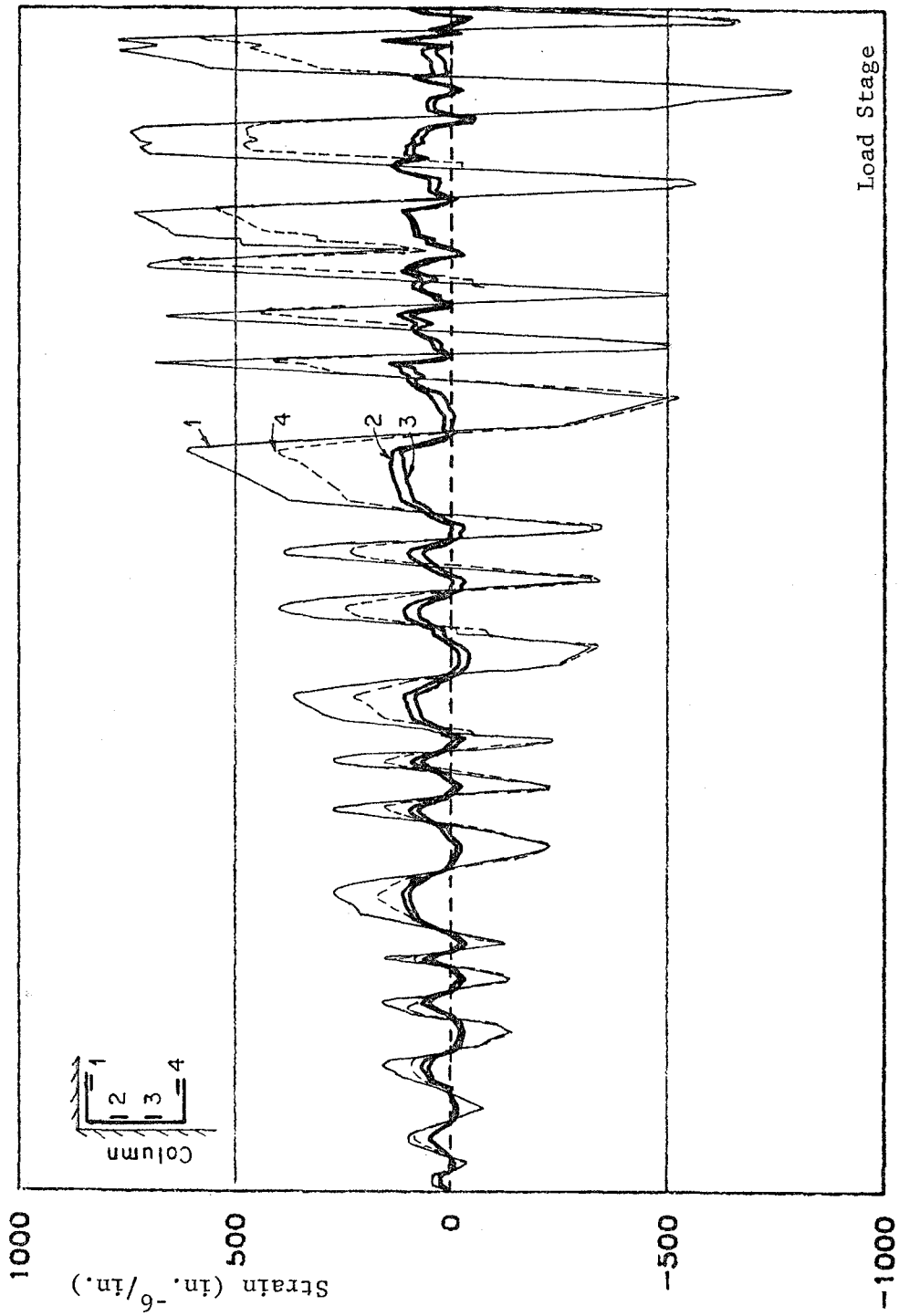

Fig. 5.18 Variation of strains in channel section

difference between web and flange strains was not quite as exaggerated.

Because the cross-section was not symmetric, and the strains were not distributed evenly, a method was devised to compute the channel load which did not take the average of the four strains. The strain distribution which was used assumed that the entire web area had a strain equal to the average of the two web strains and the flanges had a linearly varying strain which was the average web strain at the corner and the flange strain at the tip. Calculation of loads in the above manner produced loads smaller than those computed from the average, as indicated in Table 5.3.

Also shown in Table 5.3 is a comparison of the channel loads and the vertical components of the load in brace B2. Loads were calculated for the instrumented section on the channel closest to where brace B2 frames in to the channel. There was one dowel between the gages and the connection. Ratios of the channel load over the load computed from brace B2 (Avg/Comp and Dist/Comp) are listed in the last columns of the table. When the frame was loaded south and the channel was in compression, the ratio was much smaller than when the frame was pushed north. This may have been caused by differences in the relative positions of the dowels in the holes and by friction between the channel and the column when the brace was in tension.

5.3 Relative Displacement

Relative displacement, or slip, between the steel members and the concrete frame were measured in eight locations as shown in Fig. 3.27. Except for the results from the two displacement transducers at the middle connection, the load-slip curves for each location had the same general shape and showed a large increase in slip at loads greater than 200 kips. Some of the transducers became inoperable during the final cycle, so comparison of maximum slips will be made for cycle F2.

Figures 5.19 and 5.20 are load-slip curves for the second half of the test, which began with the three cycles to 0.23 percent drift or 210 kips north and 185 kips south. In both graphs, there is a huge increase in slip after the three cycles to 200 kips, especially when the frame was loaded north. The two locations represented by these graphs are both on the third-level collector tee. However, the slip at the middle connection also showed a large increase after 200 kips lateral load (Fig. 5.25), and slip on the vertical channels showed moderate increases with each new load level after 200 kips.

TABLE 5.3 Channel Loads (kips)

Applied Load	Channel Load from Average	Channel Load from Distribution	Component of Brace B2	Avg/ Comp	Dist/ Comp
North					
90	14.8	10.7	14.6	1.01	0.73
150	18.7	17.2	21.0	0.89	0.82
200	27.1	23.4	35.9	0.75	0.65
300	39.3	22.9	47.2	0.83	0.49
330	47.9	39.2	47.8	1.00	0.82
350	47.5	39.5	36.2	1.31	1.09
South					
90	-12.2	-9.1	-18.5	0.66	0.49
150	-21	-17.5	-23.6	0.89	0.74
185	-21.8	-17.1	-31.2	0.70	0.55
270	-27.2	-18.7	-48.8	0.56	0.38
290	-26.2	-16.7	-52.1	0.50	0.32
309	-33.4	-22.2	-65.1	0.51	0.34

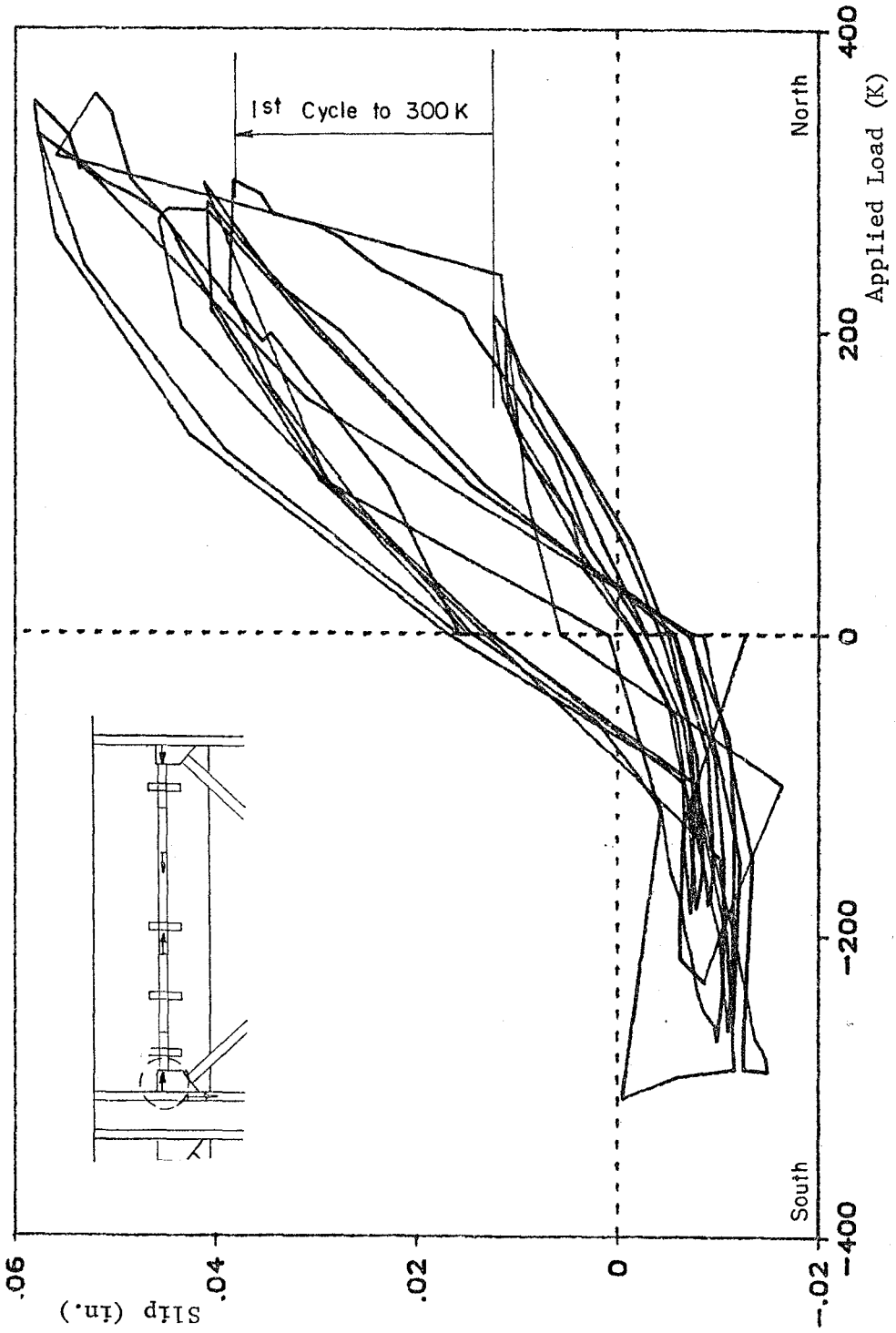

Fig. 5.19 Separation of steel connection from column

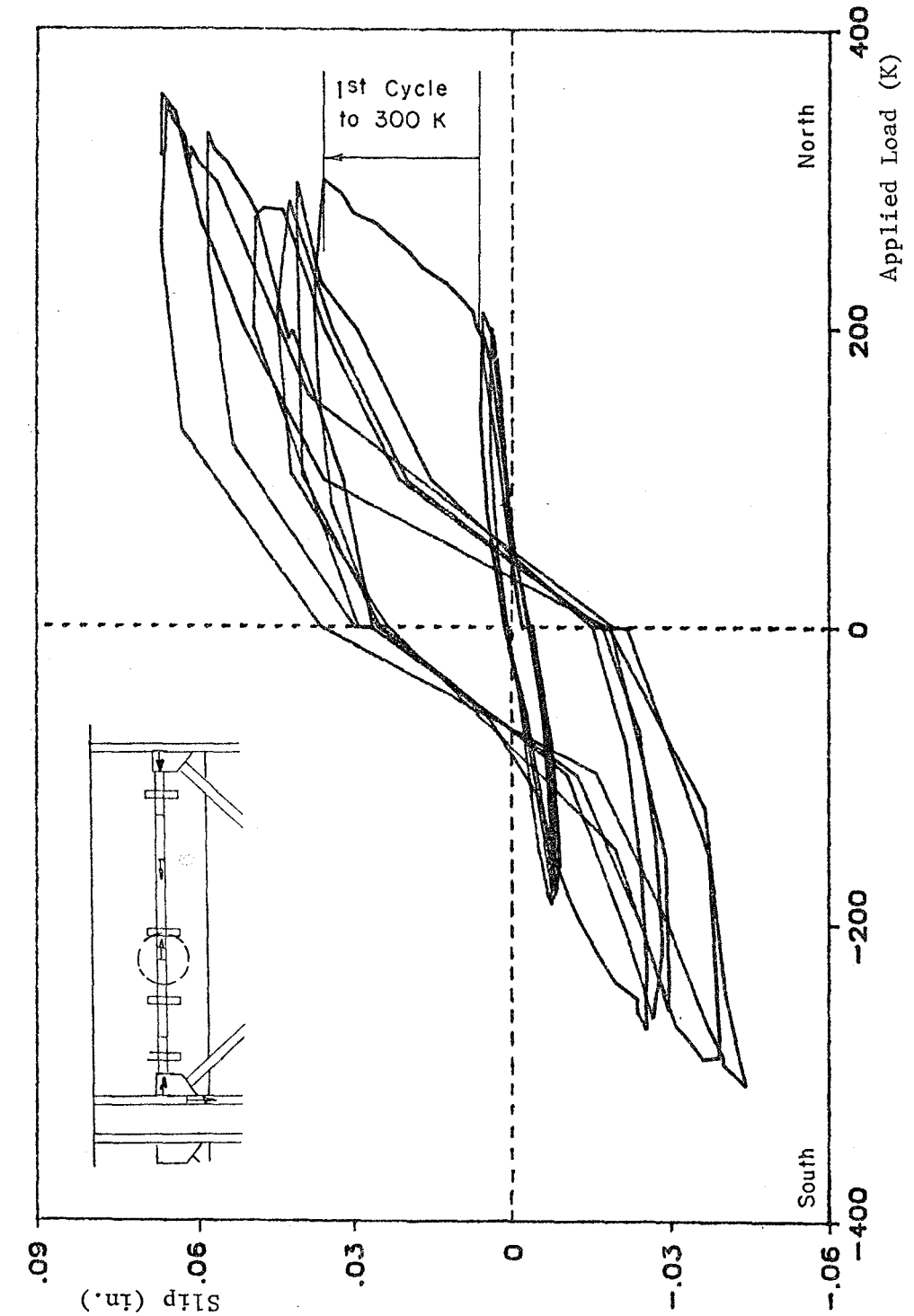

Fig. 5.20 Slip of third level collector tee

The largest displacements were observed at the four locations on the collector at the third level. The two transducers in the middle measured maximum slips of about 0.06 in. when the frame was loaded north and 0.04 in. south. The slips at the ends of the tee were about 0.06 in. north and 0.015 in. when the frame was pushed south. The largest vertical slip observed between the channel and column was .076 in. at the third level. The transducers at the middle connection recorded a maximum displacement of 0.02 in. vertically before they were removed when welds failed.

Figures 5.21 and 5.22 show the load-slip curves for the four instrumented locations on the third level collector for the three cycles to 0.36 percent drift, or about 300 kips lateral load. The curves are similar in shape showing larger slips when the frame was loaded north. The change in slope in the first cycle after 200 kips was attained is apparent.

The same set of load cycles are shown in Fig. 5.23 for the transducers measuring slip between the steel channel and concrete column. For some reason, the slip at the third level was extremely small when the frame was loaded south (channel loaded downward relative to the column).

Figures 5.24 and 5.25 display the strange results obtained from the transducers at the center X-connection. The steel always moved down and to the south relative to the spandrel for loading in both directions. In Fig. 5.25, the increase in slip after 200 kips is shown as well as the increase when the first weld broke. The graph was terminated at this point because there was a large increase in slip each time a weld broke, and the transducers were removed after the third weld failed.

5.4 Strains in Concrete Frame

The readings from the strain gages on the spandrel beam longitudinal bars were examined to determine the strains in the concrete frame. The maximum strains in the spandrel bars were about 1000 $in.^{-6}/in.$, approximately half of the strain corresponding to yield of the reinforcing bar.

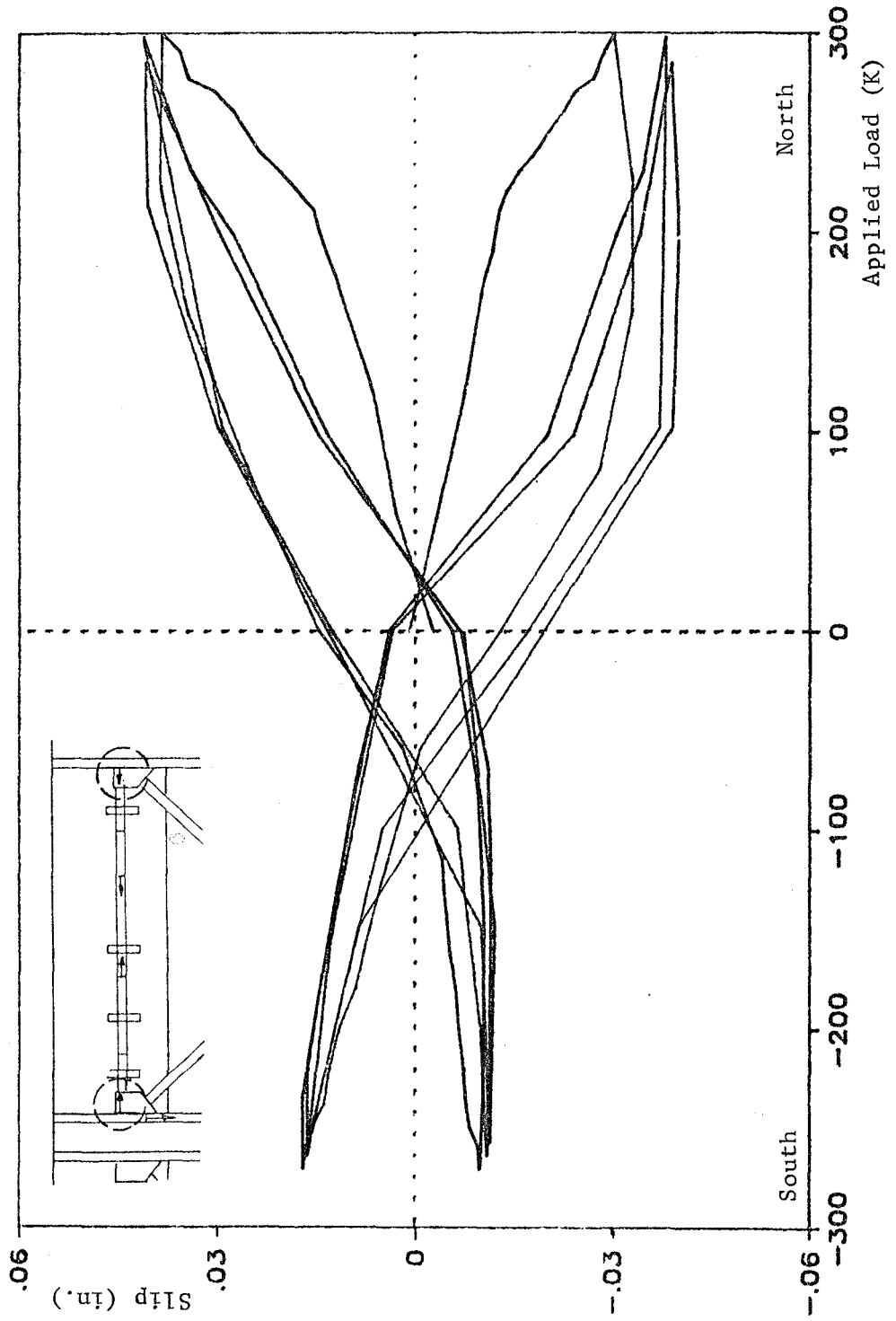

Fig. 5.21 Separation at ends of collector - 0.36% drift cycles

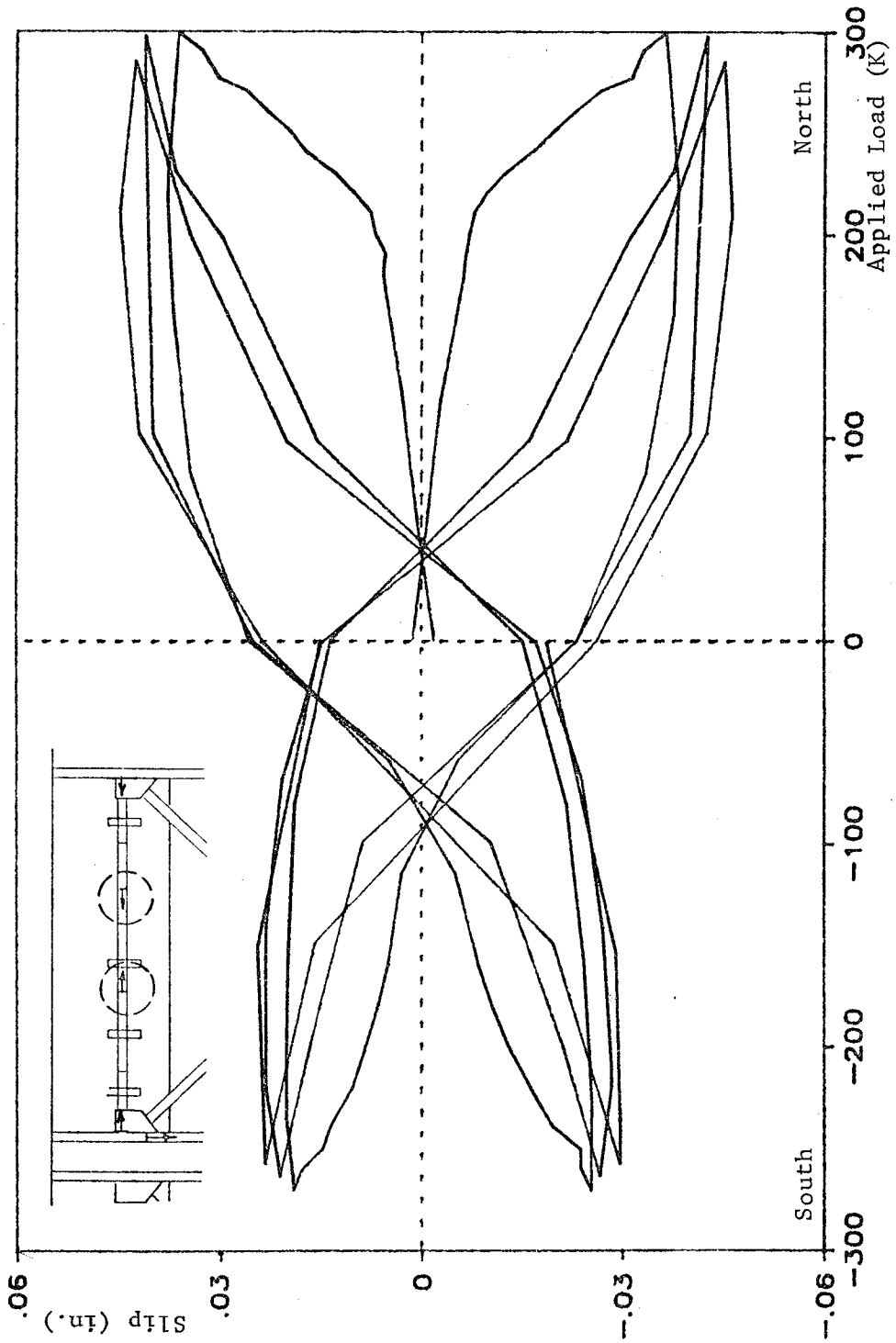

Fig. 5.22 Slips between tee and spandrel - 0.36% drift cycles

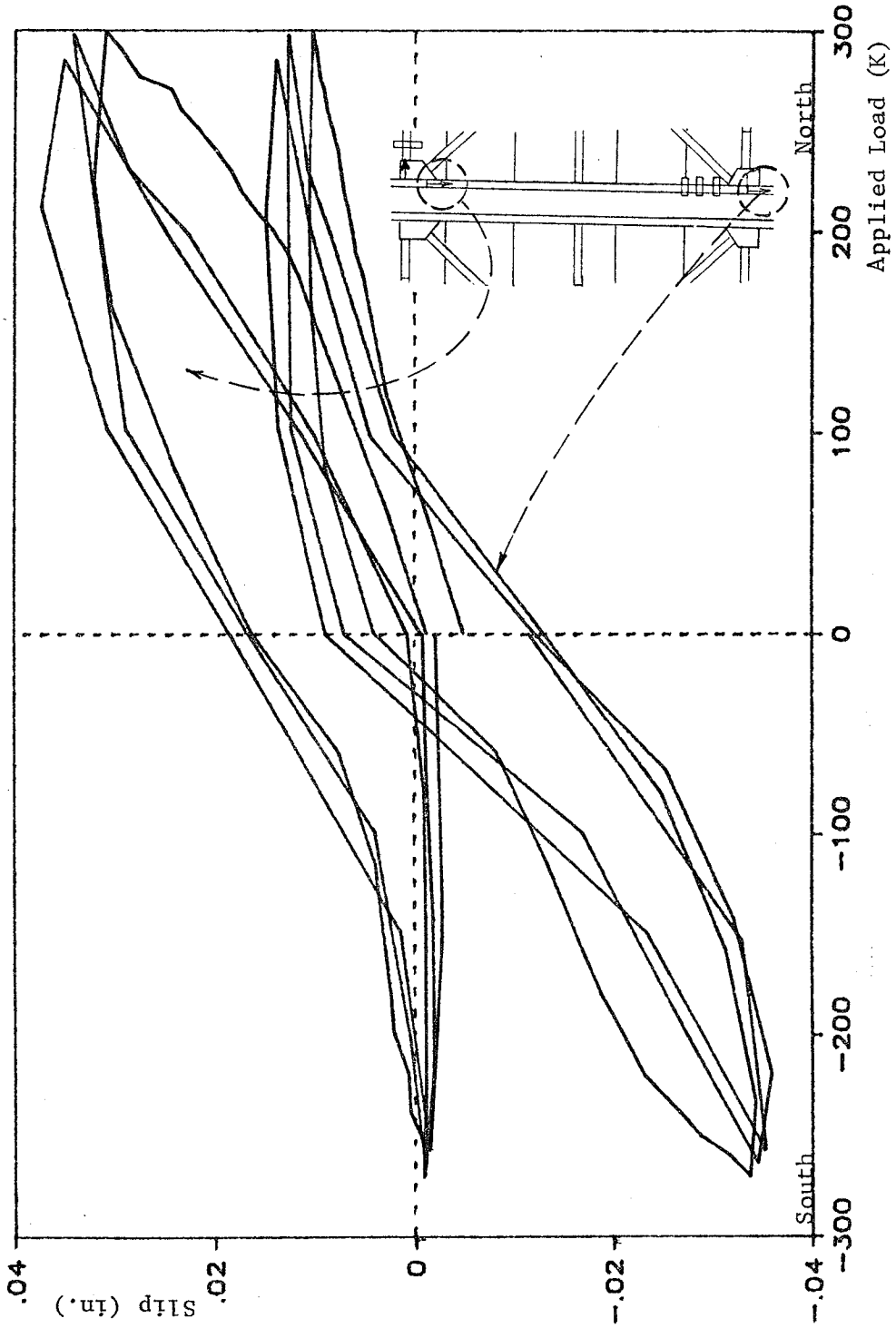

Fig. 5.23 Slips between channel and column - 0.36% drift cycles

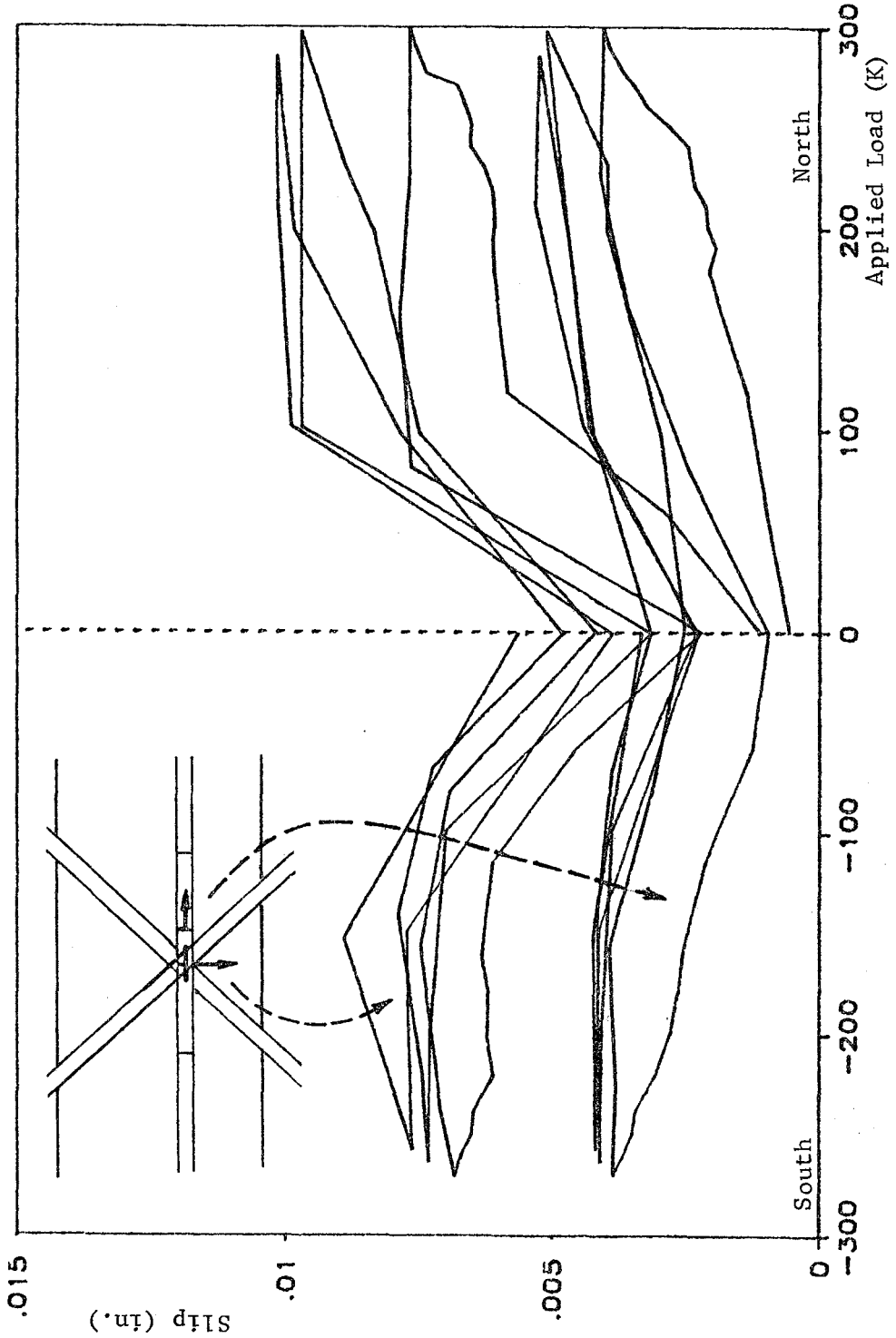

Fig. 5.24 Slips at middle connection - 0.36% drift cycles

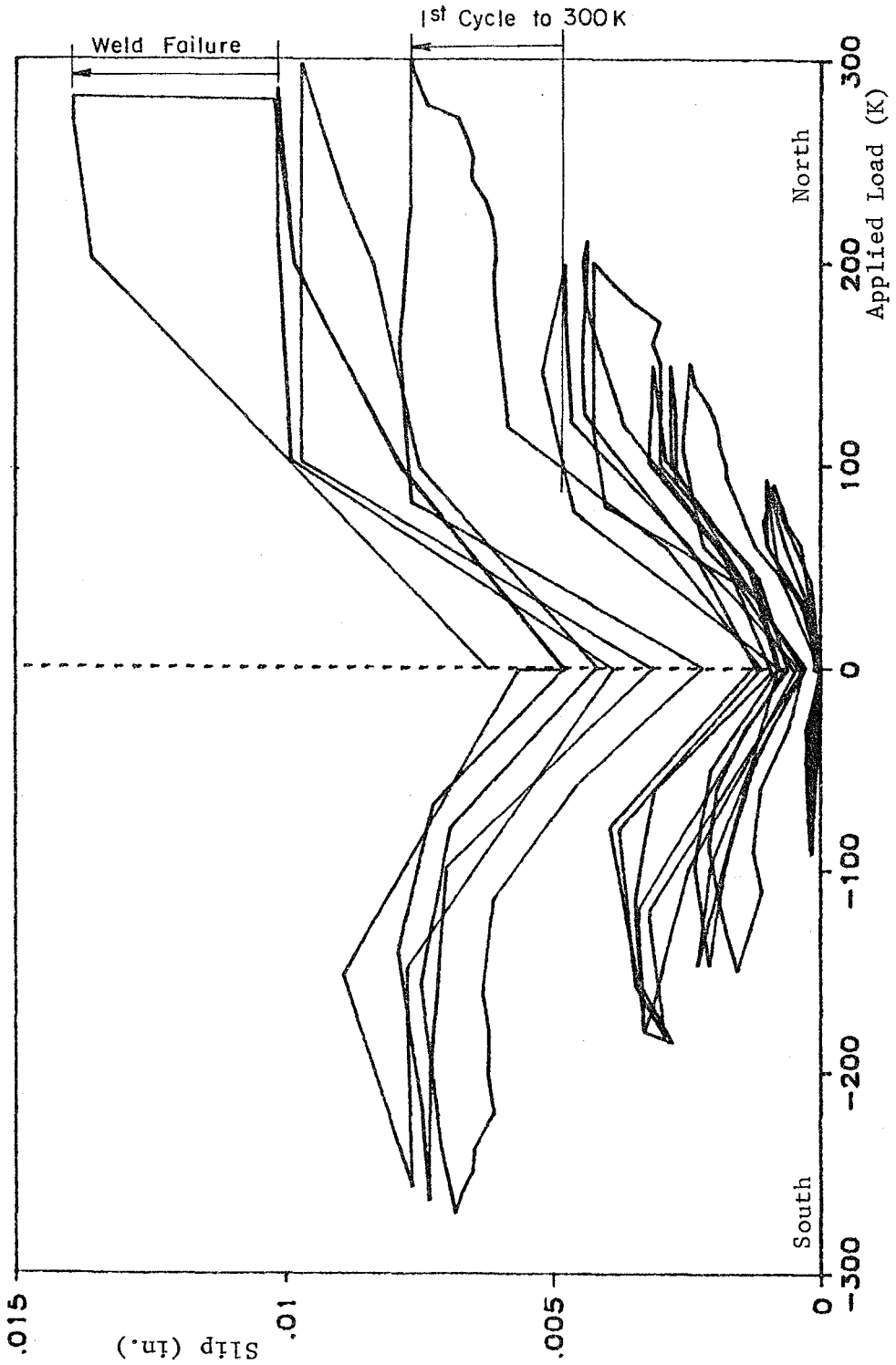

Fig. 5.25 Vertical slip at middle connection

CHAPTER 6

SUMMARY AND CONCLUSIONS

6.1 Summary of Test Program

A two-thirds, scale model of a portion of an exterior frame of a reinforced concrete building was constructed and tested. The two-bay, two-story frame modeled a type of construction popular in California during the 1950's and 1960's which consisted of deep spandrel beams and short, narrow columns. Two strengthening schemes were carried out with the purpose of increasing the lateral load capacity of the model. In this report, the second of these schemes was investigated: erection of a structural steel bracing system.

The exposed diagonal braces were six inch deep wide flange shapes, which were welded at their ends to horizontal and vertical steel collector members. Steel channels were attached to the side faces of the concrete columns with epoxy-grouted threaded rod dowels. The horizontal collectors were structural tees attached in the same manner to the spandrel faces at the floor levels. The braces were designed to carry the entire lateral shear forces computed using the 1982 Uniform Building Code.

The steel braced frame was tested to failure under reversed, cyclic loading. All of the load was applied at the third level of the model near the two columns. Reactions were applied to the frame at corresponding locations in the first level floor slab. Six of the eight braces (all four at the second level and two at the bottom level) were instrumented at mid-length for determination of axial loads.

The model strengthened by steel braces was subjected to seventeen load cycles: two preliminary cycles and five sets of three cycles, with each set at an increased drift level. The maximum loads and drift levels applied to the structure were 360 kips and 1.2 percent drift when the frame was pushed north, and 309 kips and 1.3 percent drift when the frame was loaded south. The peak lateral loads were over three times the computed design earthquake loads. The values represent the interstory drift between the second and third floors of the model, which is where the major damage occurred. Failure at the second level was caused by buckling of the compression braces, local yielding of the tension braces, weld fractures at the ends of the tension

braces, and shear failure of the columns. In addition, pullout of dowels occurred in one region of the steel channel/concrete column interface. By comparison, the first story suffered relatively minor damage consisting of shear cracking of the columns and some flexural cracking in the columns and spandrel beam.

6.2 Overall Behavior

The diagonal braces performed as they were designed in that they carried the lateral loads, thus preventing failure of the columns and possible collapse of the structure. From the beginning of the test to the point just before the first brace buckled, the four braces across the top level carried between 60 and 70 percent of the lateral load applied to the frame. Due to loss of instrumentation when a brace buckled, the total shear carried by the top level braces could not be determined for the last two cycles of the test. When the braces lost most of their load-carrying capacity due to buckling and weld failures in the final cycle, the load was transferred to the columns. Although the columns failed in shear, they were able to maintain their gravity load-carrying capacity due to the strengthening and stiffening effect of the steel channels.

The bracing system showed good redistribution of loads when a brace buckled. However, a brace weld failure produced a sudden transfer of load, which was primarily taken by the columns, especially when the entire weld connecting a brace at a joint fractured. When a brace failed at the upper level, the corresponding brace at the lower level was directly affected because most of the brace load above was transferred through the connection to the brace below. In addition, there seemed to be better transfer of load between the braces on each side of a column than between the two braces side by side in the same bay. This was observed when a middle brace buckled or when a weld connecting the brace to the collector tee failed. In both instances, the brace on the other side of the column absorbed more of the load than did the adjacent brace in the same bay.

The behavior of the steel column channels and collector tees demonstrated that the method of attaching the steel members to the concrete frame worked very well. The only instance of dowel failure occurred when the top of a channel pulled away from one side of the column at peak displacement. The dowels pulled out cones of concrete indicating that the strength and bond of the epoxy was not the problem. In that region there were fewer dowels than the design had called for because holes could not be

drilled without interference from the steel reinforcement in the columns. In addition, two of the dowels in this region had embedment lengths less than 5-1/2 inches. The need for a sufficient number of dowels with adequate embedment was demonstrated.

An important problem observed in the test of the steel braced frame was the fabrication details of the welded connections; specifically the field welds between the braces and gusset plates. Alternate details and welding procedures were suggested to ensure full penetration of the groove welds. Above all, welding must conform to the requirements specified by the American Welding Society.

The peak loads sustained by the specimen were at least three times the lateral earthquake design loads prescribed by the 1982 UBC. The shear force for the prototype building at the third story (2107 kips for seismic zone 4) divided over sixteen braced bays is 132 kips. For two bays of the two-thirds scale model, the shear force becomes 78 kips. The Uniform Building Code requires braced frames in seismic zones 2,3, and 4 to be designed for 1.25 times the computed lateral earthquake forces. Therefore, the lateral design load for the model frame is 97 kips. At this load level, the braces behaved elastically and continued to perform in a linear manner up to loads of about 290 kips when welds failed and compression braces started to bend.

The design of the steel bracing system did not include the shear strength of the columns in the calculation of the lateral load capacity. However, it was shown that the columns carried between 30 and 40 percent of the applied lateral load. Therefore, it is recommended that the lateral capacity of the system include the nominal shear strength computed from ACI equations (11.2), (11.3.1.1), and (11.17). This would be a conservative estimate of the column capacity because the steel channels approximately doubled the shear strength of the bare column.

6.3 Conclusions

The seismic strengthening system consisting of exposed structural steel diagonal braces greatly improved the performance of the reinforced concrete model which had short columns and deep beams making up the exterior frame. The braces carried the lateral loads which would be produced by an earthquake and protected the columns from shear failure. The horizontal and vertical steel collector members transferred the loads and produced good interaction between the concrete frame and steel

bracing system. In addition, the vertical steel members increased the strength and stiffness of the concrete columns. Because weld failures reduced the ductility of the steel braced frame, the fabrication and design of the welded connections required more attention. Welding and fabrication must be carefully executed and inspected to ensure satisfactory performance.

REFERENCES

1. Structural Engineers Association of California, Recommended Lateral Force Requirements and Commentary, Fourth Edition, San Francisco, California, 1975.

2. Wyllie, Loring A., Jr., "Strengthening Existing Concrete and Masonry Buildings for Seismic Resistance," Proceedings of the Second Seminar on Repair and Retrofit of Structures, Ann Arbor, Michigan, 1981, pp. 322-333.

3. Degenkolb, H.J., and Associates, Repair and Strengthening of Reinforced Concrete Structures, San Francisco, California, 1983.

4. Ogura, Koichiro, "Outline of Damages to Reinforced Concrete Structures," Proceedings of U.S.-Japan Seminar on Earthquake Engineering with Emphasis on the Safety of School Buildings, Sendai, Japan, 1970.

5. Higashi, Y., "Strengthening of Reinforced Concrete Structures," Research Report, Higashi Laboratory, Tokyo, Japan, 1981.

6. Sugano, S., "An Overview of the State-of-the-Art in Seismic Strengthening of Existing Reinforced Concrete Buildings in Japan", Proceedings of the Third Seminar on Repair and Retrofit of Structures, Ann Arbor, Michigan, 1982, pp. 328-349.

7. Sugano, S., "Guideline for Seismic Retrofitting (Strengthening, Toughening and/or Stiffening) Design of Existing Reinforced Concrete Buildings," Proceedings of the Second Seminar on Repair and Retrofit of Structures, Ann Arbor, Michigan, 1981, pp. 189-237.

8. Shimizu, Y., Higashi, Y., Endo, T., and Ohkubo, M., "Aseismic Capabilities of Strengthened Reinforced Concrete Frame," Research Report, Higashi Laboratory, Tokyo, Japan, 1981.

9. Sugano, S., and Endo, T., "Seismic Strengthening of Reinforced Concrete Buildings in Japan," Strengthening of Building Structures - Diagnosis and Theory, IABSE Symposium, Venice, Italy, 1983, pp. 371-378.

10. Kawamata, S., and Ohnuma, M., "Strengthening Effect of Eccentric Steel Braces to Existing Reinforced Concrete Frames," Proceedings of the Second Seminar on Repair and Retrofit of Structures, Ann Arbor, Michigan, 1981, pp. 262-269.

11. Sugano, S., "Aseismic Strengthening of Existing Reinforced Concrete Buildings," Proceedings of the First Seminar on Repair and Retrofit of Structures, Ann Arbor, Michigan, 1980, pp. 13-40.

12. Sugano, S., and Fujimura, M., "Aseismic Strengthening of Existing Reinforced Concrete Buildings," Proceedings of the Seventh World Conference on Earthquake Engineering, Part I, vol. 4, Istanbul, Turkey, 1980, pp. 449-456.

13. International Conference of Building Officials, Uniform Building Code, 1955 Edition, Whittier, California, 1955.

14. International Conference of Building Officials, Uniform Building Code, 1982 Edition, Whittier, California, 1982.

15. American Concrete Institute, Building Code Requirements for Reinforced Concrete (ACI 318-83), Detroit, Michigan, 1983.

16. Black, R., Wenger, W., Popov, E., "Inelastic Buckling of Steel Struts under Cyclic Load Reversals," Report No. UCB/EERC-80/40, Berkeley, California, October, 1980.

17. Wiener, D., "Behavior of Steel to Concrete Connections Used to Strengthen Existing Structures," unpublished Master's thesis, The University of Texas at Austin, August, 1985.

18. American Society for Testing and Materials, "Compressive Strength of Cylindrical Concrete Specimens," ASTM C39-72, Philadelphia, Pennsylvania, 1972.

19. Luke, P. C. C., Chon, Carlos and Jirsa, J. O., "Epoxies For Use of Grouting Reinforcing Bar Dowels in Concrete," PMFSEL Report No. 85-3, The University of Texas at Austin, May, 1984.

20. Adhesive Engineering Company, "Product Data Concresive 1411," Technical Bulletin A/E 478, San Carlos, California, 1982.

21. American Society for Testing and Materials, "Standard Methods and Definitions for Mechanical Testing of Steel Products," ASTM 370-71, Philadelphia, Pennsylvania, 1971.

22. American Welding Society, Structural Welding Code - Steel, AWS D1.1-79, Third Edition, Miami, Florida, 1978.

23. American Institute of Steel Construction, Manual of Steel Construction, Eighth Edition, Chicago, Illinois, 1980.

24. Roach, C. E., and Jirsa, J. O., "Seismic Strengthening of a Reinforced Concrete Frame Using Reinforced Concrete Piers," PMFSEL Report NO. 86-4, The University of Texas at Austin, May 1986.